1241

TRANSPORTATION RESEARCH RECORD

Railroad Transportation Issues

TRANSPORTATION RESEARCH BOARD
NATIONAL RESEARCH COUNCIL
WASHINGTON, D.C. 1989

Transportation Research Record 1241
Price: $9.00

modes
1 highway transportation
3 rail transportation

subject areas
12 planning
16 user needs
21 facilities design
40 maintenance
53 vehicle characteristics
62 soil foundations

TRB Publications Staff

Director of Publications: Nancy A. Ackerman
Senior Editor: Edythe T. Crump
Associate Editors: Naomi C. Kassabian
Ruth S. Pitt
Alison G. Tobias
Production Editor: Kieran P. O'Leary
Graphics Coordinator: Karen L. White
Office Manager: Phyllis D. Barber
Production Assistant: Betty L. Hawkins

Printed in the United States of America

Library of Congress Cataloging-in-Publication Data
National Research Council. Transportation Research Board.

Railroad transportation issues.
p. cm.—(Transportation research record, ISSN 0361-1981 ; 1241)
ISBN 0-309-04965-2
1. Railroad engineering. I. National Research Council (U.S.). Transportation Research Board. II. Series.
TE7.H5 no. 1241
[TF155]
388 s—dc20
[625.1] 90-35154
CIP

Sponsorship of Transportation Research Record 1241

GROUP 1—TRANSPORTATION SYSTEMS PLANNING AND ADMINISTRATION
Chairman: Ronald F. Kirby, Metropolitan Washington Council of Governments

Specialized and Rural Transportation Services Section
Chairman: Robert T. Goble, Carter Goble Associates, Inc.

Committee on Intercity Rail Passenger Systems
Chairman: George Haikalis, New York, New York
Secretary: S. David Phraner, Port Authority of New York and New Jersey
Murthy V. A. Bondada, Ross Capon, Robert J. Casey, John A. Dawson, William W. Dickhart, Raymond H. Ellis, Sharon M. Greene, Emmanuel S. Horowitz, Ata M. Khan, James T. McQueen, Jolene Moritz Molitoris, Ronald C. Sheck, George M. Smerk, Charles H. Smith, Cheryl D. Soon, Louis S. Thompson, Merrill L. Travis, Warren D. Weber, Walter E. Zullig, Jr.

GROUP 2—DESIGN AND CONSTRUCTION OF TRANSPORTATION FACILITIES
Chairman: Raymond A. Forsyth, California Department of Transportation

Railway Systems Section
Chairman: Robert E. Kleist, Association of American Railroads

Committee on Railroad Track Structure System Design
Chairman: J. W. Winger, P'Sumit Engineering, Inc.
Secretary: Charles L. Stanford, New York City Transit Authority
Dale K. Beachy, Earl E. Frank, Crew S. Heimer, Thomas B. Hutcheson, Ben J. Johnson, Mohammad S. Longi, W. Scott Lovelace, Jerry R. Masters, Philip J. McQueen, Howard G. Moody, Myles E. Paisley, Gerald P. Raymond, Alfred E. Shaw, Jr., W. S. Stokely, Daniel H. Stone, Marshall R. Thompson, John G. White

GROUP 3—OPERATION, SAFETY, AND MAINTENANCE OF TRANSPORTATION FACILITIES
James I. Taylor, University of Notre Dame

Facilities and Operations Section

Committee on Railroad Operations Management
Chairman: William J. Romig, Norfolk Southern Corporation
Secretary: Robert E. Heggestad, Harmon Industries, Inc.
James W. Boone, Peter J. Detmold, A. Donald Dingle, James Drogan, Howard E. Handley, Jr., Michael R. Haverty, James A. Jaroch, Robert H. Leilich, Carl D. Martland, Donald G. McInnes, George L. Pollitt, John J. Robinson, Guerdon S. Sines, Charles E. Taylor, Mark A. Turnquist, Frederic W. Yocum, Jr., Benjamin Zodikoff

Maintenance Section

Committee on Railway Maintenance
Chairman: Albert J. Reinschmidt, Association of American Railroads
Secretary: William B. O'Sullivan, Federal Railroad Administration, U.S. Department of Transportation
David M. Coleman, Ronald H. Dunn, Amir N. Hanna, Thomas B. Hutcheson, Robert A. Kendall, Richard G. McGinnis, Willis H. Melgren, Guenther W. Oberlechner, Mike Rougas, Ernest T. Selig, William J. Semioli, Harry E. Stewart, Vincent R. Terrill, Donald R. Uzarski

Elaine King, Transportation Research Board staff

Sponsorship is indicated by a footnote at the end of each paper. The organizational units, officers, and members are as of December 31, 1988.

NOTICE: The Transportation Research Board does not endorse products or manufacturers. Trade and manufacturers' names appear in this Record because they are considered essential to its object.

Transportation Research Board publications are available by ordering directly from TRB. They may also be obtained on a regular basis through organizational or individual affiliation with TRB; affiliates or library subscribers are eligible for substantial discounts. For further information, write to the Transportation Research Board, National Research Council, 2101 Constitution Avenue, N.W., Washington, D.C. 20418.

Transportation Research Record 1241

Contents

Foreword

Koppelman's paper examines the relevant issues related to the development of intercity travel demand models and evaluates existing intercity travel data sets that could be used to estimate models of intercity trip frequency, destination, mode, and air fare/service class choice. The desired properties of data needed to develop a model system that is behaviorally consistent and has a high degree of predictive accuracy are described.

Peterkofsky describes an expert support system developed to automate the selection of routings for the return of empty freight cars under special car orders (a provision of the Association of American Railroads' Car Service Rules). This system incorporates elements of artificial intelligence and operations research but also puts a human expert directly into the decision process.

Detailed track inspection procedures designed to implement Army Track Standards are described by Brown et al. These procedures are tied into the Army's railroad track maintenance management decision support system, RAILER, and can also be used to implement other track standards, such as those issued by the Federal Railroad Administration.

The paper by Sattler et al. presents a bearing capacity type of design procedure for assessing the stability of track subgrade. In particular, this paper concentrates on the incorporation of the matric suction term into the procedure to permit the use of the additional soil strength that results from the matric suction in the subgrade. Design charts have been produced that give a factor of safety against bearing capacity failure as a function of various train loads, sub-ballast thicknesses, soil types, and design matric suction values.

Excessive wheel/rail loads cause accelerated wheel/rail wear, truck component deterioration, track damage, and increased potential for derailment. Kalay and Reinschmidt present results of tests of conventional North American freight cars using both wayside and onboard measurement systems. Particular emphasis is given to wheel/rail loads resulting from suspension dynamics.

Multidimensional Model System for Intercity Travel Choice Behavior

FRANK S. KOPPELMAN

In this paper, the relevant issues concerned with development of intercity travel demand models are examined, and a behavioral framework and model system for the set of complex and interrelated choices undertaken by travelers and potential travelers in the intercity travel market are developed. The desired properties of a data set for estimation of a disaggregate intercity travel demand model system are formulated, and existing intercity travel data sets are evaluated with respect to these properties. No existing data set satisfies all the requirements for estimation of a system of disaggregate intercity demand models. Nonetheless, it is useful to use the best available data to demonstrate the proposed behavioral framework and model structure. The 1977 National Travel Survey, supplemented with data on intercity level of service, is used to estimate models of intercity trip frequency and destination, mode, and air fare/service class choice. The estimation results support the proposed behavioral structure and the corresponding model structure. Deficiencies in the estimated models are attributed to the characteristics of the data set used in this study. Collection of data specifically for estimation of a system of disaggregate intercity travel models is needed to develop a model system that is behaviorally consistent and has a high degree of predictive accuracy.

Investment in intercity transportation services has received considerable attention in recent years. Examples in the United States include consideration of high-speed rail service in Southern California (*1*), in Florida (*2*,*3*), in Ohio (*4*), between Chicago and Milwaukee (*5*), and between Las Vegas and Los Angeles (*6*). Examples in Europe inclue the Channel Tunnel and expansion of the Très Grand Vitesse network in France. Accurate prediction of total intercity travel demand and its distribution among modes is an important component of the evaluation of these large capital investments.

Reviews of intercity passenger demand modeling studies undertaken during the last two decades (*7*–*9*) identify a number of important deficiencies in the models developed. Each of these reviews concludes that a new effort is needed to develop models that will provide accurate, policy-sensitive predictions of future intercity travel and that these models should be based on analysis of individual choice behavior.

Addressed in this paper are the methodological and practical issues associated with the development of a system of intercity travel demand models based on analysis of individual travel choices. Issues concerning the modeling approach, the theoretical basis of the model system, the model structure, and data needs are examined. The best available data are then used to estimate and evaluate the proposed approach.

The Transportation Center, Northwestern University, 1936 Sheridan Road, Evanston, Ill. 60208.

MODELING APPROACH

Previous modeling approaches can be grouped into two major classes. These are the aggregate and the disaggregate approaches. Models within each class have important similarities despite the many variations employed with respect to the modeling technique, the mathematical formulation, and the variables used.

Aggregate Approach

Early emphasis was on development of aggregate models, mostly in conjunction with the Northeast Corridor Transportation Project. Several different classes of aggregate models were developed. The aggregate models, which have been used most in intercity travel modeling, are sequential models. These models consist of two linked submodels that jointly predict intercity travel volume by mode. The first model predicts total intercity travel volume for the city pair as a function of the characteristics of each of the cities and composite measures of city pair level of service taking account of the attributes of all city pair travel modes. The second model predicts the share of total intercity travel volume assigned to each travel mode as a function of level of service by each of the available travel modes. An early sequential modeling aproach (*10*) has been used in a number of intercity corridor studies (*11*).

The variables used in the aggregate sequential models are averages or totals of the corresponding individual variables. The variables that have been used in different models include area descriptors such as population, employment, economic activity and cultural attraction indices, and intercity level of service measures such as travel time, travel cost, and frequency for each travel mode. The number of variables used in any one model is limited by the aggregate estimation approach because of sample size limitations and multicollinearity among area descriptors and among level of service variables.

Although no behavioral basis supported the development of these aggregate models, they were subjected to macroeconomic reasonableness criteria and provided useful insight into intercity travel behavior. The most important results of these studies are (a) the identification of city pair activity and attraction variables and city pair level-of-service variables as statistically related to travel volume, (b) the finding that segmentation by trip purpose (business and nonbusiness) and trip distance is important, (c) the recognition of the importance of trip generation and destination changes as well as corridor mode share changes, and (d) the recognition of the

need to include travel service measures for all modes to obtain satisfactory forecasts of single mode volume.

Despite these contributions of aggregate intercity analysis, there are a number of problems with this class of models. These include lack of behavioral basis, deficiencies of aggregate estimation methods (data aggregation leads to estimation bias and multicollinearity among variables), and unsuccessful functional form (the multiplicative form of the total demand model tends to magnify relatively small input errors into large prediction errors). These deficiencies lead to poor performance of the aggregate models, which in some cases overpredicted demand by as much as 50 percent (*9*).

Disaggregate Approach

Disaggregate models have been used extensively for both analyzing and forecasting urban passenger travel demand. The few attempts to apply the disaggregate modeling approach to the analysis of intercity travel demand have been limited by the characteristics of existing data sets (*12*). The most important advantage of disaggregate model estimation is that it overcomes estimation biases inherent in the use of aggregate estimation methods and incorporates a wide range of policy-sensitive variables. Thus, these models more accurately represent the behavioral response of travelers to changes in economic activities and to changes in fare and service characteristics.

The primary characteristic of disaggregate models is their use of data that describe each individual traveler or potential traveler, his or her characteristics and environment, and the attributes of service available to him or her. This approach provides improved estimation capabilities, as well as an increased ability to represent the terminal access and egress service characteristics for intercity trips.

The disaggregate models must be formulated consistently with an underlying behavioral structure; otherwise, the models will reflect only empirical relationships with limited usefulness. A proposed behavioral framework is discussed in the next section.

BEHAVIORAL FRAMEWORK

The development of a behavioral framework for intercity travel makes it possible to identify the proper structure of the models, identify the relevant variables to be used in the various models, develop policy-sensitive models, and prepare an appropriate data set. A framework, proposed earlier (*13*), describes an individual's intercity travel as derived from the individual's daily, weekly, and seasonal activity patterns, which are, in turn, based on the individual's demographic and life-style characteristics.

The individual's intercity travel and travel-related decision are classified into four decision categories: trip generation, destination choice, mode choice, and "at destination" decisions. Each of these categories includes several dimensions. Trip-generation decisions include the dimensions of trip frequency, purpose, time of the year, and party size. Destination choice includes the destination city, location within that city, and number of stops. Mode choice dimensions are mode selection for going and returning, carrier selection, and fare-type/service-class selection. The relevant decisions "at the destination" include the stay duration, lodging arrangement, and local transportation selection.

These decisions and dimensions are interrelated; models should be structured to reflect these links. Linkages among models make it possible to capture the effect of level-of-service changes on the total demand level (i.e., induced demand) by appropriate structure and specification of the model system.

Having established an appropriate model system, the calibration of the models requires a suitable data set. The attributes of a suitable data set are discussed in the following section.

INTERCITY TRAVEL DATA REQUIREMENTS

The information required to support disaggregate intercity travel demand modeling includes

- Individual survey data, such as demographic and location (residential and work) characteristics, intercity travel behavior of travelers over a defined period, and preference rankings or observed choices among a variety of real or artificial service alternatives;
- Urban area characteristics, such as size and activity measures for the origin area and potential destinations;
- Intercity travel volume information, including counts or other estimates of travel flows by mode and fare/service class; and
- Intercity travel service data including measures of service frequency or schedule delay, line haul and access/egress travel costs, line haul and access/egress travel times, and service quality.

None of the existing data sets includes all of the desired information. These data sets are in aggregate form with two exceptions: the 1977 National Personal Transportation Study (NPTS) (*14*) and the 1977 National Travel Survey (NTS) (*15*). These disaggregate data sets include trips of 75 mi and longer during a recall period of 14 days for the NPTS and 100 mi and 3 months for the NTS. There are three major deficiencies that limit the usefulness of these data sets:

- The lack of accurate information on the residence location of respondents makes it impossible to estimate access and egress time and cost for intercity trips.
- The absence of exact origin and destination city location in many cases limits the ability to develop representative destination choice models, as well as good mode choice models, because the level of service attributes cannot be determined accurately.
- The lack of information provided about the fare class used for common carrier trips limits both the ability to model fare class choice and the usefulness of the mode choice models, because travel cost and travel time restrictions cannot be defined.

Thus, it is necessary to collect new data to develop fully behavioral intercity travel models. The design of a data collection plan is a complex process. Two important issues concerning data collection are reviewed in this section.

First, it will be necessary to collect data at both the home

or work place and on board intercity travel modes. Home- or work-based data collection is needed to identify the frequency of intercity travel and the factors that influence that frequency. On-board data collection is necessary to obtain adequate representation of travel on infrequently used modes or travel classes.

Second, detailed level-of-service data are required for all travel modes and service classes including both line haul and access/egress service measures. These variables are especially important because they represent the policy measures that influence mode choice. The definition of intercity service variables is more complex than for urban travel because of the variety of modes and fare/service classes and the multiplicity of carriers for some modes. The required intercity data cannot be obtained from survey respondents for all of the travel service alternatives but must be provided from supplementary sources.

Despite the limitation on data availability, it is valuable to demonstrate and test the validity and usefulness of the proposed conceptual and model structure. The next sections describe the use of existing data to estimate intercity mode and fare/service class models.

Data Description

The 1977 NTS collected by the Bureau of the Census, supplemented with information from other sources, provides a resource to demonstrate and test the use of disaggregate techniques to develop behavioral intercity demand models. The NTS includes information on all trips of 100 mi or more during the 3-month period for randomly selected households in 34 metropolitan areas. Each record includes information about the trip made, the area of residence, the trip destination and characteristics of that destination, and characteristics of the trip such as purpose, timing, duration, and the means of transportation used. These data were supplemented by published level of service data for the available modes and fare classes including travel time, fare, and service frequency.

To control costs, the number of city pairs for which the level of service data were collected was limited to all city pairs with observed intercity trips with origins in one of the following seven cities: Atlanta, Baltimore, Boston, Buffalo, Chicago, Los Angeles, and Washington, D.C. The resultant data set contains intercity level-of-service information for 130 city pairs.

The data set developed is considered to be equivalent to a disaggregate data set for the purpose of developing a prototype model system. However, the level-of-service data describe city pair rather than true origin-to-destination data. Thus, it is not truly disaggregate. For this reason, the models estimated will be biased compared to a complete disaggregate model system. However, it is believed that this model system will be substantially better than any estimated exclusively with aggregate data. Thus, it is a step in the improvement of intercity travel demand models.

Model Structure and Formulation

An intercity disaggregate model is a system of interdependent submodels representing choice of trip frequency, trip destination, and travel mode and other related choices. This section describes the hierarchical structure and mathematical formulation of a specific proposed model.

Model Hierarchy

The choice structure depicted in Figure 1 describes a process in which the individual first decides whether to make an intercity trip and then how many trips to make during a given period. Next, for each intercity trip, the individual selects a destination. Then, the individual selects the transportation mode. Finally, the individual selects the fare/service class for modes with multiple classes.

Alternative model structures can be formulated to provide more detailed analysis of selected aspects of intercity travel. For example, the choice of intercity travel mode can be broken into a series of choices such as private automobile versus public carrier and a subsequent choice of a specific public carrier mode. Alternatively, the model can be simplified by, for example, combining trip frequency choice (zero or one trip in the study period) with destination choice in a single model.

The travel choices in the hierarchy are interrelated. Linkages among models are used to represent relationships among travel choices. First, each travel choice in the hierarchy is made conditional on all higher-level choices. For example, the choice of travel mode is made conditional on the selection of a specific destination city. This conditioning provides the basis for characterizing the service attributes of the mode alternatives under consideration. Second, the higher-level choice is influenced by the expected choices at lower levels

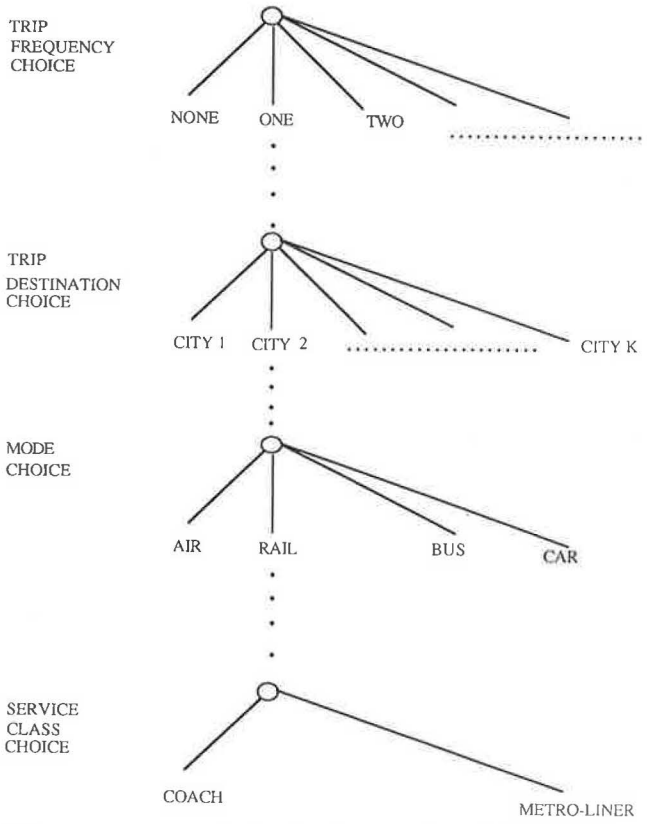

FIGURE 1 Proposed intercity disaggregate model system.

in the hierarchy. For example, the destination choice should reflect the travel service options to the destination city. However, because the mode that will be chosen is not known when the destination choice is made, the expected modal service is represented by a composite measure of the characteristics of all modes to each destination. A variety of composite measures can be formulated for this purpose (*16*). For example, the service characteristics of each mode could be weighted by the probability of being chosen. The composite service measure used in this analysis is based on specific properties of the nested logit model used in this study (*17,18*). This model is described next.

The intercity travel choice models reported in this paper are the choice of trip frequency, destination, mode, and, for air travel, fare/service class. The trip frequency is represented by a linear regression model that predicts the expected trip frequency for each traveler or potential traveler. The other choices are represented by logit models that predict the probability that each alternative in the choice set will be selected by the traveler. The logit model relates the probability of choosing an alternative, $Pr(i)$, positively to the observed utility of that alternative, V_i, and negatively to the utility of each other alternative, V_j (*19*).

The observed utility for each alternative is a function of the characteristics of the individual and the attributes of the alternative. The range of variables included can be extensive. For example, in a mode choice model, individual characteristics may include income, sex, and household automobile availability, and alternative attributes may include travel time, travel cost, and frequency of service offered by each mode. Generally, the utility function is formulated as a linear function of variables, but this is not required.

The multinomial logit model is capable of representing the choice process of an individual who is making a choice among several alternatives independent of any other choice. However, the choice process included in this study is multidimensional. That is, the individual is making choices from several choice sets (e.g., trip frequency, destination, mode, and fare class). These decisions are interrelated as discussed earlier. This interrelated choice structure can be represented by the nested multinomial logit model (*17*), which is a structured series of submodels with each submodel corresponding to one stage in the hierarchical choice process.

The formulation of the nested multinomial logit model includes a multinomial logit model at each level in the choice hierarchy. The models differ from independent multinomial logit models in two ways. First, each lower-level model is conditional on the results of the higher-level choice. Thus, the fare class choice model applies only if the air mode is chosen in the mode choice model. Second, the higher-level model includes a composite variable that represents the combined attributes of all the alternatives in the lower-level choice. Thus, the mode choice model includes a variable that represents the different fare classes for the air mode. The mathematical form of these models and the interrelationships between them are described by McFadden (*17*), Sobel (*18*), and Ben-Akiva and Lerman (*19*).

MODEL ESTIMATION RESULTS

The estimation results for intercity trip frequency, trip destination, travel mode, and fare/service class models are described in this section. The estimation of these models proceeds sequentially from the lowest- to highest-level model. The estimation results are reported and discussed in this estimation sequence.

Fare/Service Class Choice Model

The fare/service class choice model is estimated for the air mode only because the data do not provide information about a range of service classes for the other modes. Even for the air mode, the actual class chosen is not reported. However, the NTS data included information about the actual intercity travel cost. This cost was compared to fares by fare/service class to identify the chosen fare/service class.

Available fare/service classes were combined to obtain three alternatives: first, coach, and discount classes. A total of 235 trips were assigned to a fare class. This sample is too small to estimate separate fare class choice models for business and nonbusiness trips, so a single model is estimated with trip purpose included as a variable influencing choice of fare/service class.

The level of service variables included in the model are fare and daily number of departures (frequency) for each service class (not all flights included all service categories). Travel time is excluded because it is invariant over fare/service classes. The traveler's household income and trip purpose are included to account for expected differences in mode choice behavior among these groups.

The estimation results (Table 1) show that both fare and departure frequency significantly influence fare/service class choice. As expected, lower fares and increased frequency for any class increase the utility of that class.

Traveler's household income also significantly affects fare/service class choice. An increase in income leads to higher utility for first class and lower utility for discount class relative to coach class. This effect is highly significant between first class and coach class and less significant but strong between discount class and coach class.

Trip purpose is very significant in the choice between discount and coach class with business travelers being much less likely than nonbusiness travelers to take discount class. However, trip purpose has little effect on the choice between coach and first class. The probable reason for the low utility of

TABLE 1 THE FARE/SERVICE CLASS CHOICE MODEL

Variables	Parameter Estimate	(*t*-Statistic)
Alternative specific constants		
Discount class	−0.311	(0.6)
First class	−0.889	(1.2)
Level of service		
Fare cost ($)	−0.010	(2.7)
Daily departures	0.055	(4.1)
Income ($10,000)		
Discount class	−0.263	(1.3)
First class	0.350	(2.1)
Business trip		
Discount class	−1.605	(3.7)
First class	−0.160	(0.3)
Statistical Information		
Likelihood ratio index (ρ^2)	0.333	
Number of cases	235	

discount class to business travelers is the inability of business travelers to meet the restrictions associated with discount travel such as advanced reservation and minimum stay duration.

These estimation results demonstrate the feasibility of estimating a fare/service class choice model for intercity air travel. Good estimation results are obtained even with the small sample available for this purpose.

Mode Choice Models

The intercity travel modes considered in this study are car, air, rail, and bus. The intercity trips used in the mode choice analysis are round trips from home to one or more destinations and return home. Separate models are estimated for business and nonbusiness travel to account for the differences in these choice contexts.

All individuals in the sample were assumed to have all four modes available for each trip. All three common carrier modes were available for trips between all 130 city pairs included in the analysis. The data set did not include information about the car ownership of the household, and it was assumed that a car was available for all trips.

The variables considered for inclusion in this model and the rationale for their inclusion are as follows:

- Level of service variables (travel time, travel cost, and number of daily departures) represent the basic service characteristics for the alternatives.
- Composite utility of air fare/service classes reflects the combined attributes (cost and daily departures) of the three air fare/service classes (inclusion of this variable tests the effect of air fare/service class choice on mode choice). Composite utility of air classes is a monotonically increasing function of the utility of each fare/service class.
- Distance between city pairs reflects the empirically observed change in mode shares from bus, car, and rail to air as distance increases.
- Household income reflects a generally observed shift to higher-cost/higher-service alternatives with increasing income.

Collinearity problems between travel time and travel cost make it difficult to obtain significant estimates for both variables in these models. Estimation of models with only travel cost or travel time obtained significant estimates for these variables. Also, the estimation results for models with cost indicated that travel time for high-income travelers (more than \$20,000 per year in 1977) is valued much more highly than travel time for lower-income travelers. The problem of collinearity is resolved by constraining the ratios between travel time and travel cost parameters based on judgmentally selected values of time of \$60 and \$20/hr for high- and low-income business travelers, respectively, and \$45 and \$15/hr for high- and low-income nonbusiness travelers.

The estimation results are reported in Table 2 for both business and nonbusiness mode choice. The overall statistical fit is good for both models. The cost and time variables (estimated jointly) are highly significant. The bus/rail frequency variable has the correct sign and is marginally significant in the nonbusiness model. This variable could not be estimated satisfactorily in the business model because of the small number of business travelers who chose bus or rail in this data set.

The fare class composite utility variable has the correct sign, indicating that an improvement in service characteristics of any fare/service class will lead to an increase in air mode utility. This parameter is significant in the nonbusiness model

TABLE 2 MODE CHOICE MODEL FOR BUSINESS AND NONBUSINESS TRIPS PARAMETER ESTIMATE (*t*-STATISTIC)

Variables	Business Trips		Nonbusiness Trips	
Alternative constants				
Car	−0.883	(1.5)	1.687	(4.0)
Bus	−1.703	(2.2)	0.386	(0.6)
Rail	−2.227	(2.8)	0.136	(0.2)
Level of service				
Cost (\$)	−0.00460	(3.0)[a]	−0.00256	(3.8)[a]
Travel time (minutes) (high income)	−0.00460	(3.0)[a]	−0.00193	(3.8)[a]
Travel time (minutes) (low income)	−0.00153	(3.0)[a]	−0.00064	(3.8)[a]
Bus/rail frequency			0.0399	(1.9)
Composite air class utility	0.324	(1.5)	0.456	(4.0)
Income (\$10,000)				
Car	−0.0865	(0.4)	0.046	(0.3)
Bus and rail	0.354	(1.3)	−0.4910	(2.4)
Distance less than 250 mi				
Car	2.263	(4.3)	1.703	(3.8)
Bus and rail	1.994	(2.9)	0.857	(1.5)
Distance greater than 500 mi				
Car			1.796	(3.5)
Bus and rail			−0.816	(1.3)
Statistical Measures				
Likelihood ratio index (ρ^2)				
Equal shares base	0.623		0.465	
Number of cases	251		356	

[a]Cost and time parameters estimated jointly with value of time equal to \$60 and \$20/hr for high- and low-income business travelers, respectively, and \$45 and \$15/hr for high- and low-income nonbusiness travelers, respectively.

but not significant in the business trip model. It is likely that this variable would be significant in both models if the model were estimated with a larger sample. The inclusion of this variable is important because it provides a linkage with the fare/service class model.

The income variables are excluded from the business models because of poor estimation results. The effect of income in this model is through the use of income-segmented travel time parameters. The income variables in the nonbusiness model indicate little influence of income on car versus air choice but a strong negative effect on the use of bus and rail.

The distance variables indicate that the likelihood of choosing surface modes (car, bus, or rail) relative to air decreases substantially with increasing distances.

These results demonstrate the feasibility of estimating nested multinomial logit mode choice models with existing data and including the composite utility from the lower-level air mode fare/service class model.

The differences between the business and nonbusiness models reflect reasonable differences in the travel behavior for business and nonbusiness travel.

Destination Choice Models

Destination choice models for business and nonbusiness travel are estimated for a reduced set of destinations to place some limit on the requirements for gathering intercity travel service data. The data set used in this process consists of trips originating at one of seven locations, with the destination choice set including the chosen destination and four additional destinations selected randomly from the set of nonchosen destinations for which level of service data were collected. This sampling approach will produce consistent estimators for logit choice models under a wide variety of conditions (*17*).

The variables considered for the destination choice models are the city characteristics (e.g., population and recreation/cultural indices), the distance between the origin city and the destination, and the composite utility variable from the mode choice models. Further, in order to take some account of the variation in geographic destination attractiveness other than that included in the city characteristics, a set of alternative specific constants was formulated by grouping cities by geographic area.

Models were estimated for both business and nonbusiness trips because of the expectation that different city characteristics would be important for business and nonbusiness travel. Both models include the geographic destination constants, variables describing city characteristics, distance, and the composite mode utility variable from the respective mode choice model.

The destination models for business and nonbusiness trips (Table 3) show that the accessibility of the destination, represented by both the distance to the destination city and the composite mode utility variable, significantly affects destination choice. As expected, the higher the accessibility, the higher the probability that a destination will be selected. These two variables are collinear, which may explain the difference in estimation significance of the individual variables between the two models.

The attractiveness of the destination is reflected by population size and indices of museum (cultural) and other recreational resources. The larger the destination standard metropolitan statistical area, the higher the probability that this destination will be selected for business travel and the lower the probability for nonbusiness travel, all other things being equal. Taken together, the estimation results for these three variables support the conclusion that city size is an important determinant of destination choice for business travel, and other attraction indices are important for nonbusiness travel.

The geographic constants are positive and mostly significant for all areas relative to New York for business travel and

TABLE 3 DESTINATION CHOICE MODELS FOR BUSINESS AND NONBUSINESS TRIPS PARAMETER ESTIMATES (*t*-STATISTICS)

Variable	Business Trips		Nonbusiness Trips	
Regional Constants[a]				
Washington	2.040	(3.7)	−0.726	(1.4)
Northeast	1.046	(1.6)	−0.866	(1.7)
California	2.006	(3.3)	0.605	(1.4)
Southeast	2.835	(3.7)	0.081	(0.1)
Carolina & Virginia	2.867	(3.8)	−0.633	(1.1)
Midwest	1.145	(2.0)	−0.728	(1.6)
Ohio	1.936	(2.8)	−0.710	(1.3)
Texas, Arizona, Oklahoma	2.167	(2.7)	0.451	(0.7)
Denver and Omaha	2.128	(3.0)	−0.865	(1.4)
Florida	1.745	(2.0)	1.295	(2.2)
Pennsylvania	1.288	(2.0)	0.339	(0.7)
Las Vegas	2.800	(2.5)	−0.103	(0.1)
Northwest	1.776	(1.6)	1.062	(1.9)
Other Variables				
Distance (1,000 mi)	−0.988	(3.9)	−0.0717	(0.3)
Log of destination population in thousands	0.770	(2.5)	−0.2729	(1.3)
Museum index at destination	0.000143	(1.3)	0.000187	(2.3)
Recreation index at destination	0.000491	(0.9)	0.000660	(1.9)
Log sum of business mode choice	0.4233	(1.8)	0.5655	(5.4)
Statistical Measures				
Likelihood ratio index	0.256		0.313	
Number of cases	253		355	

[a]New York City is base alternative.

generally nonsignificant for nonbusiness travel with the exception of Florida and Las Vegas.

The most important result of these models with respect to the model structure put forth in this study is that the parameters for composite utility for the intercity travel modes are consistent with the proposed hierarchical structure.

Trip Generation Models

The trip generation models differ from the other models in two important ways. First, a linear regression approach is used because the formulation of a choice model for frequency choice is somewhat cumbersome. Second, the composite variable that would represent the service characteristics to destinations by the available modes is excluded because the sampling structure of the data will introduce bias in the estimation of the parameter for this variable.

Thus, the estimated trip generation models do not include any level of service measure but do include variables describing the household. These are household income, size, and structure and the age, occupation, and employment type for the head of household. Constants were tested to identify differences among origin (residence) cities. These constants, which represent the average effect of all the factors that influence the amount of intercity travel but which are not included in the model, were not significant. This suggests that the average rate of intercity trip making is not significantly affected by the variations in service among the residence cities (Atlanta, Baltimore, Boston, Buffalo, Chicago, Los Angeles, and Washington, D.C.) considered in this study.

The estimation results for business and nonbusiness trip generation (Table 4) identify household income as having a strong positive and almost equal effect on both business and nonbusiness travel. Other variables tend to be more important for either business or nonbusiness travel.

Business trip making, undertaken to serve the needs of the firm, is affected by occupation (professionals, managers, and sales people travel more than others) and type of organization (government employees and self-employed persons travel less than others).

Nonbusiness trip making, undertaken to serve the needs of the household and its members, is affected by individual and household characteristics. Interestingly, the occupation of the household head is a significant determinant of trip making, with households headed by professionals and managers making more nonbusiness trips than others.

The estimation results for the trip generation model show that intercity trip frequency is heavily influenced by the characteristics of the individual and the household. However, a large fraction of the variation in intercity trip frequency is not explained by these models. It is supposed that level of service differences are responsible for some of this variation.

Summary of Model Estimation Results

Overall, the model estimation results are consistent with the choice behavioral conceptualization proposed and the corresponding model structure. The hierarchical choice structure is supported by the estimation results for the composite variables in both the mode and destination choice models.

TABLE 4 TRIP GENERATION MODEL FOR INTERCITY TRIPS

Variable	Business Travel Parameter Estimate (t-statistic)	Non-Business Travel Parameter Estimate (t-statistic)
Household Income ($000)	0.054 (7.2)	0.067 (7.4)
Household Structure		
Non-married, no children		1.280 (3.7)
Non-married, children		0.426 (1.3)
Married, no children		0.653 (2.1)
Household Size Measures		
Number of Persons		0.590 (7.0)
Number of Children (5 to 18 years)		-0.351 (4.3)
Number of Babies (less than 5 years)		-0.743 (5.1)
Age of Household Head	-0.008 (1.6)	-0.024 (4.1)
Occupation of Household Head		
Professional	1.536 (6.2)	1.057 (4.0)
Manager	2.446 (8.7)	1.240 (4.0)
Salesman	2.518 (6.3)	
Employment Type of Household Head		
Self Employed	-0.530 (1.4)	
Government Employed	-0.714 (3.0)	
Constant	-0.079 (0.3)	0.868 (1.7)
Goodness of Fit Measures		
R^2	.130	.144
F	42.4	33.4
Sample Size	1998	1998

The importance of cost, travel time, and frequency of service in fare class and mode choice is supported by the significance of the corresponding parameters. The importance of specific demographic variables is also supported by the estimation results. Income influences class choice, mode choice for nonbusiness trips, and trip frequency. Other demographic characteristics affect overall trip making in reasonable ways. Finally, trip characteristics have an important impact on travel choices. Most important among these is trip purpose.

These estimation results are obtained despite the use of data that do not include precise origin and destination locations and thus exclude access travel times and costs, rely on travel service data obtained from published schedules rather than actual performance, and are based on a relatively small sample. It is concluded that implementation of this analysis approach with a true disaggregate sample is likely to produce results that are substantially better than those reported here.

SUMMARY AND CONCLUSION

Some of the issues associated with developing a behaviorally based disaggregate modeling approach for intercity travel are presented in this paper, and a hierarchical conceptual model for intercity travel choices is proposed. This approach can represent more accurately the decision-making process of the behavioral unit, which is the individual and his or her household.

A disaggregate type data base was developed from the 1977 NTS and used to estimate a hierarchically structured model of trip generation, destination choice, mode choice, and air fare/service class choice.

Overall, the estimation results support the conceptual structure and the corresponding model structure described in this paper. We conclude that the conceptual structure and the derived models reasonably represent the intercity travel demand relationships. Nonetheless, there are a number of deficiencies in the estimation results that can be attributed to the limitation of the data set used in this study. It appears that collection of data specifically for estimation of a system of disaggregate intercity travel models is likely to provide a basis for development of a model system that is behaviorally consistent and has a high degree of predictive accuracy.

ACKNOWLEDGMENT

The work reported in this paper was part of a research project entitled Intercity Passenger Travel Demand Analysis and Forecasting, supported in part by the FRA, U.S. Department of Transportation, through the University Research Program.

REFERENCES

1. *Bullet Train from Los Angeles to San Diego, Forecast of Ridership and Revenues.* Arthur D. Little, Inc., Cambridge, Mass., 1982.
2. Charles River Associates. *Preliminary Forecast of High Speed Rail Travel in the Miami–Orlando–Tampa Corridor.* Florida High Speed Rail Transportation Commission, 1988.
3. Peat Marwick Main & Co. *Florida TGV Project: Patronage Estimation.* Florida High Speed Rail Transportation Commission, March 1988.
4. Peak Marwick Main & Co. and F. S. Koppelman. *High Speed Rail Ridership Study: Final Report.* Ohio High Speed Rail Authority, 1989.
5. H. Baer, W. Testa, D. Vanderbrink, and B. Williams. *High Speed Rail in the Midwest.* Federal Reserve Bank of Chicago, 1984.
6. J. R. Hamburg and R. W. Keith. *Patronage Analysis and Forecast for Maglev Service—Las Vegas and Southern California.* 1988.
7. R. G. Rice, E. J. Miller, G. N. Steward, R. Ridout, and M. Brown. *Review and Development of Intercity Passenger Demand Models.* Research Report 77. University of Toronto Joint Program in Transportation, Toronto, Ontario, Canada, 1981.
8. F. S. Koppelman, G. K. Kuah, and M. Hirsh. *Review of Intercity Passenger Travel Demand Modelling: Mid-60s to the Mid-80s.* The Transportation Center, Northwestern University, Evanston, Ill., 1984.
9. M. E. Ben-Akiva and C. C. Whitmarsh. Review of U.S. Intercity Passenger Demand Forecasting Studies. Presented at the International Seminar on the Socioeconomic Aspects of High Speed Trains, Paris, 1984.
10. J. M. McLynn and T. Woronka. *Passenger Demand and Modal Split Models.* Arthur B. Young and Co., Dec. 1969.
11. J. S. Billheimer. Segmented, Multimodal, Intercity Passenger Demand Model. In *Highway Research Record 392*, HRB, National Research Council, Washington, D.C., 1972, pp. 47–57.
12. S. A. Morrison and C. Winston. An Econometric Analysis of the Demand for Intercity Passenger Transportation. *Research in Transportation Economics* (T. E. Keeler, ed.), JAL Press, Inc., 1985.
13. F. S. Koppelman and M. Hirsh. *Intercity Passenger Decision Making: Conceptual Structure and Data Implications.* The Transportation Center, Northwestern University, Evanston, Ill., 1985.
14. *1977 National Personal Transportation Study.* User Guide for Public Use Tapes. FHWA, U.S. Department of Transportation, 1980.
15. *National Travel Survey—Travel During 1977.* Bureau of the Census, U.S. Department of Commerce, Oct. 1979.
16. M. E. Ben-Akiva. *Structure of Passenger Travel Demand Models.* Ph.D. dissertation. Department of Civil Engineering, Massachusetts Institute of Technology, Cambridge, 1973.
17. D. McFadden. Modeling the Choice of Residential Location. In *Transportation Research Record 673*, TRB, National Research Council, Washington, D.C., 1978, pp. 72–78.
18. K. L. Sobel. Travel Demand Forecasting by Using the Nested Multinomial Logit Model. In *Transportation Research Record 775*, TRB, National Research Council, Washington, D.C., 1980, pp. 48–56.
19. M. E. Ben-Akiva and S. R. Lerman. *Discrete Choice Analysis: Theory and Application to Predict Travel Demand.* MIT Press, Cambridge, Mass., 1985.

Publication of this paper sponsored by Committee on Intercity Rail Passenger Systems.

Expert Support System for Modification of Railroad Car Service Rules

ROY I. PETERKOFSKY

The Association of American Railroads administers a series of policies called Car Service Rules. These rules govern the handling by one railroad of empty freight cars owned by another carrier. Among the Car Service Rules, the Special Car Orders indicate that cars of certain types will return to their owners through predetermined junctions ("outlets"). The selection of these outlets constitutes a difficult problem because it involves a tremendous amount of data and a great many discrete alternatives. These characteristics, plus many interacting factors and the conflicting objectives of equity and efficiency, preclude "optimization." Instead, the goal is to "satisfice"—to find satisfactory solutions. The Interactive Credit Balancing Machine (ICBM), a software "expert support system," provides an interactive environment for adjusting these outlets. It incorporates elements of artificial intelligence and operations research methods, but, most important, it puts a human expert directly into the decision process. ICBM automates the previous analytical approach, allowing Special Car Order outlet adjustments to be performed more quickly and in a more informed manner.

The Association of American Railroads (AAR) administers a series of policies called Car Service Rules. These rules govern the handling by one railroad of empty freight cars owned by another carrier. Among the Car Service Rules, the Special Car Orders indicate that cars of certain types will return to their owners through predetermined junctions ("outlets"). The Interactive Credit Balancing Machine (ICBM), a software "expert support system," provides an interactive environment for adjusting these outlets in minimal time, producing efficient, equitable results.

CAR SERVICE RULES

Among many other functions, the AAR administers Car Service Rules for the freight railroads of North America (*1*). Through the authority of the AAR Committee on Car Service, these rules govern the use of a railroad's equipment by other carriers.

Because no North American railroad serves the entire continent, a shipment may travel over the networks of many railroads to reach its destination. In fact, about 60 percent of U.S. rail traffic involves multiple carriers (*2*). For obvious reasons of efficiency, such shipments stay in their original cars—transloading would cause great delays (*3*). Thus, cars belonging to load-originating railroads end up in the hands of terminating carriers. Sometimes, a terminating carrier reloads such a car and sends it to yet another railroad. In the end, elements of every railroad's fleet often disperse across the continent.

As can be imagined, the railroads need to govern this process. Having invested in freight equipment, railroads want those cars back for loading. Originally, then, terminating (and en route) carriers had to return all empty cars to their owners over the reverse ("mirror image") of their loaded routes. This, however, often led to inefficiency. Sometimes, owners do not need their equipment back immediately—for instance, if they are allowed to load equipment owned by other railroads ("foreign cars"). By allowing such reloads, empty car mileage—a nonproductive expense—can be reduced (and car use improved) industrywide (*4*). The railroad industry needed detailed policies on foreign car return and reloading, guaranteeing car supply and also promoting efficiency. Such policies evolved into today's Car Service Rules.

The present set of Car Service Rules governs when railroads can reload other railroads' cars and how they should return the cars they do not reload. Different rules govern different types of cars. Some equipment, still, always travels "home" by the "reverse route" of its loaded movement. Newer concepts, however, control the movements of other car types. In general, these concepts aim to promote efficiency (minimize empty mileage) while maintaining equity (forcing no carrier to accept more than its share of empty mileage) and assuring car supply.

SPECIAL CAR ORDERS

The present array of Car Service Rules includes the Special Car Orders, such as SCO90 and SCO100. These car orders govern the movements of several equipment types, including most boxcars and plain gondolas. In their present form, the orders specify that, if a car's last loaded route included handling by its owner, the car should return home by reverse route. Otherwise (i.e., if reloaded by a terminating carrier), the car will return home through a network of predetermined outlets. An outlet indicates a junction where one railroad agrees to take on empty cars of a certain type and ownership from another railroad. The receiving railroad, generally, car-

Association of American Railroads, Research and Test Department, Freight Equipment Management Program, 50 F Street, N.W., Washington, D.C. 20001. Current affiliation: MIS-Operations Research, USAir, 2345 Crystal Drive, Arlington, Virginia 22227.

ries such a car to another railroad at another designated outlet. If its network connects to the car owner's, however, a receiving road can bring the car to the owner at any junction.

Obviously, the selection of the outlets determines which railroads will carry how much empty mileage under the Special Car Orders. Ideally, railroads would bear empty mileage in proportion to the corresponding amounts of loaded mileage (a reasonable proxy for revenue). Toward this goal, the AAR Transportation Division (TD) uses a performance measure called the obligation adjustment to evaluate the Special Car Orders and their outlet selections (*5*). Thanks to the industrywide TRAIN II information system, TD can trace all car movements and create a movement data base (*6*). On a quarterly basis, TD identifies from this data base all movements of cars operating under Special Car Orders in nonreverse route mode (i.e., after reloading—owner not in last loaded route). The TD calculates time and distance costs for these movements, both loaded and empty. Car hire rates—the costs of "renting" a foreign car—contribute to both time and distance costs; distance costs also reflect the expenses of transportation (fuel, labor, etc.). As a first step, the TD's calculations sum the loaded and empty costs for each railroad and for the entire industry. Basically, each railroad's fraction of the industry loaded cost is multiplied by the industry empty cost, producing the railroad's "fair share" of SCO90/100 empty costs. Roughly, subtracting from this figure the railroad's actual empty costs yields the obligation adjustment. A negative obligation adjustment, then, indicates a railroad carrying more empty costs than it should.

Needless to say, the participating railroads demand adjustments when major imbalances occur. To address these concerns, the TD updates the SCO90/100 outlet sets every quarter. In doing so, TD tries to move all obligation adjustments toward zero without creating extra empty mileage resulting from longer return routes. The TD closes outlets onto railroads with negative adjustment sums, replacing them with outlets onto railroads with positive adjustments. Until the present, unfortunately, TD personnel lacked good tools to support this task; they used only hand calculators and huge computer printouts of movement data. To generate potential changes of outlets, TD staff had to shuffle through tremendous amounts of paper and make many tedious calculations. Once generated, such options could only be analyzed to a limited extent: Which carrier would the empty traffic be moved onto initially? By how much would its empty costs increase? By how much would the former carrier's costs decrease? It became difficult to project an empty route further than the first few carriers, to keep track of the cumulative effects of multiple changes, and to balance best the inherent efficiency-equity trade-off. Also, of course, this effort demanded a tremendous amount of time from busy personnel, whose workload had increased because of a large new project. Therefore, the TD sought an automated tool that would allow it to perform its quarterly analyses and adjustments more quickly and in a more informed manner. This situation inspired the work described herein.

PREVIOUS STUDIES

In the past, studies have examined the mechanisms that control interline freight car movements in North America. These mechanisms include temporary directives, as well as the standing Car Service Rules. To the present, almost all work on the standing rules has taken a long-run, strategic outlook. Such studies have compared various broad configurations of Car Service Rules (e.g., Special Car Orders versus reverse route). Some of the studies have analyzed empirical evidence (*4*, *7–9*); others have used predictive modeling (*10*, *11*).

Until the present, little work has addressed short-term or tactical issues in Car Service Rules. One computer algorithm currently in use by AAR generates outlets for Special Car Orders. Based on shortest routes over a network, it essentially creates new orders for cars of a specific ownership. To our knowledge, no previous research has dealt with the modification or fine tuning of particular Car Service Rules in use. The first attempt at an interactive methodology to modify standing Car Service Rules based on past performance is discussed in this paper.

ICBM

ICBM is an "expert support system" that guides its user through the quarterly analysis of the SCO90/100 system. ICBM automates the process of searching through, sorting, and manipulating the SCO movement data. In this way, it effects great time savings in the generation of possible outlet changes. Furthermore, ICBM's simulation capabilities allow thorough evaluation of the impacts of SCO outlet changes—including all downstream and cumulative effects. ICBM is a flexible, completely menu-driven tool that presents its outputs as clearly summarized tables and graphics. As such, it can work interactively to support decisions, incorporating human expertise directly into the process. Also, it can work in decision making mode, applying a small "knowledge base" of encoded expertise, to prepare a starting solution for interactive fine tuning.

ICBM mimics the methodology used by the human "experts" in the TD. Unlike an "expert system," however, ICBM uses only a simplification of the expert logic. An expert system uses a detailed codification of the expert's "knowledge base"—always extremely difficult to assemble properly—and makes decisions automatically. ICBM, on the other hand, incorporates the human element directly into the decision process. Where an expert system tries to be the expert, the expert support system supports the expert. ICBM's simplified logic intelligently filters and summarizes data before presenting them to the user. At each step, the user makes the final decision, applying subtle elements of his or her knowledge and experience that a computer model could never fully embrace. If desired, the user can essentially put ICBM on "autopilot," letting it make decisions based only on the simple logic. Before making these results final, however, the user reviews and attempts to improve upon them. Either way, the computer does the great volume of the work—the simple, repetitive tasks—leaving the human free to concentrate on the finer points. The following sections of this paper explain the program's operation in greater detail.

POSSIBLE OUTLET CHANGES

Generation

TD personnel generate possible outlet changes largely according to a few basic rules. These rules provide a series of steps

to follow. First, the analyst identifies a railroad with a large negative obligation adjustment; he or she will work on making that value less negative. Then, the analyst finds an ownership ("mark") with cars that contribute heavily to the selected railroad's empty costs (i.e., those cars often travel empty over that railroad). Next, he or she identifies an outlet through which cars of the selected mark come onto the selected railroad—an outlet porting a large amount of empty costs onto that road. Finally, he or she considers the railroad delivering the cars through the outlet. The analyst selects an alternative outlet (junction and receiving railroad) at which that railroad might deliver the cars. Geographically, the new outlet should be relatively near the old one. A further outlet, drawing the car out of its way, may lengthen considerably the empty return route. The new receiving railroad, ideally, should have a positive obligation adjustment—or at least one more positive than that of the old receiving railroad. In other words, the new should not be bearing as much "unfair" empty mileage as the old. The "outlet change" generated consists of "closing" (deleting) the existing outlet picked in the third step and "opening" (adding) the new outlet from the last step. This will transfer empty costs from the old outlet's receiving railroad to the new receiving railroad.

At each of these steps, ICBM first ranks the alternative choices according to basic criteria. Then, the program presents the highest-ranked possibilities to the user with some supporting data. Figure 1, for example, shows a screen of hypothetical data, supporting selection of a railroad on which to work (the first step). Each railroad's abbreviation appears with its obligation adjustment value. Similar screens support later steps. The first screen leads to a screen listing car marks with the amounts of empty cost ("credit") they incur on the selected railroad (note that these positive amounts make the obligation adjustment more negative). Figure 2 shows such a screen. The third step consists of selecting an existing outlet. The corresponding screen displays such junctions with their delivering railroads and the amounts of credit they port onto the previously selected road (Figure 3 provides an example). Finally, a screen displays certain junctions of the delivering carrier of the selected outlet (Figure 4). Specifically, they are junctions close to the old outlet and where the delivering carrier connects to railroads having better (more positive) obligation adjustments than the old receiving carrier. ICBM shows these junctions as possible new outlets, with their corresponding receiving railroads and their obligation adjustment values. All of these screens show multiple alternatives preliminarily selected and ranked according to simple criteria; the user performs the final selection, using his or her expert knowledge of the decision's complexity.

```
RAILROADS WITH LARGEST NET CREDITS

   RAILROAD    OBLIGTN ADJT

     CR          -91720
     BM          -79479
     DH          -67066
     CNW         -12586
     CMNW         -4368
     DQE           -690

PLACE THE CURSOR ON THE RAILROAD YOU
WISH TO WORK ON AND HIT ENTER OR ...

     PF1 TO SEE MORE OF THE LIST
     PF2 TO GO BACK UP THE LIST
     PF3 TO RETURN TO MAIN MENU
```

FIGURE 1 Railroad selection screen.

```
CNW:  OBLIGATION ADJUSTMENT -12586

     CARMARKS CONTRIBUTING THE MOST
          TO CNW'S NET CREDIT

        MARK        CREDIT

        COP          3312
        NLG          2180
        NDM           647
        NSL           540
        NOPB          170

PLACE THE CURSOR ON THE MARK YOU WISH
   TO WORK ON AND HIT ENTER OR ...

 PF1 TO SEE MORE OF THE LIST
 PF2 TO GO BACK UP THE LIST
 PF3 TO RETURN TO CARRIER SELECTION
```

FIGURE 2 Ownership selection screen.

```
CNW:  OBLIGATION ADJUSTMENT -12586
3312 CREDIT DUE TO COP CARS

     OUTLETS BRINGING THE MOST CREDIT FOR
     EMPTY CARRIAGE OF COP CARS ONTO CNW

JUNCTION          DELIVERING RR   CREDIT

CHICAGO      IL       GTW          3068
GREEN BAY    WI       GBW           244

PLACE THE CURSOR ON THE OUTLET YOU
WISH TO WORK ON AND HIT ENTER OR ...

   PF1 TO SEE MORE OF THE LIST
   PF2 TO GO BACK UP THE LIST
   PF3 TO RETURN TO MARK SELECTION
```

FIGURE 3 Old outlet selection screen.

Some enhancements to the screen mechanism provide additional support to the decision process. For instance, the user can move up and down within the displayed lists of ranked alternatives. As an example, by paging down from the railroads with the most negative obligation adjustment values (Step 1), the user can eventually see those with the most positive values. This allows exploration into the realm of possibilities. Also, at every point in the generation process, the upper left corner of the screen displays the choices made in previous steps (see Figure 4, for example). Along with the choices appear corresponding values of appropriate quantitative indicators. Finally, rather than working in a strictly stepwise fashion, ICBM offers flexibility. The user, if so desiring, can quickly and easily flip forward and backward among

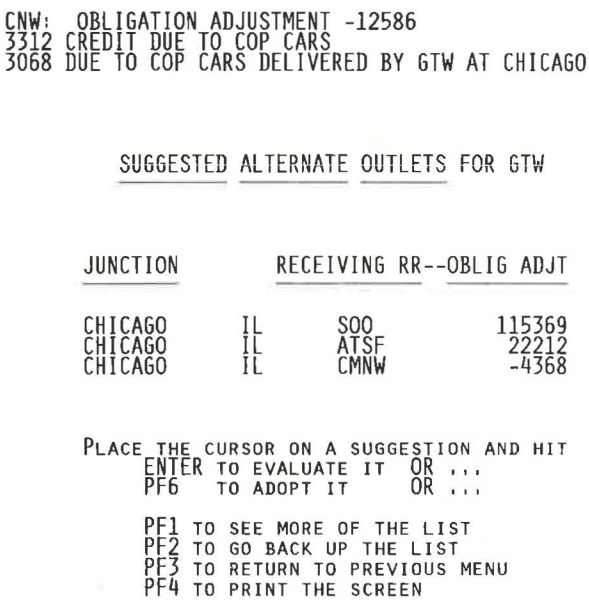

FIGURE 4 New outlet selection screen.

steps. Once again, this permits extensive exploratory analysis. All in all, ICBM's ranking and selection approach combines strong points from the analytical abilities of both computers and humans. The machine processes the bulk of the tedious, mechanistic work; it leaves the subtleties to the interacting human.

Evaluation

To evaluate a possible outlet change, ICBM identifies those movements with routings that the change would affect and simulates the routings. The program then presents the results—predicted impacts on empty mileage and obligation adjustment values—in several formats.

It is easy to determine which movements the closing of an outlet affects: those that pass through the outlet. To determine the movements affected by a new outlet's opening, though, requires a bit more effort. ICBM examines all movements of empty cars of the appropriate mark across the outlet's delivering railroad. For each such movement, the program compares the "impedances" (a network distance-based measure of transportation cost) from the movement's origin to both the new outlet and the movement's destination (*12*). If the minimum network impedance to the present destination exceeds that to the new outlet, we predict the movement's diversion to the outlet. Using this paradigm, ICBM assembles data base records for the movements that potential outlet changes will affect.

To determine the impacts of a change, ICBM "places" an empty car at the origin point of every affected movement. The program then simulates the empty return path of each such car, both with and without the changes. Initially, ICBM considers the railroad holding one of the cars placed at an origin point (the delivering carrier of the outlet being opened or closed). What options does the carrier have for the disposition of a car there? Where does it have outlets to other railroads for equipment of this type and mark? Generally, the program picks the option (outlet) to which the path from the origin point has the lowest impedance. Similarly, ICBM emulates the decision of the receiving carrier at that outlet: Where can that railroad move the car with the least impedance? This cyclic process continues until the car reaches a railroad with a network that connects directly to that of the car owner. Such railroads can deliver the car "home" at any junction with its owner. Each such junction, then, constitutes an option for the carrier. The simulation routes the car to the junction reachable with minimum impedance. That movement completes the car's simulated empty return.

After predicting these movements, ICBM estimates their costs. To determine time-based car hire charges, ICBM uses the actual average car hire rate for each group of cars (those at the same origin point); it finds these data in the movement data base. To obtain the full time cost, the program multiplies this rate by the number of cars and an estimate of the transit time for the route segment. To estimate the transit time for a route segment, the evaluation package will try three different approaches, in order. First, it will search through the movement data. It will look for actual movements between the segment's origin and destination, carried by the segment's railroad. If the program finds such a movement, it captures the actual average transit time for the movement. If this method fails, ICBM will estimate the segment's travel time from the network distance and the carrier's average empty speed (averaged over all its movements in the data base). Finally, if the carrier has no movements in the data base, the program uses the network distance and the average empty speed for all railroads (averaged over the entire movement data base) to estimate a transit time. For distance cost, ICBM simply takes the average mileage rate (distance-based car hire plus 28 cents/mi transportation cost) for the car group and multiplies it by the number of cars and the movement's network distance. Adding this to the time cost creates the estimated overall empty movement cost.

Once ICBM has predicted the effects of a change, displaying the results presents a formidable challenge. Because of the multiple decision criteria involved—minimizing each railroad's empty costs while maintaining equity among them all—clear, simultaneous communication of all impacts has the utmost importance. To balance properly the many trade-offs inherent in outlet selection, the user must apply the finest points of his or her expert knowledge; this requires that he or she absorb all of the available information. Toward this goal, ICBM provides simulation results in two different table formats, as well as in graphical form.

Figure 5 shows the format of the first table, giving details of "before" and "after" empty return routes—routes simulated, respectively, without and with the change. Each line of the table represents one carrier's segment of an empty route. The record gives the carrier's abbreviation, the locations where it began carrying the cars and where it handed them over to the next carrier, and the corresponding empty mileage and cost data. The program can also show the two empty routes in graphical form, traced out on a map of North America. This allows the analyst to recognize immediately if one route is significantly longer or more circuitous than the other. To complete its presentation of the results, ICBM offers a table summarizing cost and mileage effects by railroad, as well as overall (Figure 6). For each affected railroad, this

EMPTY ROUTES AFFECTED BY CHANGES

	RR	FROM		TO		CARMILES	CREDIT
BEFORE CHANGES	GTW	KALAMAZOO	MI	CHICAGO	IL	295	105
	CNW	CHICAGO	IL	DES MOINES	IA	837	294
	IAIS	DES MOINES	IA	COUNCIL BLUFIA		149	61
	UP	COUNCIL BLUFIA		PRINEVILLE	JOR	3543	1157
AFTER CHANGES	GTW	KALAMAZOO	MI	CHICAGO	IL	295	105
	SOO	CHICAGO	IL	ST PAUL	MN	876	319
	BN	ST PAUL	MN	PRINEVILLE	JOR	3569	1299

(#2 OF 4 ROUTES AFFECTED)
2 CARS

PF1 ADOPT CHANGES
PF2 SEE SUMMARY OF EFFECTS BY RR
PF3 RETURN TO OUTLET SELECTION MENU
PF4 PRINT SCREEN
PF7 SEE OTHER AFFECTED ROUTES

FIGURE 5 Route display table.

EFFECTS OF CHANGES ON SCO90 RAILROADS

RR	OBLIGATION ADJUSTMENT BEFORE	AFTER	CHANGE	(%)	CHANGE IN CARMILEAGE	CHANGE IN # CARS HANDLED
BN	11586	10187	-1394	(12%)	35692	8
CNW	-12586	-9942	2642	(21%)	-8374	-8
SOO	115369	109600	-5769	(5%)	876	8
UP	-440	717	1157	(263%)	-27337	-8

SYSTEMWIDE EMPTY CARMILEAGE CHANGE: -857 (INCL. NON-SCO90 RRS)
(52978 --> 52121) 643 (SCO90 RRS ONLY)

PF1 ADOPT CHANGES
PF2 RETURN TO ROUTE DISPLAY
PF3 RETURN TO OUTLET SELECTION MENU
PF4 PRINT SCREEN

FIGURE 6 Railroad summary table.

chart indicates the values of the obligation adjustment both before and after the change, along with the absolute and percentage changes in that value. In addition, the table indicates the change in empty car mileage for each railroad. Finally, the table shows the changes in empty car mileage summed over all railroads and over those roads participating in the Special Car Order system. These tables and graphics, it appears, provide an effective way to inform the user of the impacts of a potential outlet change. The analyst, then, can evaluate the utility of the change.

Acceptance or Rejection

After examining the simulation's estimates of cost and mileage impacts, the user can apply his or her expertise to decide whether to adopt a change. Designed for maximum flexibility, ICBM also allows the user to adopt interactively generated changes without evaluation or to enter changes directly for evaluation or adoption.

When the user chooses to adopt a change, ICBM updates the working table of outlets and recalculates the obligation adjustments of all affected railroads. In addition, the program modifies the entire movement data base to reflect the routing changes uncovered by the simulation. Furthermore, the package maintains quick-reference lists of all changes adopted and of all changes evaluated but rejected. These facilities, along with utilities for quick rejection of previously adopted changes and quick adoption of previously rejected changes, afford great flexibility. The user can easily move backward and forward among the different steps of generating alternatives, evaluating them and observing their effects both independently and in concert.

Having passed judgment on a change, the user returns to the first step of the alternative-generating phase. Presented with the updated obligation adjustments, he or she may deem the modified results satisfactory and terminate the session. Alternatively, he or she may choose to repeat the generation-evaluation-judgment process one or more times, until reaching a final, satisfactory solution.

AUTOSELECT MODULE

If the user desires, he or she can instruct ICBM to operate independently. The program will then generate, evaluate, and accept or reject outlet changes by itself, without human interaction. To do this, the software will apply the simple criteria used to rank alternative choices in interactive mode. Now, however, the program will select the highest-ranked option at each step, rather than merely suggesting it. Additional simple criteria (quantitative and qualitative) applied to the simulation results determine whether changes enter the working solution. As it rejects potential changes, ICBM works lexicographically down the lists of options, from the last step up. To start, it takes the first choice from each step. If it rejects the change thus generated, it next tries the first choice at each of the first three steps but the second choice at the fourth step. After exhausting choices at the fourth step, ICBM generates an alternative with the first choices from Steps 1 and 2, the second from Step 3, and the first from Step 4. This process continues until discovery of a change that qualifies for adoption. Then, with the obligation adjustments and movement data updated, the process continues at the next carrier-carmark combination (the next choice at Step 2). After cycling through all of the choices at all four steps, the program reorders the choices and starts over (with first choices at each step). This loop continues until one of three events occurs. If new obligation adjustments ever satisfy a simple criterion (they are all reasonably close to zero), we have a satisfactory solution and stop seeking improvement. If, however, a full cycle (all combinations of first through last choices at every step) passes without the generation of any acceptable changes, the heuristic terminates without "satisficing" (obtaining a satisfactory solution). Finally, the user can intervene to stop the process at any time.

Because of the incomplete nature of this heuristic method, its working solution is never accepted by the user as final. The user always reviews the changes made automatically and discards any he or she considers unacceptable. The analyst will apply the finer points of his or her expertise here, perhaps generating desirable changes that the machine missed. Although the AUTOSELECT module does not provide complete results, it usually gives a good starting solution. Again, the system will preprocess the bulk of the work but leave the difficult fine tuning to human intelligence. Through this approach, the AUTOSELECT module can save even more of the user's time than can the interactive module alone. Use of the AUTOSELECT module, however, requires that the user carefully examine the machine's decisions before finally adopting them.

CONCLUSIONS

The adjustment of the Special Car Order outlet sets constitutes a difficult problem. Based on a tremendous volume of data, the AAR TD must select from among a huge number of alternatives. Because of the poor structure and discrete nature of the set of alternatives, even generating options is difficult. The many interacting factors and conflicting objectives involved add to the difficulty. In spite of these obstacles, the ICBM produces good solutions to the problem, requiring a fraction of the time needed by the existing methodology.

ICBM's approach incorporates elements of artificial intelligence (expert systems) and operations research (network models and simulation). By making the human element an integral part of the decision process, however, ICBM gains significant advantages over the other two approaches. The development of a detailed "knowledge base" or mathematical utility function always requires extensive, timely consultation with the users—in this case, very busy ones. By eliminating this need, ICBM's approach allowed faster development of the package and made it more palatable to the TD. In addition to demanding much time, the development of detailed models of complex decisions invariably includes imperfections. These cost yet more time and trouble and decrease the likelihood of a system's acceptance by its users. ICBM's user-friendly methodology, directly involving the user as it does, obviously lends itself to understanding by the user. As such, it engenders the user's trust. This, together with the program's flexibility and its ability to let the user make the actual decisions, greatly eases the system's implementation.

Serendipitously, ICBM has yielded some unexpected gains. Through automation, the system eases user access and queries into the huge, once-forbidding movement data base and the outlet tables. In this manner, the system has made previously unknown problems obvious. For example, inefficient, circuitous routes become striking when seen on a map. Broadly, ICBM is getting TD users involved in the computational modeling effort that supports their operations. Previously, the TD had remained somewhat removed from this work. By bringing users in, ICBM will deepen the TD staff's understanding of the process. Thus, the benefits of increased net effectiveness will extend from ICBM to other related projects.

Although the ICBM methodology has many advantages, it also has its weaknesses. These, however, carry over mostly from the nonautomated techniques that served as its model. For instance, ICBM uses historical data as a forecast of the future; this quarter's adjustments address last quarter's problems. The system does not explicitly consider seasonal variations, random fluctuations, or the like. We hope, however, that the human element—the user's expert knowledge—considers such factors. Another weakness is that ICBM assumes no changes in loaded movements because of the outlet adjustments. In reality, outlet changes can affect railroad behavior, particularly the reload-or-return decision. Political factors and the difficulty of modeling this decision, however, necessitate the assumption. In general, any "irrationalities" of the user will carry through to the results of ICBM.

Despite these weaknesses, we can surely say that ICBM works better than the existing methodology. ICBM's weaknesses all appear in the nonautomated techniques as well. ICBM, at least, gets the job done much faster and allows the user to make decisions in a much more informed manner. Based on such improvements and its relatively easy development, this decision support system would appear successful.

The actual benefits of ICBM will be difficult to quantify. Most obviously, it will save a great deal of valuable TD staff time. Whereas the manual quarterly analysis of the SCO90/100 system usually takes about 2 person-weeks, ICBM should allow its completion in a few days. This order-of-magnitude reduction will save more than 1 person-month every year. Beyond this, ICBM's results will be indirect or without a yardstick for comparison. For example, better equity among participating railroads can increase their satisfaction with the Special Car Order system. If this contributes to the longevity of the system, it could mean a lot; just for boxcars, SCO90 saves 15 to 30 million empty car mi/year (*11*). This equates to between $5 and $10 million annually, industrywide. Because it brings better choices of outlets, ICBM can help the system save even more empty miles. Overall, ICBM might bring great and varied benefits. At the very least, by automating and clarifying the decision process, it will help the TD fulfill its mission more efficiently and effectively.

ACKNOWLEDGMENTS

Special thanks are due Rick Hobb of the AAR TD. He was instrumental in the development of ICBM and provided many comments on this paper. Peter French, Director of the AAR Freight Equipment Management Program (FEMP), also provided helpful commentary; so did four anonymous referees. Tori Schwartz of RAILINC Corporation put the movement data in the proper form, and Tom Warfield of the FEMP helped to bring it all together. Finally, many members of the FEMP staff, past and present, developed software routines that ended up directly or indirectly incorporated into ICBM. The author thanks them all.

REFERENCES

1. *Code of Car Service Rules/Code of Car Hire Rules.* Circular OT-10. Transportation Division, Association of American Railroads, Washington, D.C., April 1987.
2. J. H. Armstrong. *The Railroad—What It Is, What It Does.* Simmons-Boardman, Omaha, Nebr., 1982.
3. E. Coughlin. *Freight Car Distribution and Car Handling in the U.S.* Association of American Railroads, Washington, D.C., 1956.
4. *Freight Car Utilization Impacts of Railroad-Customer Relationships, Volume 2: Substituting Free Runners for Assigned Cars.* Report R-444. Freight Car Utilization Program, Association of American Railroads, Washington, D.C., Sept. 1980.
5. *Special Car Order 90.* Presented at a Seminar of the Association of American Railroads, Transportation Division, Washington, D.C., Sept. 1984.
6. *Tele-Rail Automated Information Network.* Transportation Division, Association of American Railroads, Washington, D.C., May 1985.
7. A. D. Dingle. *Freight Car Clearinghouse Experiment: Evaluation of the Expanded Clearinghouse.* Report R-293. Freight Car Utilization Program, Association of American Railroads, Washington, D.C., Jan. 1978.
8. *Analysis of Car Service Rules, Orders, and Directives: The Impact of Car Service Rules on Car Utilization.* Report R-369. Freight Car Utilization Program, Association of American Railroads, Washington, D.C., May 1979.

9. *Proposal for Change in the Railroad Industry-Wide Car Management System.* Report R-379. Freight Car Utilization Program, Association of American Railroads, Washington, D.C., June 1979.
10. *The Extent that Car Service Rules Restrict Freight Car Utilization.* ADD Systems, Burlingame, Calif., May 1972.
11. *Research Report 1984–1985.* Association of American Railroads, Washington, D.C., 1986.
12. A. L. Kornhauser. *Development of an Interactive Graphics Computer Model for the Nationwide Assignment of Railroad Traffic.* Final Report. FRA, U.S. Department of Transportation, Washington, D.C., 1977.

Publication of this paper sponsored by Committee on Railroad Operations Management.

Detailed Inspection of U.S. Army Railroad Trackage and Application to Civilian Short-Line Railroads

DAVID G. BROWN, DONALD R. UZARSKI, AND RICHARD W. HARRIS

The U.S. Army Construction Engineering Research Laboratory has developed a railroad track maintenance management decision support system called RAILER. The detailed track inspection procedures are designed to implement the recently issued Army Track Standards in a manner consistent with the larger goals of RAILER, thus promoting both track safety and track maintenance management. The inspection procedures are divided into six track component areas, and field inspection forms have been developed that guide the inspector through the inspection of each component area. The inspection procedures include measures for dealing with track components that are hidden, such as by vegetation or road crossings. In addition to the Army Track Standards, the inspection procedures can also support other track standards such as those propagated by the FRA or designed by a private operator. This property serves to facilitate a transfer to the civilian sector. The inspection procedures also take advantage of the RAILER computer software to ease the overall burden of the inspector.

RAILER is a decision support system for track maintenance management developed at the U.S. Army Construction Engineering Research Laboratory (USA-CERL) (*1*, *2*). It is currently being implemented at selected Army installations. Although primarily designed for Army use, RAILER was constructed to also facilitate technology transfer to the civilian sector for use by the commercial railroad community, especially short lines and industrial networks.

As a decision support tool, RAILER can be used, in part, to develop annual and long-range work plans, develop budgets, determine condition levels, and estimate maintenance and repair costs. RAILER uses personal computer-based software developed at USA-CERL to accomplish these tasks. The data base includes several information types, the most important of which are inventory and inspection. The inventory data elements are discussed in a paper by Uzarski et al. (*3*). The RAILER detailed inspection procedures are discussed here; a complete description of these procedures is presented in a USA-CERL technical report (*4*).

BACKGROUND

Commercial railroads are governed by the safety inspection requirements of the FRA (*5*). Individual railroad companies may also have their own inspection procedures for locating defects for maintenance planning. However, U.S. Army track networks do not fall under the auspices of the FRA, nor do Army track inspectors. Because of their varied duties and responsibilities, these Army track inspectors also do not have the same intimate knowledge of their networks as do track section foremen, track inspectors, and road masters in the commercial sector. Until recently, the Army's approach to track safety and track maintenance management was not very structured. Army track was divided into just two components for maintenance management—ties and trackage—and track inspection procedures were only generally described (*6*). Also, inspection intervals tended to be infrequent.

To facilitate efficient maintenance management of Army track and safe railroad operations, the Army has developed RAILER and issued detailed track maintenance standards (*7*). The standards serve the dual function of ensuring safety and identifying maintenance needs. The safety aspects are covered through the inspection frequency and the imposing of operating restrictions associated with certain defects. These operating restrictions are 10 mph, 5 mph, and "No Operations." Maintenance needs are determined through specific defect identification. Accordingly, the track standards provide a fundamental basis for track inspection and evaluation.

Many of the decision support tasks that RAILER is designed to perform require an assessment of track conditions, current and future. These conditions are determined by inspection with respect to the new Army Track Standards. While these standards are quite precise, they do not delineate specific inspection procedures. Such procedures were developed for RAILER. The inspection procedures outlined in this paper expand on and modify the previously documented interim detailed inspection procedures (*1*, *2*).

INSPECTION PROCEDURE CHARACTERISTICS

The RAILER detailed inspection procedures were developed primarily to fulfill two interrelated tasks. The first is to promote safe Army railroad operations by incorporating the technical aspects of the U.S. Army Track Standards into practical procedures. Second, the procedures provide a means for capturing the defect information in a format that facilitates

U.S. Army Construction Engineering Research Laboratory, P.O. Box 4005, Champaign, Ill. 61824.

use within the RAILER system for track maintenance management. The inspection procedures have the following characteristics:

- The inspection procedures are divided into component areas consistent with the Army Track Standards and the RAILER inventory data elements (*8*).
- Thorough detailed field inspection forms are used to guide the inspector through the inspection of each component area.
- Procedures are included for dealing with track components that are hidden, such as by vegetation or road crossings.
- Although the inspection procedures are designed to capture all discrepancies with the Army Track Standards, the procedures are at the same time flexible and thorough enough to support other track standards (such as those propagated by the FRA).
- The inspection procedures take advantage of the RAILER computer software to ease the burden of the inspector.

These interrelated characteristics are discussed more fully in the following subsections.

Inspection Component Areas

For convenience, the inspection procedures are divided into six track component areas:

1. Tie inspection;
2. Vegetation inspection;
3. Rail and joint inspection;
4. Other track components inspection;
5. Turnout inspection; and
6. Track geometry inspection.

The components included in "Other track components" are the bridge approach, ballast/subgrade, car bumper, car stop, culvert, ditch, derail, drain, embankment, grade crossing, gage rod, hold down device, insulated component, rail anchor, rail crossing, signals, signs, shim, spike, storm sewer, and tie plate.

The inspection procedures primarily consist of specific visual observations and manual measurements of the track structure, which may be augmented by automated data collection for track geometry and for rail and joint defects. A complete regular manual inspection would include the first five component areas; manual track geometry inspection is usually conducted only when there are specific indications of potential problems. (Examples of these indications include visual observations and reports of rough riding from the engine crew.)

The segmentation of the inspection process by component areas permits significant flexibility. For example, a track may be inspected for only one or two components, or all components, depending on the purpose of the inspection. This flexibility also allows the order in which component areas and track segments are inspected to be tailored for the particular network layout. Such an inspection plan is illustrated in Figure 1. For example, with a single isolated loading track, it may be advantageous to inspect some components in one direction and other components while walking back. However, with two parallel loading tracks, it may be better to inspect some or all components of one track in one direction and the same components of the other track while walking back.

Field Inspection Forms

The inspection process is organized around five field inspection forms. One of these forms deals with three component areas: ties, vegetation, and rail and joints. A completed example of this form is presented in Figure 2. An explanation of various categories in this figure is given as follows:

- In the column for Inspection Impaired by Vegetation or Other Material, the inspector has entered four lengths of track where tie inspection was impaired. The lengths were 10, 30, 70, and 25 ft, respectively. Addition (+) signs are used to separate the lengths. The lengths are then totaled below (135 ft).
- The various tie defects are delineated in the columns. Hash marks are used to note defects and then totaled.

Vegetation Inspection

Vegetation growth is noted in feet of affected track. Results of the vegetation inspection were as follows:

- There were four occurrences of low severity (Growing in Ballast, Interferes with Walking, etc.) vegetation growth. The occurrences were 10, 50, 20, and 200 ft in length, for a total of 280 ft.
- A 50-ft length of vegetation growth prevented track inspection.
- No vegetation growth serious enough to interfere with train movements was found.

Rail and Joint Inspection

Rail and joint inspection found the following defects:

- All bolts were loose (ABL) in a joint in the left rail at Station 1+00.
- The end batter (ENB) at joints was greater than ¼ in. in both rails starting at Station 1+00 and continuing over 10 joints.
- There was a broken or cracked joint bar (BCB) in the right rail at Station 2+20.
- Some joints had improper bolt pattern (IBP). Starting at Station 2+50 and continuing for 200 ft, about 50 percent of the joints had the improper pattern.
- Several lengths of inspection impairment were noted. Inspection was impaired for one quarter (one side of one rail) for an 8-ft length. For two-, three-, and four-quarters coverage, the lengths of impairment were 6, 8, and 4 ft, respectively. The line totals are then multiplied by the quarters of coverage to get the quarter lengths (Q.L.). The quarter lengths are then summed and divided by 4, which gives the equivalent length of complete inspection impairment.

These forms are designed to guide the inspector through a structured inspection process. This is especially well illustrated by the turnout inspection form (see Figure 3). Mastering the inspection procedure associated with using this form requires a minimal amount of training, despite the large amount of information that is collected. In this case, the four blocks

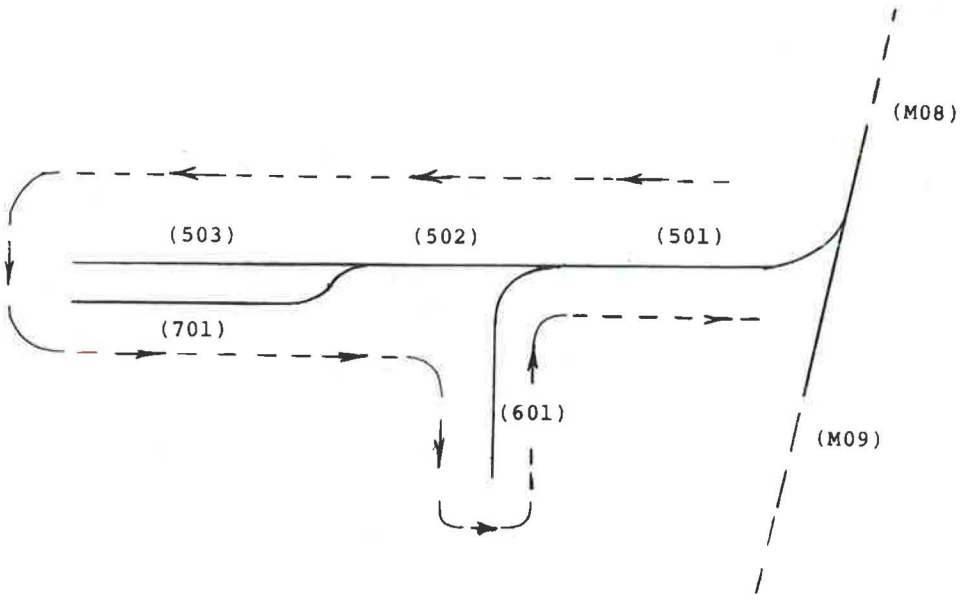

Inspection Plan for Tracks 5, 6, and 7

Segment	Component Areas
501	Ties and Other Track Components
502	Ties and Other Track Components
503	All Components
701	All Components
502	Vegetation and Rail and Joints
601	Ties and Other Track Components
601	Vegetation and Rail and Joints
501	Vegetation and Rail and Joints

FIGURE 1 Example of inspection plan.

on the form lead the inspector through the inspection; the inspector simply has to fill in the various blanks and circle the appropriate responses.

The other inspection forms are presented in an abbreviated fashion in Figures 4 through 6. The form depicted in Figure 4 can be used to continue the visual rail and joint inspection (see Figure 2) or for automated rail inspection. Because many rail defects are not visible (and hence can only be detected with specialized equipment), the continuation form depicted in Figure 4 lists more rail and joint defects than the form depicted in Figure 2. When used with automated rail inspection, the continuation form serves as a data transfer medium between the commercially prepared report (list of defects) and RAILER.

The track geometry inspection form (see Figure 5) is generally only used for manual inspection. Automatically collected track geometry data can be transferred directly from the geometry test equipment onto floppy disks for processing within the RAILER system. An explanation of segments of Figure 5 is given as follows.

- In Segment 101, Station 5+50, the gage is 57.8 in.
- In Segment 101, Station 7+00, the crosslevel is +1.5 in. (using the left rail as reference), the alignment is 0.5 in. in both the left and right rails, the profile of the left rail is 1.1 in., and the profile of the right rail is 0.5 in.
- In Segment 101, Station 7+05, the crosslevel is +0.5 in. (using the left rail as reference).
- In Segment 102, Station 9+00, the alignment of the left rail is 1.1 in., and the profile of the left rail is 1.5 in.
- In Segment 102, Station 10+50 (in Curve 1C1), the gage is 56.7 in., the crosslevel is +2.0 in. (using the left rail as the reference), the left alignment is 4.0 in., and the right alignment is 4.0 in.

Impaired Track Inspection

Sometimes grade crossings or material, such as excessive ballast and vegetation, will interfere with track inspection. This can be a particular problem where seldom used tracks may

TRACK SEGMENT #: M01 | SEGMENT BEGINNING LOCATION: 0+89 | INSPECTOR: SKW | DATE: 10-1-88

TIE DEFECTS

CHECK IF DEFECT FREE	INSPECTION IMPAIRED BY VEGETATION OR OTHER MATERIAL	NUMBER OF DEFECTIVE OR MISSING TIES	CONSECUTIVE DEFECTIVE OR MISSING TIES 2	3	4	5	ALL JOINT TIES DEFECTIVE OR MISSING	IMPROPERLY POSITIONED (skewed, rotated, bunched)	TIE CENTER-TO-CENTER DISTANCE ALONG EITHER RAIL > 48"
☐	LENGTH(TF): 10+30+70+25	////// ////// ////// ////// //	///	/	//		//	////	
	TOTAL(TF): 135								
TOTAL	%:	#: 22	#: 3	#: 1	#: 2	#: 0	#: 2	#: 4	#: 0
COMMENTS:									

VEGETATION

CHECK IF DEFECT FREE	GROWING IN BALLAST, INTERFERES WITH WALKING, BRUSHES SIDES OF ROLLING STOCK, FIRE HAZARD, INHIBITS SIGN VISIBILITY	PREVENTS TRACK INSPECTION	INTERFERES WITH MOVEMENT OF TRAINS OR TRACK VEHICLES	COMMENTS:
☐	LENGTH(TF): 10+50+20+200	LENGTH(TF): 50	LENGTH(TF): 0	
	TOTAL(TF): 280	TOTAL(TF): 50	TOTAL(TF): 0	
	%:	%:	%:	

RAIL and JOINT DEFECTS

DEFECT CODE(s)	RAIL (lt, rt both)	LOCATION (station)	LENGTH (TF)	DENSITY (%)	QTY (#)	COMMENTS
ABL	(L) R B	1+00				
ENB	L R (B)	1+00			10	
BCB	L (R) B	2+20				
IBP	L R (B)	2+50	200	50		
	L R B					
	L R B					
	L R B					
	L R B					
	L R B					
	L R B					
	L R B					
	L R B					

RAIL DEFECT CODES
- BHC = BOLT HOLE CRACK
- BRC = BREAK - COMPLETE
- BRB = BROKEN BASE
- CDH = CHIP / DENT IN HEAD
- CRB = CORRODED BASE
- COR = CORRUGATION
- CRH = CRUSHED HEAD
- ENB = END BATTER > 1/4"
- EGB = ENGINE BURN
- FLK = FLAKING
- FDL = FRACTURE - DETAIL - LARGE
- FDS = FRACTURE - DETAIL - SMALL
- FEL = FRACTURE - ENGINE BURN - LARGE
- FES = FRACTURE - ENGINE BURN - SMALL
- HWS = HEAD / WEB SEPARATION
- OVF = OVERFLOW
- L13 = RAIL LENGTH < 13'
- RSD = RUNNING SURFACE DAMAGE
- SHL = SHELLING
- SHH = SPLIT HEAD - HORIZONTAL
- SHV = SPLIT HEAD - VERTICAL
- SWB = SPLIT WEB
- TCE = TORCH CUT END
- TCH = TORCH CUT HOLE
- WRS = WEAR - SIDE
- WRV = WEAR - VERTICAL
- WDD = WELD DEFECT

CHECK IF DEFECT FREE	1/4's	INSPECTION IMPAIRED BY VEGETATION OR OTHER MATERIAL (LF)	LINE TOTAL (LF)	Q.L. (LF)	SUM of QL (LF):
☐	1	8	8	8	60
	2	6	6	12	TOTAL= SUM QL/4 (TF):
	3	4+4	8	24	15
	4	4	4	16	%:

JOINT DEFECT CODES
- ABL = ALL BOLTS IN JOINT LOOSE
- ABM = ALL BOLTS ON A RAIL END MISSING OR BROKEN
- BBB = BOTH BARS BROKEN (breaks at any location)
- BCC = BOTH BARS CENTER CRACKED
- BCB = BROKEN OR CRACKED BAR (not through center)
- CCB = CENTER CRACKED, CENTER BROKEN OR MISSING BAR
- IBP = IMPROPER BOLT PATTERN
- IBT = IMPROPER SIZE/TYPE BOLT
- ISB = IMPROPER SIZE / TYPE BAR
- LJB = LOOSE JOINT BAR(s)
- LBT = LOOSE JOINT BOLT(s)
- MBT = MISSING/BENT/CRACKED OR BROKEN BOLT(s)
- 1BT = ONLY 1 BOLT PER RAIL END
- RG1 = RAIL END GAP >1" BUT < 2"
- RG2 = RAIL END GAP > 2"
- RM1 = RAIL END MISMATCH > 3/16" BUT < 1/4"
- RM2 = RAIL END MISMATCH > 1/4"
- TCB = TORCH CUT JOINT BAR

FIGURE 2 Completed inspection form for ties, vegetation, and rail and joints.

TRACK SEGMENT #: M01	TURNOUT ID #: 1TP	INSPECTOR: RHI	DATE: 10-1-88

GENERAL			TIES	
Line and Surface	Good (Fair) Poor		Number of Defective or Missing Ties	4
Switch Difficult to Operate	(N) Y		Maximum # of Consecutive Defective or Missing Ties	2
Crib Areas Dirty or Fouled	(N) Y		# of Occurences where Joint Ties are Defective or Missing	0
Less Than FOUR Functional Rail Braces on EACH Stock Rail	(N) Y		# of Improperly Positioned Ties (skewed, rotated, bunched)	0
Flangeways Dirty or Fouled	(N) Y		# of Occurences where Tie Center to Center Spacing on Either Rail > 48"	0

	COMPONENT	DEFECT FREE	IMPROPER SIZE/ TYPE/POSITION	LOOSE	CHIPPED/WORN/BENT/ CRACKED/BROKEN	MISSING
SWITCH & STAND	Rail Braces (Chairs)	Y		2		4
	Switch Points	Y			1	
	Point Rails	(Y)				
	Switch Stand	Y	Y	(Y)	Y	Y
	Target	(Y)	Y	Y	Y	Y
	Point Locks/Lever Latches	(Y)				
	Connecting Rod	(Y)	Y	Y	Y	Y
	Switch Rods	(Y)				
	Switch Clips	Y		2		
	Bolts	Y		3		
	Cotter Keys	(Y)				
	Slide Plates	(Y)				
	Heel Fillers	(Y)				
	Heel Joint Bars	(Y)				
	Heel Joint Bolts	Y				4
FROG	General	(Y)	Y	Y	Y	Y
	Point & Top Surface	Y			(Y)	
	Bolts	(Y)				
GUARDRAILS	Guard Rails	(Y)				
	Fillers	(Y)				
	Bolts	Y		7		5

MEASUREMENTS (in)

	COMPONENT	LEFT	RIGHT
POINTS & JOINTS	Switch Point Gap	0.2	0.0
	Gauge at Switch Points	56.5	
	Gauge at Joints in Curved Closure Rail	1st: 56.625 2nd:	

COMMENTS: SOME TIES COVERED WITH BALLAST

	COMPONENT	STRAIGHT SIDE	TURNOUT SIDE
FROG & GUARDRAILS	Gauge at Point	56.5	56.5
	Guard Check Gauge	54.625	54.625
	Guard Face Gauge	52.875	52.875
	Frog Flangeway Width	1.75	1.75
	Frog Flangeway Depth	1.75	1.5
	Guardrail Flangeway Width	1.875	1.875

FIGURE 3 Completed turnout inspection form.

CHECK IF RAIL AND JOINT CONTINUATION: ✓ | INSPECTOR: R H II | DATE: 10-1-88

RAIL and JOINT DEFECTS

DEFECT CODE(s)	RAIL (lt, rt both)	LOCATION (station)	LENGTH (TF)	DENSITY (%)	QTY (#)	COMMENTS
BRB	① R B	M03	16+00			
SHL	L R ⑧	M03	16+00		3	
BHC	L ⑧ B	M03	17+20			
	L R B					
	L R B					
	L R B					
	L R B					
	L R B					
	L R B					
	L R B					
	L R B					
	L R B					
	L R B					
	L R B					
	L R B					
	L R B					
	L R B					
	L R B					
	L R B					
	L R B					
	L R B					
	L R B					
	L R B					
	L R B					

RAIL DEFECT CODES

000 = DEFECT FREE
BHC = BOLT HOLE CRACK
BRC = BREAK - COMPLETE
BRB = BROKEN BASE
CDH = CHIP / DENT IN HEAD
CRB = CORRODED BASE
COR = CORRUGATION
CRH = CRUSHED HEAD
ENB = END BATTER > 1/4"
EGB = ENGINE BURN
FCM = FISSURE - COMPOUND
FTL = FISSURE - TRANSVERSE - LARGE
FTS = FISSURE - TRANSVERSE - SMALL
FLK = FLAKING
FDL = FRACTURE - DETAIL - LARGE
FDS = FRACTURE - DETAIL - SMALL
FEL = FRACTURE - ENGINE BURN - LARGE
FES = FRACTURE - ENGINE BURN - SMALL
HWS = HEAD / WEB SEPARATION
OVF = OVERFLOW
L13 = RAIL LENGTH < 13'
PPR = PIPED RAIL
RSD = RUNNING SURFACE DAMAGE
SHL = SHELLING
SHH = SPLIT HEAD - HORIZONTAL
SHV = SPLIT HEAD - VERTICAL
SWB = SPLIT WEB
TCE = TORCH CUT END
TCH = TORCH CUT HOLE
WRS = WEAR - SIDE
WRV = WEAR - VERTICAL
WDD = WELD DEFECT

JOINT DEFECT CODES

ABL = ALL BOLTS IN JOINT LOOSE
ABM = ALL BOLTS ON A RAIL END MISSING OR BROKEN
BBB = BOTH BARS BROKEN (breaks at any location)
BCC = BOTH BARS CENTER CRACKED
BCB = BROKEN OR CRACKED BAR (not through center)
CCB = CENTER CRACKED, CENTER BROKEN OR MISSING BAR
IBP = IMPROPER BOLT PATTERN
IBT = IMPROPER SIZE/TYPE BOLT
ISB = IMPROPER SIZE / TYPE BAR
LJB = LOOSE JOINT BAR(s)
LBT = LOOSE JOINT BOLT(s)
MBT = MISSING/BENT/CRACKED OR BROKEN BOLT(s)
1BT = ONLY 1 BOLT PER RAIL END
RG1 = RAIL END GAP >1" BUT < 2"
RG2 = RAIL END GAP > 2"
RM1 = RAIL END MISMATCH > 3/16" BUT < 1/4"
RM2 = RAIL END MISMATCH > 1/4"
TCB = TORCH CUT JOINT BAR

FIGURE 4 Completed rail and joint inspection continuation form.

be hidden by vegetation or other material and where significant track lengths may be paved (such as around warehouses and marshalling areas). If not properly accounted for, significant amounts of inspection-impaired track could cause profound overestimation of general track quality and consequent underestimation of necessary repair materials. This occurs when it is implicitly and erroneously assumed that defects not seen (and hence not recorded) do not exist. Furthermore, even a few linear feet of foreign material may hide serious defects affecting the safety of railroad operations.

Inspection-impaired track is accounted for separately within the RAILER detailed track inspection procedures for each of three component areas: ties, rail and joints, and other track components. These are separated for two reasons. First, foreign material that obscures one component might not impair the inspection of another component. For example, rail and joints can often be easily inspected when the ties are covered by ballast or soil. Second, the nature and extent of obscuring foreign material may change between the inspection of two component areas. For example, during the time between a tie inspection and an "other track components" inspection (which may be more than a month), gravel may have been accidentally spilled on the track, obscuring tie plates and spikes ("other track components").

INSPECTOR(s): RH II — DATE: 10-1-88

TRACK SEGMENT NUMBER	LOCATION (station)	CURVE ID NUMBER	GAGE (in)	REFERENCE RAIL (lt,rt)	CROSS LEVEL (in)	ALIGNMENT(in) LEFT	ALIGNMENT(in) RIGHT	PROFILE(in) LEFT	PROFILE(in) RIGHT	COMMENTS
101	5+50		57.8	L R						
101	7+00			(L) R	1.5	0.5	0.5	1.1	0.5	
				L R						
102	9+00			L R		1.1		1.5		
102	10+50	1C1		(L) R	2.0	4.0	4.0			
				L R						
				L R						
				L R						
				L R						

FIGURE 5 Completed track geometry inspection form.

COMPONENT CODE	DEFECT CODE	LOCATION (station)	LENGTH (TF)	DENSITY (%)	QTY (#)	IMMEDIATE HAZARD
BS	BAD	0+00	100			(N) Y
CU	OBF	0+50				(N) Y
GR	LOS	0+90				(N) Y
SP	IMP	1+40	200	50		(N) Y
SP	MIS	1+50				(N) Y
EM	ERO	2+10	20			(N) Y
CU	STD	2+50				N (Y)

CHECK IF DEFECT FREE ☐

1/4	INSPECTION IMPAIRED BY VEG. OR OTHER MAT'L (LF)	LINE TOT.(LF)	Q.L. (LF)	SUM OF QL(LF):
1				
2				TOTAL= SUM QL/4 (TF):
3				
4				%:

COMMENTS: CULVERT AT 2+50 IS BROKEN AND TRACK HAS SETTLED BADLY

FLANGEWAY MEASUREMENTS

COMPONENT CODE	LOCATION (e.g. sta or road, etc.)	MIN DEPTH (in)	MIN WIDTH (in)	FOULED	COMMENTS
(GC) RR	INFANTRY ROAD	1.5	1.6	N (Y)	
(GC) RR	PARKING LOT 5	0.5	2.0	N (Y)	
GC (RR)	SEGMENT 107	2.0	1.9	(N) Y	
(GC) RR	STA 1+60	1.4	1.9	(N) Y	

COMPONENT CODES

BS = BALLAST / SUBGRADE	GC = GRADE CROSSING
BA = BRIDGE APPROACH	RA = RAIL ANCHOR(s)
CB = CAR BUMPER	RR = RAIL CROSSING
CS = CAR STOP	SS = SIGNS / SIGNALS
CU = CULVERT	SP = SPIKE(s)
DL = DERAIL	SW = STORM SEWER
DR = DRAIN	TP = TIE PLATE(s)
EM = EMBANKMENT	OT = OTHER (specify in comments)
GR = GAGE ROD(s)	

DEFECT CODES

BRK = BROKEN	NFL = NON - FUNCTIONAL
CRB = CRACKED / BENT	OBF = OBSTRUCTED FLOW
BAD = BALLAST - DIRTY	PMP = PUMPING
ERO = EROSION	SET = SETTLEMENT
IMP = IMPROPER POSITION	SLS = SLOPE STABILITY
IST = IMPROPER SIZE / TYPE	STD = STRUCTURAL DETERIORATION
ISA = INSUFFICIENT AMOUNT	SUD = SURFACE DETERIORATION
LOS = LOOSE	TCA = TORCH CUT / ALTERED
MIS = MISSING	WAS = WASHOUT

FIGURE 6 Completed other track components inspection form.

Ties are considered inspection impaired if less than half of the top surface is visible. The other two component areas use the concept of quarters for inspection impairment. For example, if the base on one side of only one rail is covered, then rail and joint inspection is one-quarter impaired. At the other extreme, four-quarters inspection impairment occurs when the base on both sides of both rails is covered. Quarters of inspection impairment are also used with "other track components"; the only difference is that the inspection impairment criterion is whether or not the spike heads are visible (instead of the rail base).

For each of the three component areas, obscuring foreign material is accounted for in terms of (equivalent) linear track feet and percentage of track length. These are calculated within the RAILER computer software based on data collected in the field during track inspection and can also be calculated manually if RAILER is not computer implemented. The field entries associated with inspection-impaired track are illustrated in Figures 2 and 6. An explanation of various categories shown in Figure 6 is given as follows:

- The ballast (component code: BS) is dirty (defect code: BAD) starting at Station 0+00 and continuing for 100 ft. This is not an immediate hazard.
- A culvert (CU) is clogged so that flow is obstructed (OBF). The culvert is a discrete item located at Station 0+50. This is not an immediate hazard.
- Three gage rods (GR) are loose (LOS). The first loose gage rod is located at Station 0+90. This is not an immediate hazard.
- Some spikes (SP) are improperly positioned (IMP) because of an improper spike pattern. Starting at Station 1+40 and continuing for 200 ft, about 50 percent of the spikes are improperly positioned. This is not an immediate hazard.
- A spike (SP) is missing (MIS) at Station 1+50. This is not an immediate hazard.
- An embankment (EM) is experiencing erosion (ERO) starting at Station 2+10 and continuing for 20 ft. This is not an immediate hazard.
- A culvert (CU) has suffered structural deterioration (STD). The culvert is located at Station 2+50. This defect is marked as an immediate hazard, and the comment indicates that the track has "settled badly," which could lead to unsafe car movement (e.g., rocking) if the track is used.

Flangeway Measurements

- A grade crossing (component code: GC) that crosses Infantry Road has an effective minimum flangeway depth and width of 1.5 in. and 1.6 in., respectively. The flangeways are fouled.
- A grade crossing (GC) that crosses Parking Lot 5 has an effective minimum flangeway depth and width of 0.5 in. and 2.0 in., respectively. The flangeways are fouled.
- A rail crossing (RR) that crosses Segment 107 has an effective minimum flangeway depth and width of 2.0 in. and 1.9 in., respectively. The flangeways are not fouled.
- A grade crossing (GC) located at Track Station 4+60 has an effective minimum flangeway depth and width of 1.4 in. and 1.9 in., respectively. The flangeways are not fouled.

In addition to undesirable foreign material, grade crossings (paved areas) also obscure track inspection. Grade crossing length is a RAILER inventory data element. This data element is used within the RAILER software to account for the effect of grade crossings on track inspection. For this reason, the inspection impairment associated with grade crossings can be ignored during track inspection field procedures if RAILER is computer implemented. Otherwise, the effect of grade crossings is accounted for in the field in conjunction with undesirable foreign material.

This process quantifies, for each of the three component areas, the amount of track that cannot be properly inspected. Procedures for using this information to estimate the hidden defects are still under development.

Relationship to Track Standards

Track maintenance or safety standards describe desired or acceptable track conditions. In addition, track standards may indicate the relative severity of various deviations from these acceptable track conditions (as the Army standards do).

The first immediate goal of the detailed inspection procedures described here is implementing the Army Track Standards in a manner consistent with the RAILER program. However, RAILER is also designed to accommodate other track standards. For example, a version of RAILER is being developed for the U.S. Army in Europe that will incorporate German Track Standards. Also, it is envisioned that RAILER will be eventually transferred to the civilian/private sector for use by short lines, industrial networks, and possibly some branch line operations. These operators may wish to incorporate FRA or their own track standards.

In order to accommodate this flexibility, the inspection procedures are designed (as much as possible) to collect raw data, which are later compared within the computer with the appropriate standards (or possibly multiple standards). For example, instances of three consecutive defective ties are noted as raw data during tie inspection (see Figure 2). This defect implies a 10-mph operating restriction in the Army Track Standards. However, in some industrial situations, such as in a steel mill operation where eight-axle ladle cars regularly carry molten iron, management could elect to impose a more restrictive 5-mph limit, or perhaps prohibit all train movements, whenever three consecutive defective ties are encountered.

The analysis of the inspection data relative to a given set of track standards is provided in three RAILER "Comparison Reports" that vary in their level of detail. These are a Condition Summary, a Condition Comparison by Inspection Type (component area), and a Detailed Comparison. An example of the Condition Comparison by Inspection Type report is presented in Figure 7. The comparison results can be tied to a locally developed maintenance policy so that a Maintenance and Repair (M&R) report can be generated for work planning. This report can be generated in two levels of detail, an M&R Summary and a Detailed M&R. An example of the summary level is presented in Figure 8.

Use of a Computer to Simplify Inspection Procedures

Inspecting for all the defects specified in the Army Track Standards is a significant task. Therefore, an important con-

RAILER Page: 1
Condition Comparison Date: 12/21/1988
by Inspection Type Report

Report Criteria: Condition Comparison by Inspection Type for All Track Segments.

TRACK SEGMENT #	NO OPERATION	5 MPH SPEED LIMIT	10 MPH SPEED LIMIT	FULL COMPLIANCE	DEFECT FREE
1001	TURNOUTS			TIES	VEGETATION
1002			TURNOUTS	TIES	VEGETATION
1003				TIES T/O GEOM	TURNOUTS VEGETATION
1004				TIES	TURNOUTS
1005			TURNOUTS	T/O GEOM	TIES VEGETATION
1006		TURNOUTS	TIES	T/O GEOM VEGETATION	
1007	FLNGWAY MEA		TIES	TURNOUTS VEGETATION	T/O GEOM
1008			TIES		VEGETATION
101	FLNGWAY MEA TIES			TRACK COMP	VEGETATION

FIGURE 7 Condition Comparison by Inspection Type report.

RAILER Date: 12/21/1988
M&R Summary Report

Condition After Repairs: Full Compliance Track Category: All
Policy: IN-HOUSE Track Use: All

Track Segment #	Maintenance Standard Condition	Total Cost to Raise Condition to Desired Level
1001	OUT OF SERVICE	$2,002.00
1002	10 MPH SPEED LIMIT	$1,534.00
101	OUT OF SERVICE	$1,327.00
102	OUT OF SERVICE	$3,327.00
103	10 MPH SPEED LIMIT	$991.00
701	OUT OF SERVICE	$2,072.00
L01	5 MPH SPEED LIMIT	$1,469.00
L02	10 MPH SPEED LIMIT	$1,227.00
L03	OUT OF SERVICE	$8,783.00
P01	5 MPH SPEED LIMIT	$3,556.00
		$26,288.00

FIGURE 8 Maintenance and Repair Summary report.

sideration in developing these inspection procedures was easing, as much as possible, the burden of the inspector. This was accomplished in several ways, including, as discussed previously, in the design of the inspection forms.

The RAILER computer software provides another means to this end. The focus on collecting raw data (as discussed previously) is an important example. This is especially true of measurements such as those obtained during turnout inspection (see lower portion of form presented in Figure 3). The inspector does not need to know the acceptable value ranges and the cut-off points for different operating restrictions (severity levels). The inspector only needs to properly make the measurement(s) and enter the values on the form. These values are later compared with the standards, either in the computer or by hand if RAILER is not computer implemented.

The computer software is also designed to prevent the entry of some obviously inconsistent defect combinations such as rail anchors that are pumping (see in Figure 6 Component Code RA and Defect Code PMP). This increases the reliability of the inspection process.

SHORT-LINE APPLICABILITY

Potential technical transfer to the civilian sector is an important consideration in research conducted by the federal government. Early in the development of RAILER, it was observed that many characteristics associated with Army track maintenance management are also true for commercial short lines and industrial networks. These common characteristics include general track quality, service levels and types of operations, and the availability of local expertise.

Therefore, potential use by short lines was a strong consideration throughout the development of RAILER. This was partially accomplished by introducing into RAILER the necessary flexibility to accommodate those areas in which the Army's needs are not completely consistent with those of potential civilian users. An example of this flexibility is the ability to develop within RAILER customized track standards as discussed previously. The RAILER detailed inspection procedures provide the same benefits for short-line users, as they do for Army users.

FIELD TESTING

The detailed inspection procedures described here have been under development for over 3 years. They have evolved into their present form with the concurrent development of the Army Track Standards. Both involved considerable revision during their history. The development was an iteration process; needed information was ascertained, procedures were then developed to collect the information, these procedures were field tested, and revisions were made. The overall goal was to be able to easily collect the necessary information with trained installation track inspectors.

Many weeks were spent in the field testing the procedures. Teams were sent to the Tooele Army Depot, Utah; Ft Devens, Massachusetts; Ft Stewart, Georgia; and Hunter Army Airfield, Georgia. Additionally, the Urbana, Illinois, yard of the Consolidated Rail Corporation (Conrail) served as a local site. Generally, data collection procedures were first developed in the laboratory and tested locally. Then, field trips to the installations were scheduled to uncover procedural shortcomings. The various locations were chosen to provide the great variety of operating, climatic, and maintenance differences that were needed to properly test and evaluate the data collection procedures. Also, the field work permitted the researchers to test the practical requirements of the Army Track Standards. Feedback to the developers of the standards resulted in some changes. Those, in turn, resulted in inspection changes and data collection modifications.

The field work has shown that inspection productivity rates are strongly dependent on the condition of the track (i.e., the more defects there are, the longer the inspection takes). The inspections may only progress at a slow walking pace. This is because many of the defects are quite finite and require acute attention to be observed. Also, for the same reason, it was found that it can be nearly impossible for a single inspector to inspect all of the components concurrently. In fact, it may take up to three passes of the track by one inspector to note all of the defects for all of the components. The track can be inspected by one person, but a team of two significantly improves the efficiency; it can be nearly impossible for one person to perform certain manual track geometry inspection tasks.

Based on the range of conditions found at the various installations, one inspector could completely inspect, on foot, approximately 0.3 mi/hr. Turnouts take approximately 15 min each to inspect (time actually spent at the turnout). These are average rates and include allowance for nonproductive walking time (time lost walking back from the end of a terminating track at the completion of an inspection). They do not include travel time to and from the network portion being inspected.

A two-person inspection team was found to be able to inspect at a rate of approximately 0.8 mi/hr. Turnout inspection can be reduced to approximately 8 min.

None of the above productivity rates includes time for manual track geometry measurements.

Track inspection from a moving track vehicle, even at slow speeds (<5 mph), resulted in a number of missed defects.

CONCLUSIONS AND RECOMMENDATIONS

The detailed inspection procedures described in this report were developed for use within the RAILER system. The inspection data collection forms were developed to facilitate relative ease in data collection and recording, as well as eventual loading into installation RAILER data bases for processing and analysis. Testing has shown that this has been accomplished.

These same detailed inspection procedures were designed to satisfy the requirements of the Army Track Standards. The methods and procedures described in this report can be used to satisfy the inspection requirements of those track standards.

Also, these inspections are currently intended to satisfy several maintenance management requirements at both the network and project levels (*1*, *2*). At the network level, these include identifying safety problems, assessing conditions, developing long-range work plans, budgeting, and prioritizing work for the entire network. Project-level management focuses

on specific track segments and includes quantifying work needs associated with preparing job orders and contracts, determining the cause of the track problems, and selecting the most feasible M&R alternative.

The detailed track inspection procedures are explicitly designed to provide the information required for project-level management, in which detail becomes very important. However, much of that detailed information is not needed for network-level management tasks. Network-level management tasks are performed at least annually, whereas project-level tasks are performed only when and where needed. Thus, most management tasks are at the network level.

The authors believe that management needs should dictate data requirements, not vice versa. Specific information should be collected only when needed to satisfy management needs. Accordingly, simplified track inspection procedures are being formulated as part of the Track Structure Condition Index (TSCI) development currently under way at USA-CERL. The TSCI will measure the "health" of both individual track segments and the overall network. This measure will be the prime tool for network-level management tasks. The new simplified inspection procedures will capture just enough information to perform those tasks, yet at the same time be sensitive enough to identify critical defects requiring immediate attention for safety reasons. The spirit and intent of the Army Track Standards will still be met. A tangible benefit consisting of a significant reduction in inspector hours would result. The detailed inspection procedures described in this report would be reserved for project-level management tasks.

ACKNOWLEDGMENTS

The authors would like to acknowledge members of the U.S. Army Pavement and Railroad Maintenance Committee, chaired by the RAILER system project sponsor, Robert Williams, from the U.S. Army Engineering and Housing Support Center, for their significant contributions to the development of the RAILER detailed inspection procedures. The cooperation of Conrail for the ongoing use of their Urbana, Illinois, yard is greatly appreciated.

Special appreciation goes to the group at USA-CERL who worked on these procedures. Thanks go especially to Don Plotkin, who contributed much to the early development of these procedures and was a codeveloper of the Army Track Standards. Thanks also go to Debra Piland, Mike Britton, and Joshua Crowder for coordinating the relationship between the inspection procedures and the RAILER computer software. The efforts of David Coleman from the U.S. Army Waterways Experiment Station in codeveloping the Army Track Standards are also acknowledged.

REFERENCES

1. D. R. Uzarski, D. E. Plotkin, and D. G. Brown. *The RAILER System for Maintenance Management of U.S. Army Railroad Networks: RAILER I Description and Use.* Draft Technical Report. U.S. Army Construction Engineering Research Laboratory, Champaign, Ill., 1988.
2. D. R. Uzarski and D. E. Plotkin. Interim Method of Maintenance Management for U.S. Army Railroad Track Networks. U.S. Army Construction Engineering Research Laboratory, Champaign, Ill., 1988.
3. D. R. Uzarski, D. E. Plotkin, and S. K. Wagers. Component Identification and Inventory Procedures of U.S. Army Railroad Trackage. In *Transportation Research Record 1131*, TRB, National Research Council, Washington, D.C., 1987, pp. 89–98.
4. D. R. Uzarski, D. G. Brown, R. W. Harris, and D. E. Plotkin. *Maintenance Management of U.S. Army Railroad Networks—The RAILER System: Detailed Track Inspection Manual.* Draft Technical Report. U.S. Army Construction Engineering Research Laboratory, Champaign, Ill., 1988.
5. *Track Safety Standards.* Office of Safety, FRA, U.S. Department of Transportation, Nov. 1982.
6. RPMA *Component Inspector's Handbook.* U.S. Army Facilities Engineering Support Agency, May 1979.
7. *Railroad Track Standards.* TM 5-628. U.S. Army Headquarters, Assistant Chief of Engineers, Oct. 1988.
8. D. R. Uzarski, D. E. Plotkin, and D. G. Brown. *Maintenance Management of U.S. Army Railroad Networks—The RAILER System: Component Identification and Inventory Procedures.* Technical Report M-88/13. U.S. Army Construction Engineering Research Laboratory, Champaign, Ill., 1988.

The views of the authors do not necessarily reflect the position of the Department of the Army or the Department of Defense.

Publication of this paper sponsored by Committee on Railway Maintenance.

Bearing Capacity Approach to Railway Design Using Subgrade Matric Suction

PAMELA SATTLER, D. G. FREDLUND, M. J. KLASSEN, AND W. G. ROWAN

A bearing capacity type design procedure for assessing the stability of the track subgrade is presented in this paper. The current phase of the research concentrates on the incorporation of the matric suction term into a bearing capacity design procedure. This permits the design procedure to use the additional strength of the soil resulting from the matric suction in the subgrade. A previous research program has enabled the measurement of the matric suction in the subgrade of a tie-track system. Design charts have been produced for various train loads, subballast thicknesses, soil types, and design matric suction values. The design charts give a factor of safety against bearing capacity failure as a function of the above parameters. Stresses in the subgrade are predicted using the computer program GEOTRACK for various design train loads, subballast thicknesses, and soil parameters. The ultimate bearing capacity is determined using bearing capacity theories that have been modified to accommodate the layered track system and also incorporate the additional strength of the soil resulting from matric suction. A comparison of predicted stresses and the bearing capacity defines the factor of safety against a bearing capacity failure.

The design of an adequate railway system has developed over a long period of time. In fact, railways were built before the advent of modern soil mechanics. It is not surprising, therefore, that the technology associated with railway design has remained largely empirical, from a soil mechanics standpoint. Although this approach has served quite well, Canadian Pacific Railways, Canadian National Railways, and the Transportation Development Center have embarked on research programs at the University of Saskatchewan that give consideration to the benefits that could accrue from the application of modern soil mechanics knowledge to railway design.

The present research program has concentrated on the effect of soil suction in the subgrade of the track structure. Soil suction is defined as negative pore-water pressure referenced to the pore-air pressure. The pore-water pressure above the groundwater table is negative and when referenced to the pore-air pressure becomes a variable that varies in response to the surrounding microclimate. Figure 1 illustrates typical negative pore-water pressure profiles in the upper layers of a soil.

Previous research conducted at the University of Saskatchewan for the railway companies has enabled the measurement of soil suction in the subgrade of a tie-track system (*1*). The objective of a recent research program was to develop a bearing capacity design procedure for the railway ballast-subballast-subgrade system, incorporating soil suction into the design procedure. This permits the design procedure to use the additional strength of the soil resulting from soil suction. Further details on the bearing capacity design procedure that has been developed are discussed in a report by Sattler and Fredlund (*2*).

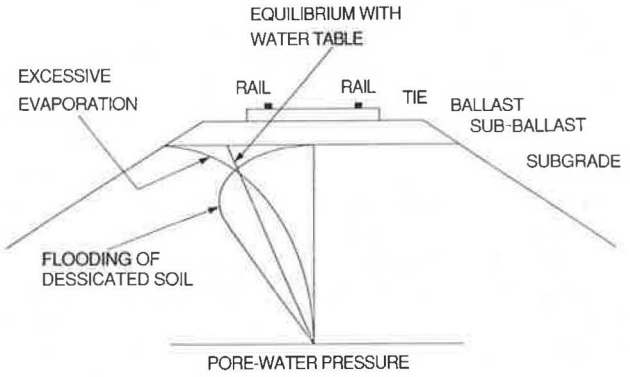

FIGURE 1 Idealized pore-water pressure profiles beneath a railroad track.

The design procedure that has been developed is a bearing capacity approach to the problem. Previously, railway design has concentrated on minimizing stresses in the rails, in the ties, and in the subgrade. The bearing capacity approach provides a measure against which the subgrade stresses can be compared. The strength of the subgrade is computed using a conventional bearing capacity equation with the incorporation of the soil suction term, whereas the stresses in the subgrade are estimated using a computer stress model. A comparison of subgrade strength and subgrade stresses provides bearing capacity factors of safety for various subgrade properties and loading conditions. It is the development of this bearing capacity approach that is given primary consideration in this paper.

HISTORY OF BEARING CAPACITY APPROACH TO RAILWAY DESIGN

An examination of the literature reveals two facets to the railway design problem: (a) the predictions of stress distributions beneath the tie-track structure and (b) the evolution

P. Sattler and D. G. Fredlund, Department of Civil Engineering, University of Saskatchewan, Saskatoon, Saskatchewan, Canada S7N 0W0. M. J. Klassen, Canadian Pacific Railways, Windsor Station, P.O. Box 6042, Station A, Montreal, PQ, Canada H3C 3E4. W. G. Rowan, Transportation Development Center, 200 Dorchester Boulevard West, Suite 601 West Tower, Montreal, PQ, Canada H2Z 1X4.

of the bearing capacity equation to include layered systems and subgrade soil suction.

The most notable contributions to railway design are those of Talbot (*3–9*). Talbot assumed that the rail-tie system acted as a beam continuously supported on a homogeneous, elastic medium. This became known as the beam-on-elastic-foundation approach to railway design. At the same time that railway design approaches were being developed, Boussinesq was developing similar procedures for computing stress distributions beneath a loaded structure for modern soil mechanics (*10,11*). The first contribution to the development of theories of stress distribution beneath a layered system was presented by Burmister in his analyses of airport runways (*12*). The advancement of the digital computer in the 1970s resulted in the development of numerous models to predict the stresses beneath the complex tie-track structure.

A model combining Burmister's three-dimensional elasticity solution and a structural analysis model that solves for the tie-ballast reaction was proposed by Kennedy and Prause in 1978 (*13*). Their MULTA model predicts reasonable values for tie loads and tie-ballast pressures; however, accurate modeling of the ballast and subgrade system becomes more difficult. Developers of the GEOTRACK model (*14*) chose to adopt the MULTA model's representation of the tie and rail components because the structural analysis model provided accurate results. However, modeling of the ballast-subgrade system was replaced with a model representing a series of continuous plates (*14*). The GEOTRACK model was chosen for predictions of stress distribution and is later discussed in more detail.

Characterization of soil strength beneath a loaded structure has conventionally been expressed as a bearing capacity. The first equations for bearing capacity by Terzaghi (*15*) were later extended by Meyerhof to include the effects of foundation shape, eccentric loading, base roughness, and varying groundwater conditions (*16–18*). The extension of bearing capacity theories to multilayered systems was first attempted by Broms in 1965 for applications to highway systems (*19*). More recently, work by Hanna and Meyerhof (*20*) has extended the conventional bearing capacity equation to layered soils treating the upper granular material as a continuation of the footing that punches into the weaker subgrade material, in many ways like a driven pile.

The extension of conventional soil mechanics to unsaturated soil mechanics has opened the way for determining the bearing capacity of railway subgrades in a less empirical manner. The soil suction term can be incorporated into the bearing capacity equation much like shear strength extensions of unsaturated soil mechanics. The result is that the ultimate bearing capacity can now be reasonably estimated from measurements of the subgrade shear strength parameters and the subgrade soil suction. Stress distributions can now be predicted with reasonable reliability using computer models. A comparison of predicted stress distributions and estimated bearing capacity provides a measure of the factor of safety against failure of the railway subgrade.

PREDICTION OF STRESS DISTRIBUTIONS

The prediction of the three-dimensional stress state beneath a loaded tie-track structure is accomplished through the use of the GEOTRACK computer model (*14*). The GEOTRACK model emphasizes the geotechnical behavior of the tie-track structure and provides a reasonable representation of the soil layers. Figure 2 illustrates that the rails are modeled as elastic beams supported by ties that are also represented as elastic beams. The ties are divided into 10 segments, each segment capable of transmitting a load to the ballast surface. Each soil layer is characterized by a flexible plate of a given modulus of elasticity, Poisson's ratio, and stress-dependent modulus equation. Reasonable predictions for the stress distributions beneath the loaded tie-track structure are provided by the GEOTRACK computer model.

The first step in using the GEOTRACK model for predictions of stress distributions beneath the loaded tie-track structure was to perform a sensitivity analysis on the computer generated output to the variations in input parameters. Stewart and Selig (*21*) published the results of a sensitivity analysis for the GEOTRACK model. The sensitivity analysis performed at the University of Saskatchewan confirmed the results of Stewart and Selig.

The parameters considered were (a) axle load, (b) ballast E modulus, (c) subgrade E modulus, (d) granular depth, (e) tie spacing, and (f) tie modulus. Although significant sensitivity was determined for tie spacing and tie modulus, the tie spacing was fixed at 0.508 m (20 in.), and the tie modulus was fixed at 1.65×10^7 kPa (2.4×10^6 psi). Therefore, the design procedure was documented so that the user could change parameters that would vary from the standards assumed. The vertical stresses were used for comparison to the bearing capacity results. Therefore, all sensitivity analyses used the vertical stress distribution as a guide to determine parametric sensitivity.

The sensitivity analysis determined which parameters should be varied for the purposes of developing design charts. It was decided to keep the ballast modulus constant at 241 MPa, to vary the subballast modulus from 103.5 to 241 MPa, and to

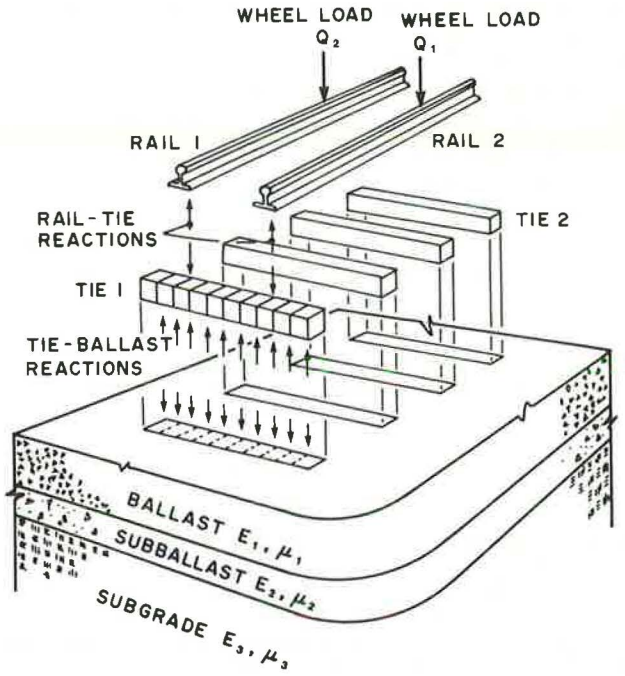

FIGURE 2 Forces and elements in the GEOTRACK model.

vary the subgrade modulus from 6.9 to 103.5 MPa. Two ballast depths of 203 and 305 mm were used. Four subballast depths, 203, 406, 610, and 813 mm, were used for each case. Complete documentation on the parameters input to the GEOTRACK model can be found in a report by Sattler and Fredlund (*2*). A total of 64 computer runs were generated for each of six different axle loads making a total of 384 GEOTRACK computer runs.

Following the data generation process for all of the varying parameters, it was necessary to reduce the data to values that could be compared to the ultimate bearing capacity. Figure 3 illustrates typical vertical stress output from the GEOTRACK computer model for a subgrade modulus of 69.0 kPa, subballast modulus of 241.5 MPa, a total granular depth of 610 mm, and an axle load of 184 kN. A postprocessing graphics package was written for the GEOTRACK model for the purpose of plotting the output. Figure 3 represents a typical plot produced by the postprocessing package GEOPLOT.

Two geometries must be considered for bearing capacity analysis: (a) geometry parallel to the track and (b) geometry perpendicular to the track.

A sectional view of the geometry perpendicular to the track can be used to represent the two most critical failure conditions: (a) the failure of the complete tie-track system for the length of the track as shown in Figure 4 and (b) the failure of a portion of the track beneath the heavily stressed outer third of the tie and the distance of a double truck loading as shown in Figure 5. The failure conditions represented by Figure 5 are often recognized in the field where bearing capacity failures occur. The failure geometry depicted in Figure 4 is usually of lesser significance and is better analyzed using slope stability methods of analysis.

A sectional view of the geometry parallel to the track can be used to represent two failure conditions: (a) the local failure of an individual tie punching into the subgrade as shown in Figure 6 and (b) the failure of a portion of the track corresponding to the loading that occurs beneath a double truck arrangement between two cars as depicted in Figure 7. Field experience suggests that the failures represented by Figures 6 and 7 may occur in the absence of subballast for weak clay subgrades. The failure geometry depicted in Figure 7, in which the track is pushed up in a wave ahead of the moving cars, is a dynamic effect that could be important particularly where braking occurs on curves. These two failure mechanisms are presented, but emphasis is placed on the more critical failure geometries represented by Figures 4 and 5.

The failure geometry depicted in Figure 6 is analyzed by the Hanna and Meyerhof approach (*20*) to bearing capacity,

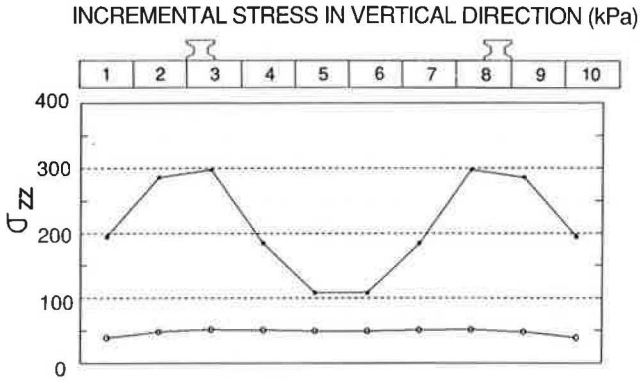

FIGURE 3 Typical vertical stress output from GEOTRACK and GEOPLOT.

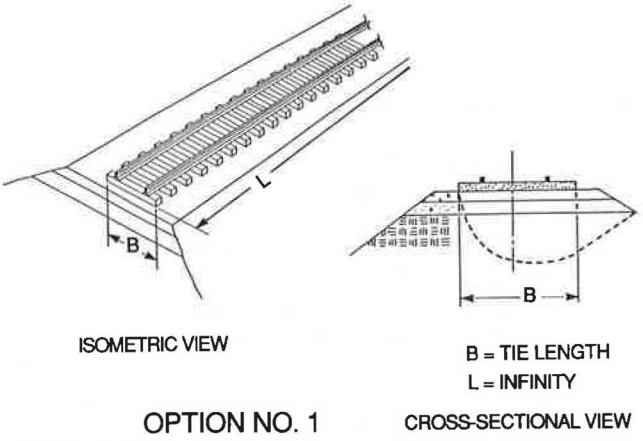

FIGURE 4 Failure geometry for the complete tie-track system for the length of the track.

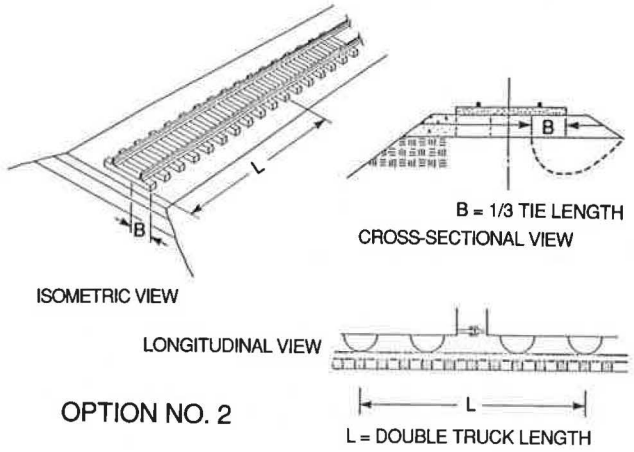

FIGURE 5 Failure geometry for the heavily stressed outer third of the tie and the distance of a double truck loading.

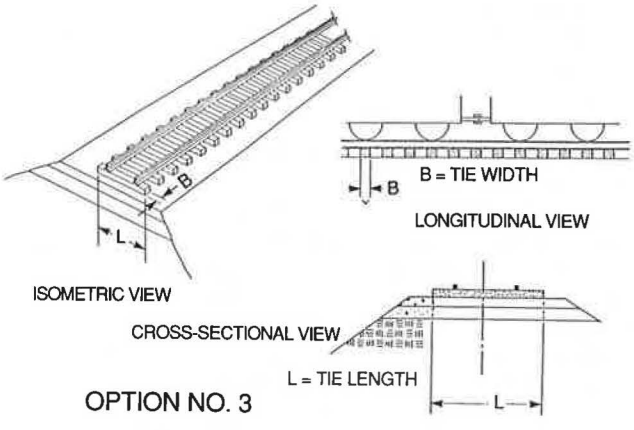

FIGURE 6 Failure geometry for the local failure of an individual tie punching into a weak subgrade.

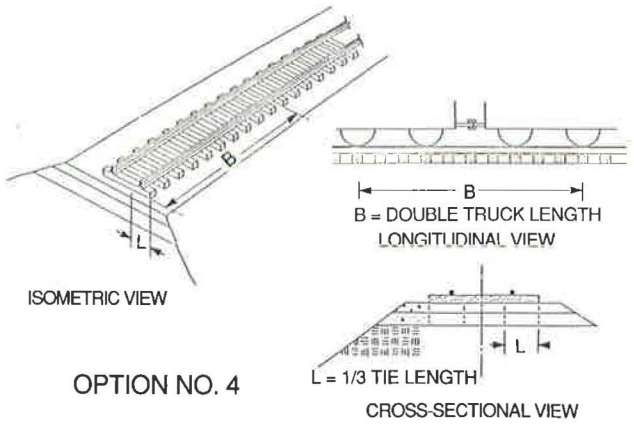

FIGURE 7 Failure geometry for a portion of the track beneath a double truck arrangement for weak subgrades.

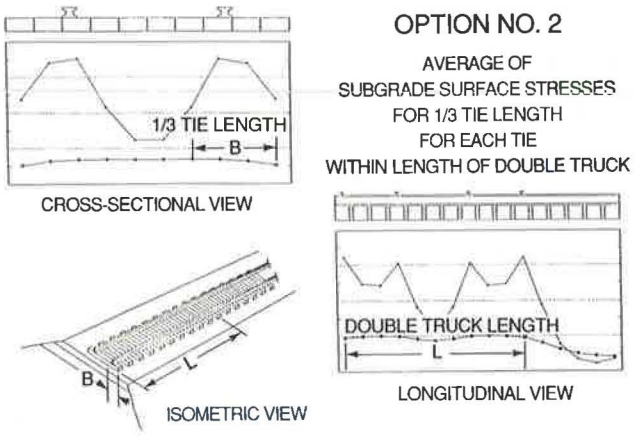

FIGURE 8 Option 2 Stress Averaging Technique.

whereas the geometries illustrated in Figures 4, 5, and 7 are all analyzed by the Broms approach (*19*) to bearing capacity.

The necessity to create a program that averages the stress distribution comes from the fact that a bearing capacity analysis produces a unique value to represent the strength of the soil, whereas a stress analysis program, like the computer program GEOTRACK, creates a stress distribution (i.e., several values of stress beneath several different locations of the railway track structure). Because comparison of one value for the bearing capacity to several values representing the stress distribution would result in confusion, it was decided to average the stress distribution for comparison to the bearing capacity.

There are four averaging techniques corresponding to each of the four bearing capacity options. Only the Option 2 Averaging Technique is presented in the figures. Each option corresponding to an averaging technique also corresponds to a bearing capacity loading configuration. In other words, the Option 2 Averaging Technique presented in Figure 8 must be compared to the Option 2 Bearing Capacity Loading Configuration presented in Figure 5.

Figure 8 shows the averaging technique for Option 2. The stress distribution beneath the most heavily loaded outer one-third of the tie is averaged for a distance beneath the track equal to the length of two closest trucks. For bearing capacity computations, the width, B, is equal to one-third of the tie length and the length, L, is equal to the length of a double truck loading. The bearing capacity option corresponding to Option 2 of the Stress Averaging Technique is a Broms approach and is presented in Figure 5.

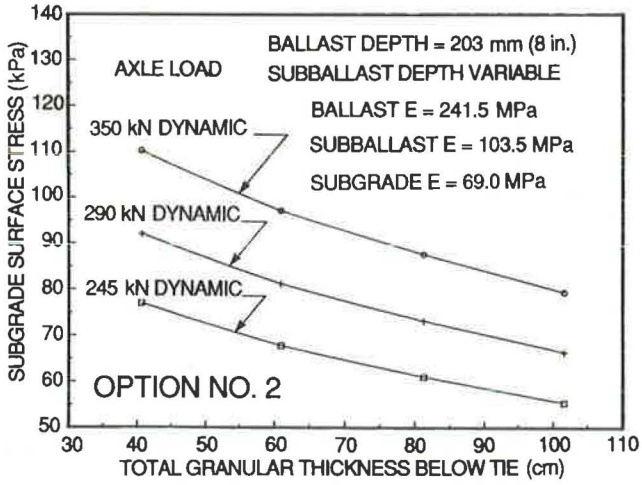

FIGURE 9 Averaged subgrade surface stress from several GEOTRACK computer runs for comparison to the Broms approach.

Figure 9 illustrates the results of 24 separate GEOTRACK computer runs on one set of ballast, subballast, and subgrade moduli for which the subgrade stresses have been averaged for later comparison to the Broms bearing capacity values. The three axle loads (245, 290, and 350 kN) shown in the charts correspond to (a) a 100,000-kg (220,000-lb) car, (b) a 119,000-kg (263,000-lb) car, and (c) a 143,000-kg (315,000-lb) car, respectively. For dynamic loading conditions, the axle load was increased by 50 percent to account for wheel speed and impact loadings. (In other words, a 245-kN dynamic load has been modeled as a 367-kN static load.)

ULTIMATE BEARING CAPACITY

Two methods are used for the estimation of the bearing capacity beneath a loaded track structure. The Hanna and Meyerhof approach applies only to weak clay subgrades, whereas the Broms approach applies to the stronger clays, glacial tills, silt, and sand subgrades. The soil suction term is incorporated into both procedures.

Hanna and Meyerhof Bearing Capacity Approach

Figure 10 illustrates the bearing capacity equation for the Hanna and Meyerhof approach. The failure mechanism assumes that a soil mass of the upper sand layer of approximately pyramidal shape is pushed into the lower clay layer. At the point of limiting equilibrium, the sum of forces in the vertical direction yields an equation for the ultimate bearing capacity. Laboratory data collected by Hanna and Meyerhof reveal an appropriate equation for the passive earth resistance based on an assumed coefficient of punching shear (*20*). The resulting bearing capacity equation is as follows:

$$q_u = cN_c + \gamma_1 H^2 (1 + 2D/H) K_s \tan \phi'/B - \gamma_1 H \qquad (1)$$

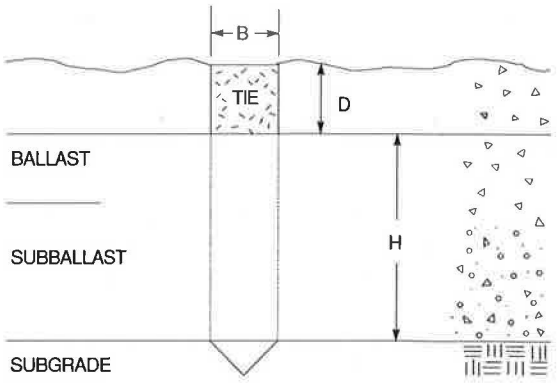

$$q_u = cN_c + \gamma_1 H^2(1+2D/H)\,K_s \tan\phi'/B - \gamma_1 H$$

FIGURE 10 Illustration of the bearing capacity equation for the Hanna and Meyerhof approach.

where

c = total cohesion of the clay subgrade,
N_c = bearing capacity factor,
γ_1 = unit weight of overlying dense sand (or ballast and sub-ballast),
H = thickness of dense sand below the bottom of the footing (or railway tie),
D = depth of embedment of the footing (or railway tie),
K_s = coefficient of punching shear resistance (determined from published charts),
ϕ' = friction angle of the upper dense sand (or ballast and sub-ballast), and
B = width of footing (or railway tie, depending on the geometry considered).

The soil suction term is incorporated into the Hanna and Meyerhof equation by replacing the undrained shear strength of the clay with the more rigorous c' and ϕ^b terms, illustrated as follows:

$$c = c' + (u_a - u_w)\tan\phi^b \qquad (2)$$

where

c' = the effective cohesion of the subgrade,
$(u_a - u_w)$ = design suction value for the subgrade, and
ϕ^b = rate of increase in shear strength with respect to soil suction.

Figure 11 illustrates the components of the total cohesion term, c.

Kraft and Helfrich (*22*) suggest that the Hanna and Meyerhof approach to computing the bearing capacity is quite accurate for shallow footings. If an individual tie can be assumed to act in the same manner, then the results should also apply to the case of the geometry perpendicular to the track (Figure 6). The replacement of the cohesive strength term with unsaturated soil parameters renders the computations more rigorous because the strength can be related to microclimatic conditions. Kraft and Helfrich suggested that the Hanna and Meyerhof approach cannot be extended to stronger deposits while still maintaining reliable predictions.

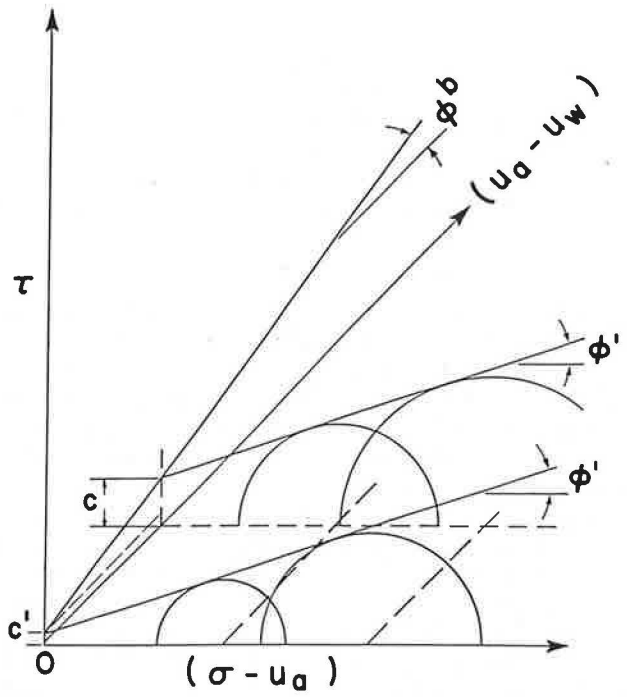

$$c = c' + (u_a - u_w)\tan\phi^b$$

FIGURE 11 Components of the total cohesion term.

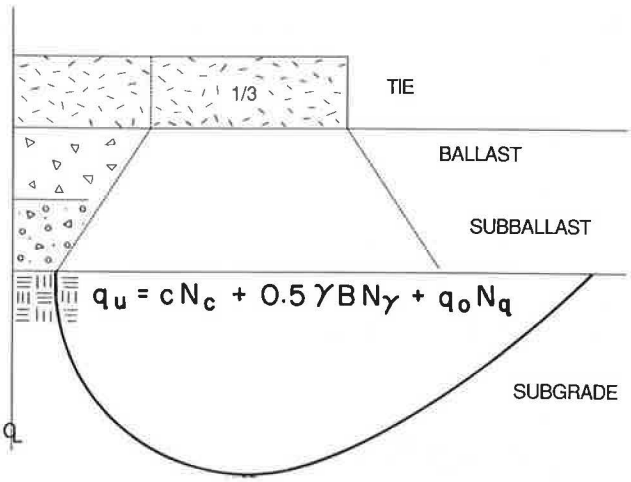

FIGURE 12 The Broms approach to bearing capacity for highway pavements.

Broms Bearing Capacity Approach

The Broms approach to computing bearing capacity is illustrated in Figure 12. When the rail-tie system is considered as a contiguous unit placed on the ballast and subgrade, the Broms approach provides a reasonable estimate of the general bearing capacity failures that occur under field conditions. The equation for bearing capacity bears the same form as the conventional bearing capacity equation:

$$q_u = cN_c + 0.5\gamma BN_\gamma + q_o N_q \qquad (3)$$

where

N_c, N_γ, N_q = bearing capacity factors,
c = total cohesion,
γ = unit weight of the overlying ballast and subballast material,
B = width of the footing (or railway tie loaded area, depending on the geometry considered), and
q_o = surcharge loading.

Again the equation can be modified to replace the undrained shear strength parameter with the unsaturated soil parameters. Broms suggested incorporation of the χ parameter to account for the degree of saturation of the subgrade (*19*). The present formulation will treat the stress state variables in an independent manner, thereby eliminating the need for the χ parameter.

The subgrade bearing capacity for various total cohesion values of a clay subgrade, as computed from the Broms approach, is illustrated in Figure 13. Figure 13 presents typical bearing capacity values for a clay with a total cohesion ranging from 0 to 100 kPa and a ϕ' angle ranging from 10 to 25 degrees. The second term in the bearing capacity equation becomes negligible for the small ϕ angles, and, hence, the width assumed for the tie-track system becomes insignificant to the computations.

Bearing Capacity Factors

The bearing capacity factors are computed from the following equations:

$$N_q = e^{(\pi \tan \phi')} \left(\frac{1 + \sin \phi'}{1 - \sin \phi'} \right) \quad (4)$$

$$N_c = (N_q - 1) \cot \phi' \quad (5)$$

$$N_\gamma = 1.5 (N_q - 1) \tan \phi' \quad (6)$$

where ϕ' is the friction angle of the subgrade material.

The equations are derived from Brinch-Hansen (*23*) and Vesic (*24*). Other published equations for the bearing capacity factors could also be used.

PREPARATION OF BEARING CAPACITY DESIGN CHARTS

A comparison of the predicted stresses from the computer model to the ultimate bearing capacity computed from the above methods provides a factor of safety against failure.

A bearing capacity factor of safety greater than one does not imply that a bearing capacity failure could not occur. This results from the fact that the bearing capacity approach produces a single value to represent the strength of a heterogeneous subgrade system in which planes of weakness may exist. In addition, the choice of design values for the soil parameters, track structure, and loading configuration is subject to error, which may be cumulative for each of the many design values that enter into the analysis.

A bearing capacity factor of safety 2.5 to 3.0 is often used for shallow foundations. Current research and implementation of the design procedure suggest that smaller bearing capacity factors of safety be used in railway design. At present, it is suggested that the bearing capacity factor of safety should be in the range of 2.0 to 2.5. It may be necessary to change this value after more experience is obtained with its use.

Design charts for various geometries, train loads, soil parameters, and stress-dependent moduli can be produced. It is not the purpose of the authors in this paper to present the design charts, but rather to present the procedure from which charts can be produced. A typical design chart for a clay subgrade is illustrated in Figure 14. Figure 14 was produced from a comparison of the stress distributions in Figure 9 to the bearing capacity for a clay in Figure 13.

The design charts are produced from comparisons of the stress distributions for the GEOTRACK computer program to the bearing capacity estimates. The bearing capacity factor of safety (BCF) is defined as:

$$BCF = \frac{\text{Ultimate bearing capacity}}{\text{Predicted average stress}} \quad (7)$$

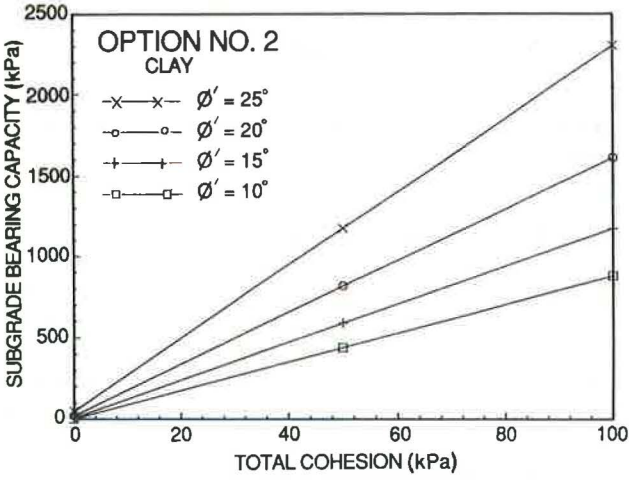

FIGURE 13 Subgrade bearing capacity as a function of total cohesion for a clay subgrade by the Broms approach.

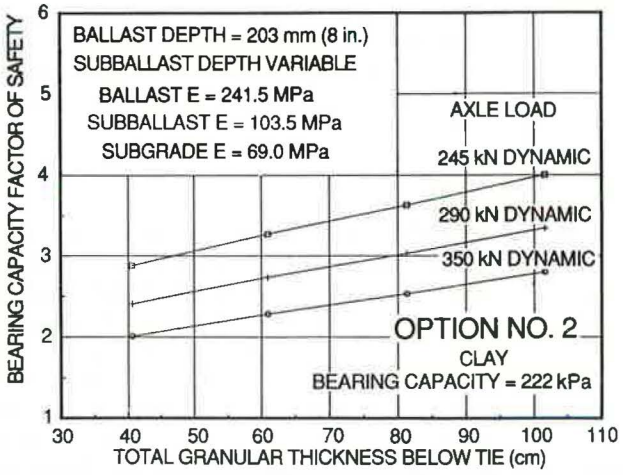

FIGURE 14 Typical bearing capacity design chart for a clay subgrade.

Computer programs have been written to perform the computations for each of the procedures used in the final production of the design charts. Complete documentation for the computer programs is presented in a report by Sattler and Fredlund (*25*).

SUMMARY

In this paper, the authors illustrate a proposed bearing capacity approach to railway design that can be used with present design methods as a complementary design tool. Soil suction is incorporated into bearing capacity theories for layered systems to arrive at the bearing capacity of the subgrade below the tie-track system. Design charts can be produced for various train loads, subballast thicknesses, soil types, and design suction values. The procedure that can be used to develop the design charts is presented. The implementation of the design charts for an example location will be presented in a future publication.

ACKNOWLEDGMENTS

The authors wish to acknowledge the financial contributions provided by Canadian National Railways (CN Rail), Canadian Pacific Railways, and the Transportation Development Center of Transport Canada. Their support has made possible this research. Sincere appreciation is expressed to W. E. Jubien of CN Rail for his contributions toward this study.

REFERENCES

1. P. van der Raadt, D. G. Fredlund, A. W. Clifton, M. J. Klassen, and W. E. Jubien. Soil Suction Measurements at Several Sites in Western Canada. Presented to the Session on Geotechnical Problems in Arid Regions, Committee A2L06, TRB, National Research Council, Washington, D.C., 1987.
2. P. J. Sattler and D. G. Fredlund. *The Development of Bearing Capacity Design Charts for Track Systems.* Document TP9521E; Final Report. The Transportation Development Center, Transport Canada, Montreal, Quebec, 1988.
3. A. N. Talbot. First Progress Report on the Special Committee to Report on Stresses in Railroad Track. *Transactions*, ASCE, Vol. 82, or Proceedings A.R.E.A., Vol. 19, 1918.
4. A. N. Talbot. Second Progress Report. *Transactions*, ASCE, Vol. 83, or Proceedings A.R.E.A., Vol. 21, 1920.
5. A. N. Talbot. Third Progress Report. *Transactions*, ASCE, Vol. 86, or Proceedings A.R.E.A., Vol. 24, 1923.
6. A. N. Talbot. Fourth Progress Report. *Transactions*, ASCE, Vol. 88, or Proceedings A.R.E.A., Vol. 26, 1925.
7. A. N. Talbot. Fifth Progress Report. *Transactions*, ASCE, Vol. 93, or Proceedings A.R.E.A., Vol. 31, 1930.
8. A. N. Talbot. Sixth Progress Report. *Transactions*, ASCE, Vol. 97, or Proceedings A.R.E.A., Vol. 35, 1934.
9. A. N. Talbot. Seventh Progress Report. *Transactions*, ASCE, Vol. 104, or Proceedings A.R.E.A., Vol. 42, 1941.
10. K. Terzaghi and R. B. Peck. *Soil Mechanics in Engineering Practice.* John Wiley & Sons, Inc., New York, 1948.
11. H. O. Ireland. Railroad Subgrade Stresses. *Proc., American Railway Engineering Association*, Bulletin 641, 1973, pp. 382–386.
12. D. M. Burmister. The Theory of Stresses and Displacements in Layered Systems and Applications to Design of Airport Runways. Proc., 23rd Annual Meeting of the Highway Research Board, Chicago, Ill., Vol. 23, HRB, National Research Council, Washington, D.C., 1943, pp. 126–148.
13. J. C. Kennedy, Jr. and R. H. Prause. Development of Multilayer Analysis Model for Tie-Ballast Track Structures. In *Transportation Research Record 694*, TRB, National Research Council, Washington, D.C., 1978, pp. 39–47.
14. C. S. Chang, C. W. Adegoke, and E. T. Selig. GEOTRACK Model for Railroad Track Performance. *Journal of the Geotechnical Engineering Division*, ASCE, Vol. 106, No. GT11, 1980, pp. 1201–1218.
15. K. Terzaghi. *Theoretical Soil Mechanics.* John Wiley & Sons, Inc., New York, 1943.
16. G. G. Meyerhof. The Ultimate Bearing Capacity of Foundations. *Geotechnique*, Vol. 2, 1951, pp. 301–332.
17. G. G. Meyerhof. Influence of Roughness of Base and Groundwater Conditions on the Ultimate Bearing Capacity of Foundations. *Geotechnique*, Vol. 5, 1955, pp. 227–242.
18. G. G. Meyerhof. Some Recent Research on the Bearing Capacity of Foundations. *Canadian Geotechnical Journal*, Vol. 1, No. 1, 1963, pp. 16–26.
19. B. B. Broms. Effect of Degree of Saturation on Bearing Capacity of Flexible Pavements. Presented at 43rd Annual Meeting of the Committee on Flexible Pavement Design, Ithaca, New York, 1965.
20. A. M. Hanna and G. G. Meyerhof. Design Charts for Ultimate Bearing Capacity of Foundations on Sand Overlying Soft Clay. *Canadian Geotechnical Journal*, Vol. 17, 1980, pp. 300–303.
21. H. E. Stewart and E. T. Selig. Predicted and Measured Resilient Response of Track. *Journal of the Geotechnical Engineering Division*, ASCE, Vol. 108, No. GT11, 1982, pp. 1423–1442.
22. L. M. Kraft and S. C. Helfrich. Bearing Capacity of Shallow Footing, Sand Over Clay. *Canadian Geotechnical Journal*, Vol. 20, 1983, pp. 182–185.
23. J. Brinch-Hansen. A Revised and Extended Formula for Bearing Capacity. Bulletin 28. Danish Geotechnical Institute, Copenhagen, Denmark, 1970, pp. 5–11.
24. A. S. Vesic. Analysis of Ultimate Loads of Shallow Foundations. *Journal of the Geotechnical Engineering Division*, ASCE, Vol. 99, 1973, pp. 45–73.
25. P. J. Sattler and D. G. Fredlund. *GEOTRACK and GEOPLOT, STRESS, BEARING, and COMPARE User's Manuals (Subgrade Stress Analysis and Bearing Capacity).* Document TP9523E. Submitted to the Transportation Development Center, Canadian National Railways, and Canadian Pacific Railways, 1988.

Publication of this paper sponsored by Committee on Railroad Track Structure System Design.

Overview of Wheel/Rail Load Environment Caused by Freight Car Suspension Dynamics

SEMIH KALAY AND ALBERT REINSCHMIDT

It has been a well-established fact that excessive wheel/rail loads cause accelerated wheel/rail wear, truck component deterioration, track damage, and increased potential for derailment. The economic and safety impact of the increased wheel rail loads can only be ascertained by a total characterization of the wheel/rail loads. In this paper, a comprehensive set of experimental results obtained from on-track testing of conventional North American freight cars using both wayside and on-board measurement systems are presented. The particular emphasis is given to the wheel/rail loads resulting from suspension dynamics. The dynamic wheel/rail environment addressed in this paper is limited to dynamic performance regimes such as rock-and-roll and pitch-and-bounce, hunting, and curving. The strong dependence of the dynamic response of a railway vehicle on a truck suspension system has been illustrated by comparison of controlled test results for vehicles of different types.

Growing understanding of the interactions between vehicle and track continues to provide benefits in both performance and safety. Recent advancements in freight car modeling and testing procedures have enhanced the understanding of wheel/rail dynamics and continue to provide guidance in dynamic system testing (*1*,*2*). Development of experimental techniques to accurately measure the wheel/rail loads using instrumented wheel sets has made it possible to determine the total load environment seen under railway cars over long stretches of track (*3*). Many large-scale on-track tests have been conducted by railway researchers to characterize the dynamic performance of railway vehicles using state-of-the-art computer-based data acquisition systems (*4*–*6*).

The Association of American Railroads (AAR) has been an active participant in conducting extensive analytical and experimental vehicle dynamics research through the years. In this paper we have attempted to bring together the results of some of the experimental research conducted by the AAR, regarding dynamic load environment for conventional freight cars.

The forces generated at the wheel/rail interface depend on many factors, such as the geometry of the wheel and rail, vehicle weight and suspension system, vehicle speed, and track stiffness and damping properties. It should not be assumed that the wheel/rail loads remain constant in magnitude and a constant increase in the static loads could accurately represent the dynamic effects. Nevertheless, most conventional techniques for vehicle and track structural design use assumed dynamic load factors that represent only the effects of maximum dynamic load conditions (*7*). The most serious problem with these types of assumptions is that they neither make any distinction for the effects of suspension design used in different types of freight cars nor describe the variety of track conditions found in revenue service. Ideally, for design of track and freight car structures, a total description of the load spectra including low-frequency high-dynamic loads should be used (*8*).

Our purpose in this paper is to provide an overall understanding of the dynamic load environment encountered under typical North American freight cars. The dynamic forces that are covered in this paper are associated with low-frequency response of the car body to lateral and vertical track excitations. The longitudinal dynamic loads that result from train action and thermal effects are excluded.

The low-frequency dynamic loads are primarily associated with vehicle suspension dynamics and cause much of the track/vehicle damage because they are transmitted to all of the vehicle and track components. The loads associated with high-frequency response, such as those from wheel/rail impacts at discrete rail anomalies and flat wheels, are not included unless they occurred in conjunction with low frequency phenomena.

We begin the paper with a brief description of the loads that take place at the wheel/rail interface and their measurement techniques. The test results obtained from a series of vertical dynamic performance tests are described: both the rock-and-roll and pitch-and-bounce responses that result from typical track irregularities are presented. On-track test results for 70-, 100-, and 125-ton freight cars using wayside and vehicle-borne instrumentation are presented. Next, measurement of vertical track irregularities using an instrumented freight car is described. The vertical load environment developed by the response of this car to both revenue and controlled test track irregularities is given. This is followed by a description of the lateral and vertical loads produced during hunting of an empty and loaded 100-ton car. Finally, the wheel and rail loads developed under steady-state and dynamic curving of 100- and 125-ton cars are presented.

DESCRIPTION OF WHEEL/RAIL LOADS

A conventional freight car consists of a load carrying body supported by two rail trucks. The standard three-piece truck uses two wheel sets connected to two side frames through a very stiff primary suspension system and a bolster connecting

Association of American Railroads, 3140 South Federal Street, Chicago, Ill. 60616.

to the side frames through a secondary suspension system. The wheels, rigidly attached to an axle, are coned to provide self-steering action for the vehicle. The primary function of the suspension system is to provide guidance and stability and to isolate the car body from random track forces.

The wheel/rail forces that take place at the wheel/rail interface are composed of three components: vertical, lateral, and longitudinal forces. The vertical forces from the static weight of the car are attenuated or accentuated in magnitude because of the dynamic effects, such as those induced by the wheel tread and/or rail surface irregularities. The lateral forces result from the response of the vehicle to lateral track irregularities, creep, and wheel flange forces that arise from lateral instability and curving. Finally, the longitudinal forces are produced by the effects of train action, traction, and braking.

In qualitative terms, the forces acting on a freight car wheel set can be viewed in two broad categories: the wheel/rail contact forces and external forces (*1*). The external forces include the suspension forces, vehicle forces from gravity and couplers, and tractive and brake forces. The wheel/rail contact forces consist of normal and tangential forces acting at the contact patch at the wheel/rail interface. The normal forces act perpendicularly to the plane of contact. For large lateral wheel set excursions, the component of the force exerted on the wheel by the rail normal to the contact patch has a large lateral component, which is referred to as the flange force. The tangential forces in the contact plane are the longitudinal creep forces acting parallel to the direction of travel and lateral creep forces parallel to the wheel set's axis of rotation. Because of the tapering, when the wheels are forced to run outside the equilibrium rolling line, wheel creep or slip takes place. Resulting elastic deformations between the wheel and rail give rise to the lateral and longitudinal creep forces that balance all the forces exerted by the vehicle suspension system. The maximum creep force occurs during gross sliding of the wheel over rail and is determined by the product of normal force and the coefficient of friction by Coulomb's law of friction.

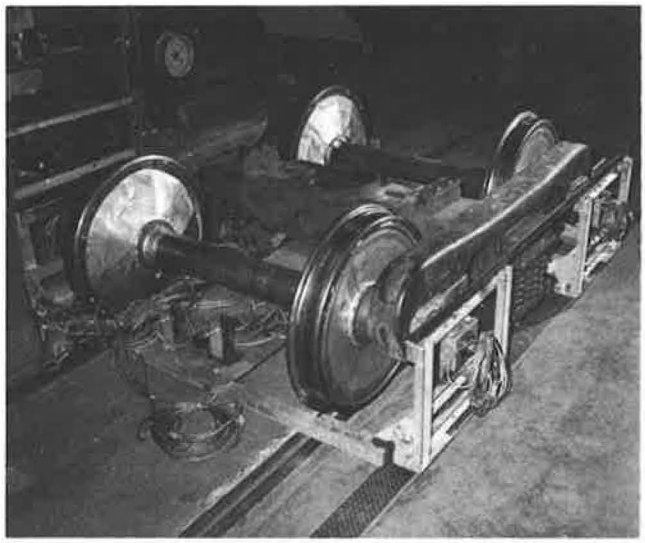

FIGURE 1 An instrumented wheel set.

WHEEL LOAD MEASUREMENTS

An accurate measurement of the dynamic forces developed at the wheel/rail contact patch is of utmost importance to characterize the dynamic performance of railway vehicles. Over the past decade, advances in finite element stress analysis techniques and electronics have made it possible to accurately measure these forces.

The instrumented wheel set and instrumented rail are the two fundamental measurement techniques for the determination of dynamic wheel/rail forces (*9–11*). In either case, strain gages are mounted on the wheel plate or on the spokes, if a spoked wheel is used, or on the rail, and the measured strains are translated into the wheel/rail forces. In either case, the triaxial components of the forces can be measured continuously.

The force measurements made by using instrumented wheel sets provide the load spectra for the specific car and the track segment it is used on. And the instrumented rail section provides the load spectra at a location in the track for a variety of cars. The wheel/rail load measuring wheel sets reported in this paper were developed by the IIT Research Institute (*11*). In this design, each wheel has strain gages mounted on the wheel plate connected to form six separate full Wheatstone bridges: three vertical, two lateral, and one position. The locations of the strain gages on the wheel plate are determined from an analytic study of strains on the surface of the wheel. The vertical bridges respond primarily to vertical loads acting on the wheel. The position bridge is used to determine the lateral position of the line-of-action of the vertical load. The remaining two bridges are used for lateral load measurements.

The electrical signals from the strain gage bridges are further processed to provide continuous vertical and lateral load measurements by using a dedicated microprocessor for each wheel set. The raw data are scaled and processed in real time to remove cross-talk effects that result from the interaction of the vertical and lateral bridge signals. Figure 1 shows such an instrumented wheel set.

VERTICAL DYNAMICS

A conventional freight car is supported by two trucks that are connected to the body through a suspension system with coil springs. As described previously, the primary objective of the suspension system is to have the wheels follow the track surface as closely as possible and to isolate the car body from the damaging vibrations induced by track irregularities. A car body supported on front and rear springs oscillates in a combination of pitching and bouncing about the center of gravity in the vertical plane. Similarly, car body roll, yaw, and sway oscillations arise from the relative motions between the vehicle and its trucks through the suspension system.

A mechanical system supported by springs will have natural frequencies that are inherent dynamic characteristics resulting from mass-stiffness effects. As a result, any mechanical system in motion will have critical speeds determined by the natural frequencies. Harmonic responses occur when the vehicle is subjected to periodic track surface irregularities such as jointed rails or even poor welds. Resonance occurs when the frequency at which the vehicle travels over the equally spaced rail joints coincides with the natural frequency of the car body on its suspension system. When resonance occurs, danger-

ously large oscillations occur, and the vehicle components experience excessive loads.

Car body roll and bounce motions are the most commonly encountered dynamic phenomena in North American railroad environment. There are two reasons for this. First, the vehicle roll and bounce natural frequencies are in the 1- to 2-H range, and resonance conditions can be induced by external forces within the operational speed range of these vehicles. Second, the track conditions that induce roll and bounce motions—staggered and nonstaggered rails—are always present in the track.

The result of excessive body roll and bounce is high dynamic loads imposed on the track and truck components resulting in spring bottoming, wheel lift, and track damage. Therefore, the effects of increased vertical and lateral wheel loads need to be investigated for their impact on maintenance and safety.

In general, response of a vehicle to staggered and nonstaggered track irregularities can be addressed by rock-and-roll and pitch-and-bounce evaluation. Both analytical and experimental methods are used in this evaluation. In the following subsections, selected results obtained from various vertical dynamics performance tests using typical 70-, 100-, and 125-ton cars are presented.

Rock-and-Roll

70-Ton Cars

In early 1986, as part of the High Productivity Integral Train Project, the Railmaster intermodal concept was tested at the Transportation Test Center in Pueblo, Colorado (*12*). The vehicle consisted of three modified highway vans with 70-ton frame-braced three-piece trucks. The trucks had a special adaptor bolster to couple the vans together. The trucks had variable column damping and D5 secondary suspension springs.

The rock-and-roll tests were run over an 800-ft tangent test section with 39-ft staggered rail joints with 0.75-in. maximum cross-level elevation. Test speeds ranged from 10 to 25 mph. The test results for the rear van are presented in the following paragraphs.

The vertical wheel loads for the leading axle of the rear truck were measured using a 33-in. instrumented wheel set. Figure 2 shows the maximum wheel loads for the right wheel versus speed, where most of the dynamic activity occurred within a critical speed range of 19 to 24 mph. At 23.3 mph, maximum wheel loads were 26 kips, and the corresponding 95th percentile of L95 values (a statistical parameter defining a level that is exceeded 5 percent of the time) was 22.7 kips. The static wheel load on this lightly loaded 70-ton truck was about 12 kips. Therefore, the ratio of a maximum vertical wheel load to its static level, representing dynamic augmentation, was about 2.2. The maximum lateral wheel loads (not shown here) were as high as 8 kips. The peak lateral/vertical (L/V) ratios resulting from the peak lateral loads were about 0.5.

The measurements of spring deflections indicated that spring bottoming did not occur during resonant roll motion of the vehicle. The maximum peak-to-peak car body roll angles were about 6 degrees.

In order to determine the load environment as affected by high curvature and cross-level variations, the same vehicle was tested in the 7.5-degree curve on the Balloon loop at the Transportation Test Center in Pueblo, Colorado (TTC). The test track had 4.5 in. of superelevation resulting in a balance speed of approximately 30 mph.

Figure 3 shows how the peak vertical loads varied as speed increased from 14 to 35 mph. Maximum wheel loads of 27 and 23 kips, experienced on the low and high rails near the critical roll speed of 23 mph, represent dynamic load factors of 2.3 and 1.9, respectively. The peak lateral loads were 9.6 kips on the low rail and 7.3 kips on the high rail at 23 mph.

The maximum vertical loads measured on the leading truck of the vehicle, which were shared by two adjacent vans, were

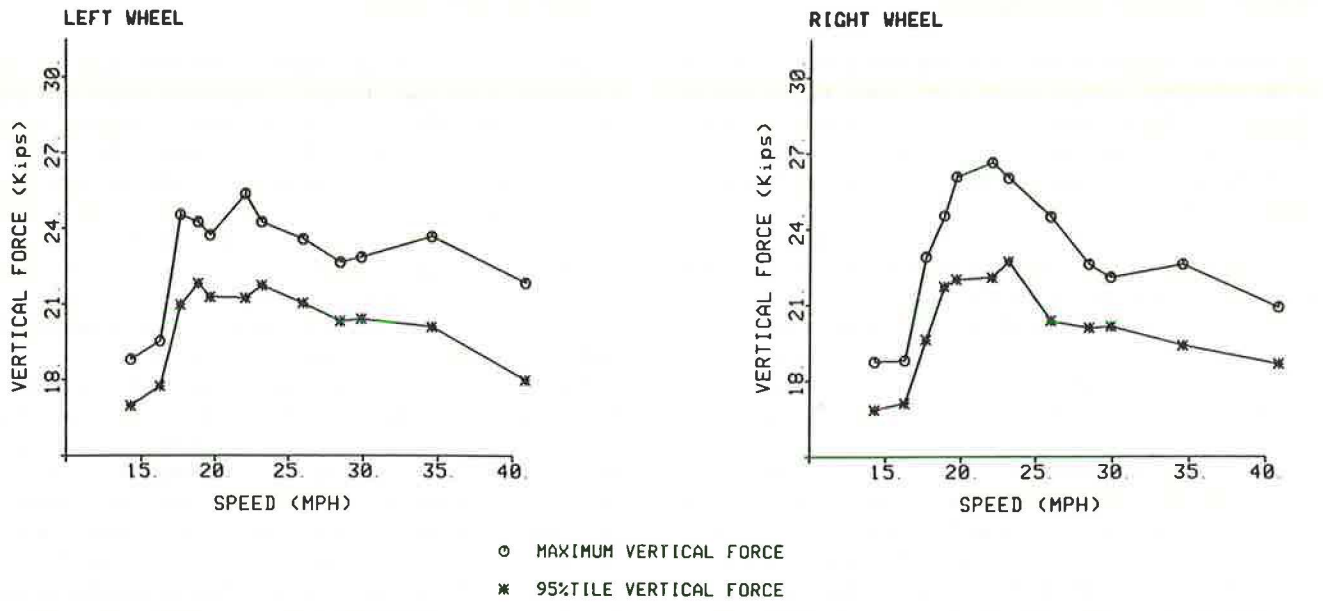

FIGURE 2 Maximum vertical wheel load versus speed for a lightly loaded 70-ton truck, measured with tangent rock-and-roll tests using instrumented wheel set data.

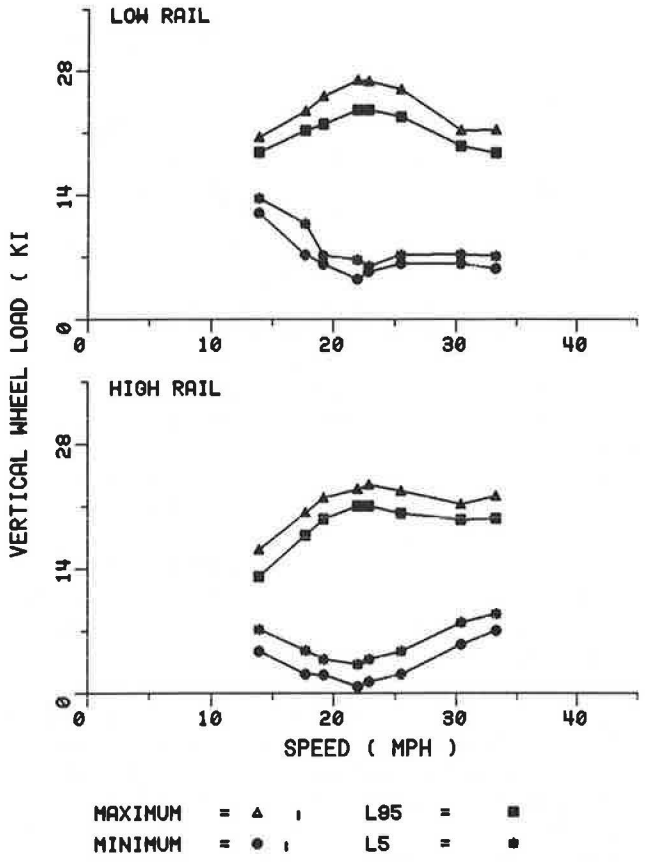

FIGURE 3 Maximum vertical wheel load versus speed for a lightly loaded 70-ton truck, measured with 7.5-degree-curve rock-and-roll tests using instrumented wheel set data.

of the same order. Peak vertical load on the high rail on the 7.5-degree curved track was about 34 kips, which represented a dynamic load factor of 1.8 (the static wheel load on the shared truck was 19 kips). The maximum lateral load on the high rail was about 12 kips. Suspension spring bottoming was not experienced at any speed at which the vehicle was tested.

In light of these results, the dynamic wheel loads produced during roll resonance of a vehicle equipped with 70-ton frame-braced trucks varied from 1.8 to 2.3. These results are not meant to represent the dynamic load environment seen under a standard 70-ton car during roll resonance. It should be kept in mind that these data are intended to provide limited information for a special freight car equipped with 70-ton trucks. We were unable to compare these results with those of the standard 70-ton cars because the experimental studies leading to quantification of the dynamic load environment under standard 70-ton cars are not well reported in current literature.

100-Ton Cars

As part of the High Performance Covered Hopper Car Project (*13*), one of the most comprehensive on-track dynamic performance test series of 100-ton covered hopper cars was conducted at the TTC in the early 1980s. The vehicle was instrumented with transducers to measure the accelerations and displacements at both the car body and truck levels. Instrumented wheel sets were used on the leading truck of the test vehicle to measure the vertical and lateral loads during rock-and-roll motion of the vehicle. The tests were run over 400-ft tangent and 7.5-degree curved test sections, with 39-ft staggered rail joints set at 0.75-in. cross-level elevation. Test speeds ranged from 10 to 25 mph.

Figure 4 shows the maximum and minimum levels of the wheel loads for the loaded car on tangent track. Peak maximum loads were developed at speeds near resonant roll speed of the vehicle. The maximum wheel load experienced at the critical roll speed of 17 mph—78,000 lb—represents a dynamic load factor of 2.4. It is seen from this figure that in a speed range from 15.5 to 18 mph, extended wheel lifts occurred. During maximum roll response, the car body rolled as much as 10 degrees peak-to-peak.

The dynamic loading and unloading of the leading axle of the leading truck were also very severe on the curved track. Figures 5 and 6 show peak low- and high-rail vertical loads with respect to vehicle speed. Near the critical roll speed of

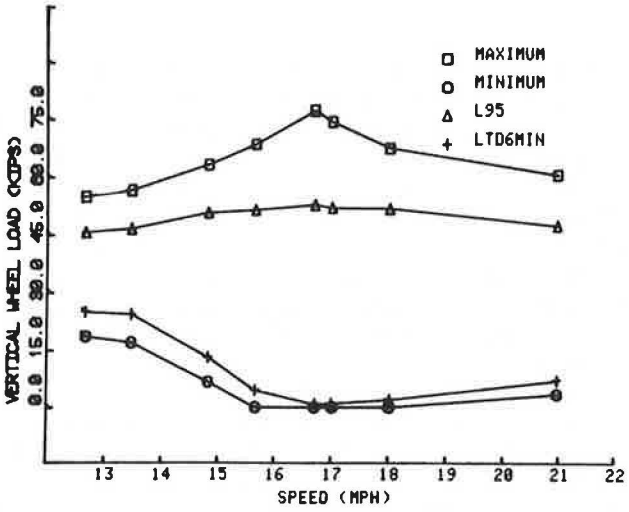

FIGURE 4 Vertical wheel loads under a 100-ton loaded hopper car, measured with tangent rock-and-roll tests using instrumented wheel set data.

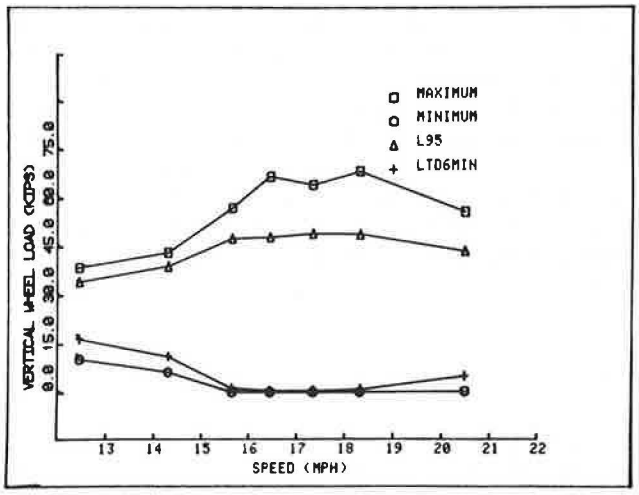

FIGURE 5 High-rail vertical wheel loads for a 100-ton loaded hopper car, measured with curved track roll tests.

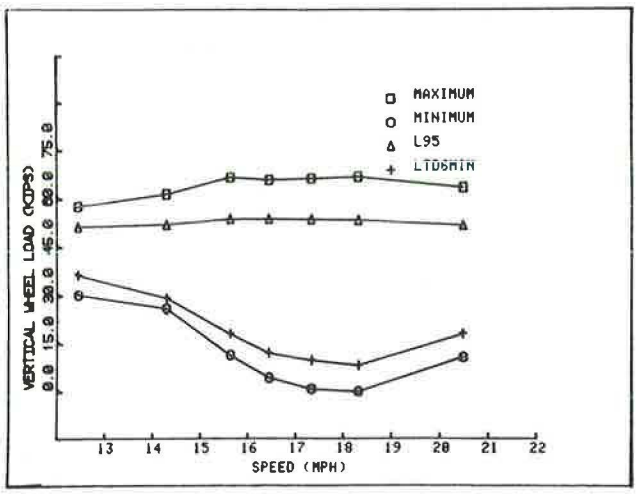

FIGURE 6 Low-rail vertical wheel loads for a 100-ton loaded hopper car, measured with curved track roll tests.

17 mph, the peak loads were as high as 68,500 lb on the high rail. At speeds ranging from 15.5 to 18.5 mph, extended wheel lifts occurred on the high rail; duration of 100 percent wheel unloading was at least 250 sec. The low-rail loads were higher than the high-rail loads, consequently the low-rail wheel unloading was less than that of the high rail. It should be noted that, on a 7.5-degree curve with 4.5-in. superelevation, higher dynamic loads develop on the low-rail side because of the offset of the car's center of gravity resulting from unbalanced running conditions, along with the increased roll in the low-rail direction.

In conclusion, the peak vertical loads developed during resonant roll motion of the 100-ton loaded car on tangent and curved tracks were comparable and equally severe. In both cases the measured loads were more than twice the static wheel load, and the resulting car body roll angles were as high as 10 degrees peak-to-peak.

Track loading resulting from rock-and-roll motions of a vehicle at critical speeds is severe. As a result of excessive body roll, the weight of the vehicle may shift into the side bearings. Suspension spring bottoming occurs, and resulting violent undamped motions cause excessive loading of one side of the vehicle with the other side lifting clear of the track. The asymmetric loading of the track structure along the direction of travel produces excessive stresses on the track components at the weakest point in the track structure resulting in accelerated deterioration and additional loss of track geometry. With increasing cross-level elevation, the vehicles operating over the same track section experience higher and higher loads bringing about additional geometry loss resulting in increased derailment propensity.

125-Ton Cars

The 125-ton dynamic load environment is relatively new to the railroads, but it is getting increased attention in recent years, particularly with the upcoming Facility for Accelerated Service Testing (FAST) tests. Preliminary tests consisted of a series of rock-and-roll tests using a consist of five 125-ton covered hopper cars. These tests were conducted at the TTC in early 1988 to quantify the loading environment and response of a typical track under heavy axle loads.

The test track consisted of 20 39-ft staggered rail sections with a maximum of 0.75-in. cross-level difference. Three adjacent cribs were instrumented for vertical and lateral load measurements. As shown in Figure 7, at speeds from 16 to 20 mph, coincident with the critical roll speeds of the vehicles, dynamic rail loads ranging from 80,000 to 110,000 lb, accompanied by excessive wheel unloadings, were measured.

Figure 8 shows the maximums of all of the wheel loads measured under the fourth car, which had the worst response characteristics. The vehicle appears to experience its maximum amplitude response near 16 mph, with the exception of the leading axle of the leading truck, which had increasing loads.

Vertical loads presented for the 125-ton cars were measured using wayside instrumentation. Instrumented wheel set data, which represent a continuous wheel load trace over all 20 irregularity waves, are not currently available for this car.

However, wheel load data taken from an instrumented wheel set of a 125-ton truck equipped with a primary suspension system are available (*14*).

This vehicle was tested on the same perturbed roll track at TTC over a speed range of 10 to 25 mph. At the resonant roll speed of 18 mph, probability distributions of the left vertical and lateral wheel loads over both the tangent and rock-and-roll sections are presented in Figures 9 and 10, respectively. The tangent track response was obtained at the same speed on the track section located just before the perturbed track. The distribution curves were plotted on Gaussian probability paper, so that the characteristics of the probability distribution functions are emphasized. The solid straight line in these plots is typical of random data, and it represents the measured distribution function of the instantaneous values of the wheel loads on the smooth tangent track. In the case of the roll response, the typical distribution functions give nonlinear plots, typical of sinusoidal waveforms. The low probability events represented by the tail ends of the distribution curve correspond to excessive wheel loading and unloading.

For this vehicle, the maximum vertical and lateral wheel loads were 77,000, and 33,000 lb, respectively. It is seen from the results for the two 125-ton trucks, one equipped with a primary suspension system and one without, that the dynamic loads seen under premium trucks were 40 percent lower. In other words, the maximum dynamic load factor for the standard truck was 2.8 times the static load, as compared with the premium truck, which had a maximum wheel load of 1.8 times the static load.

Pitch-and-Bounce

70-Ton Cars

Fatigue analysis of freight cars adapted by the AAR recommends the collection of load spectra for different types of cars over a broad range of track at a variety of train speeds. While collecting environmental load data from the operation of a 70-ton boxcar during FEESTs (freight equipment environmental sampling tests), bolster loads in excess of 1.8 *g* were

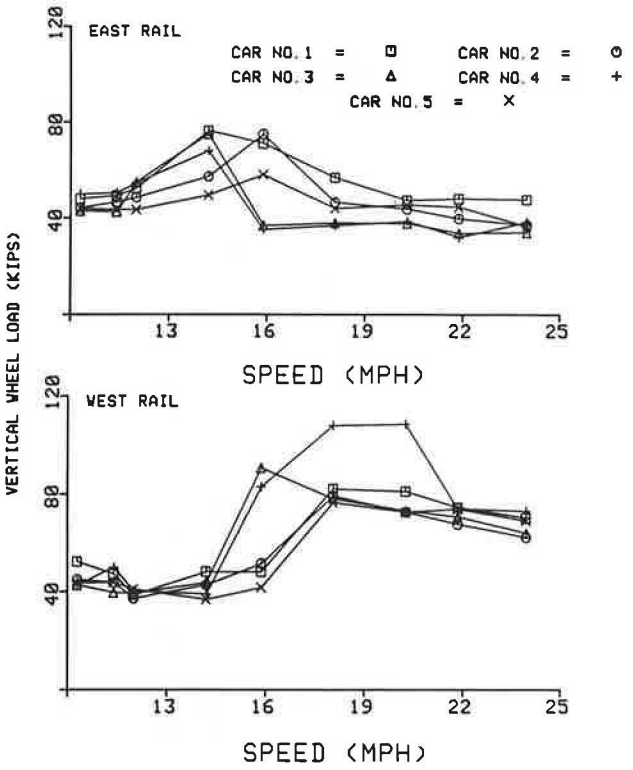

FIGURE 7 Vertical rail loads under a 125-ton loaded covered hopper car, measured with tangent track bounce tests using wayside data.

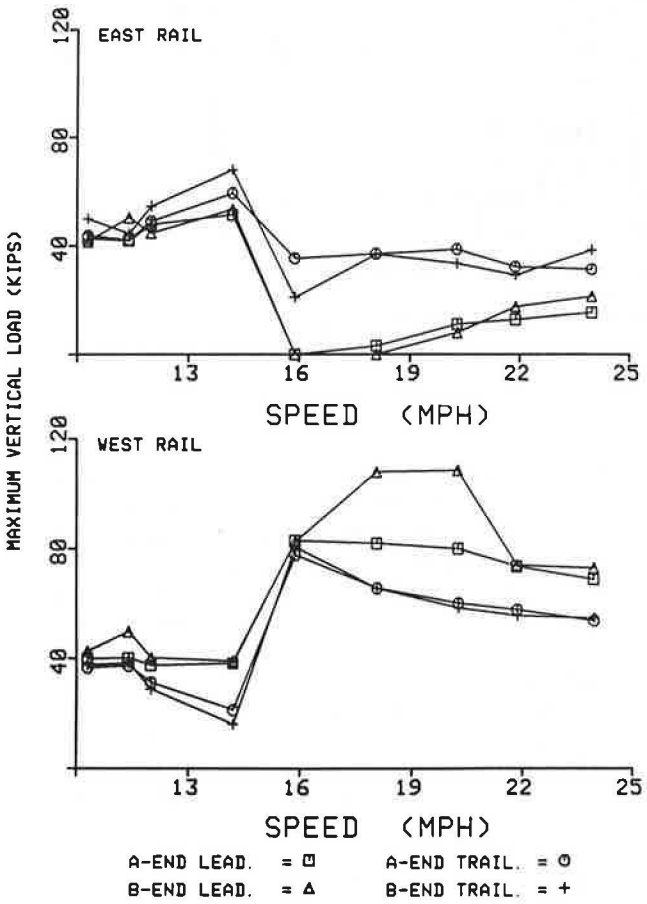

FIGURE 8 Vertical rail loads versus speed for a 125-ton loaded hopper car, measured with tangent rock-and-roll tests using wayside data.

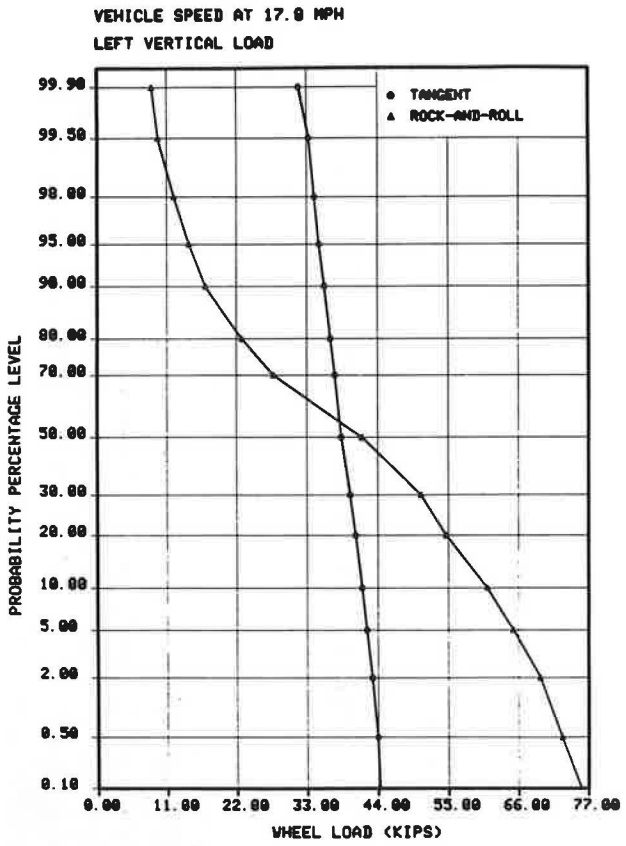

FIGURE 9 Probability of distribution of vertical wheel loads for a loaded 125-ton truck, measured using instrumented wheel set data.

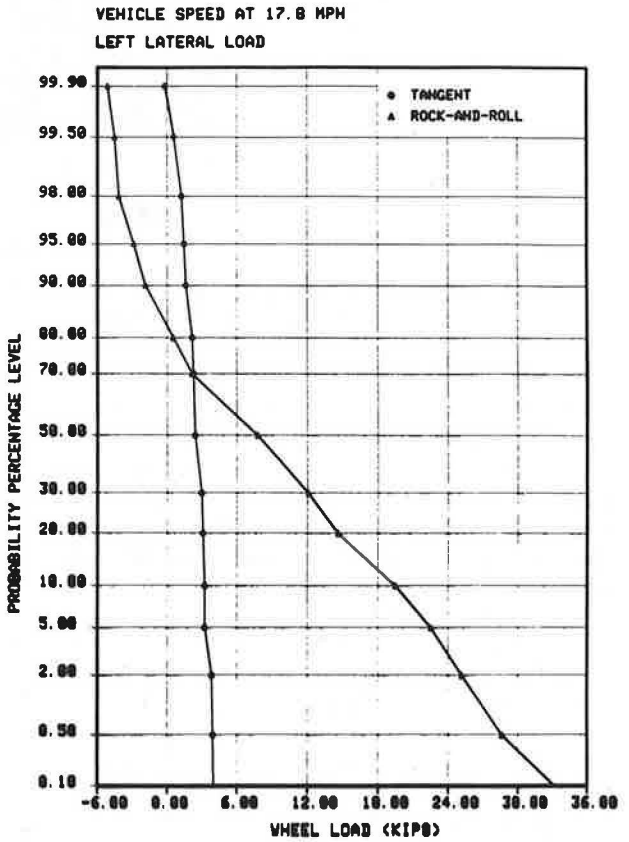

FIGURE 10 Probability of distribution of lateral wheel loads for a loaded 125-ton truck, measured using instrumental wheel set data.

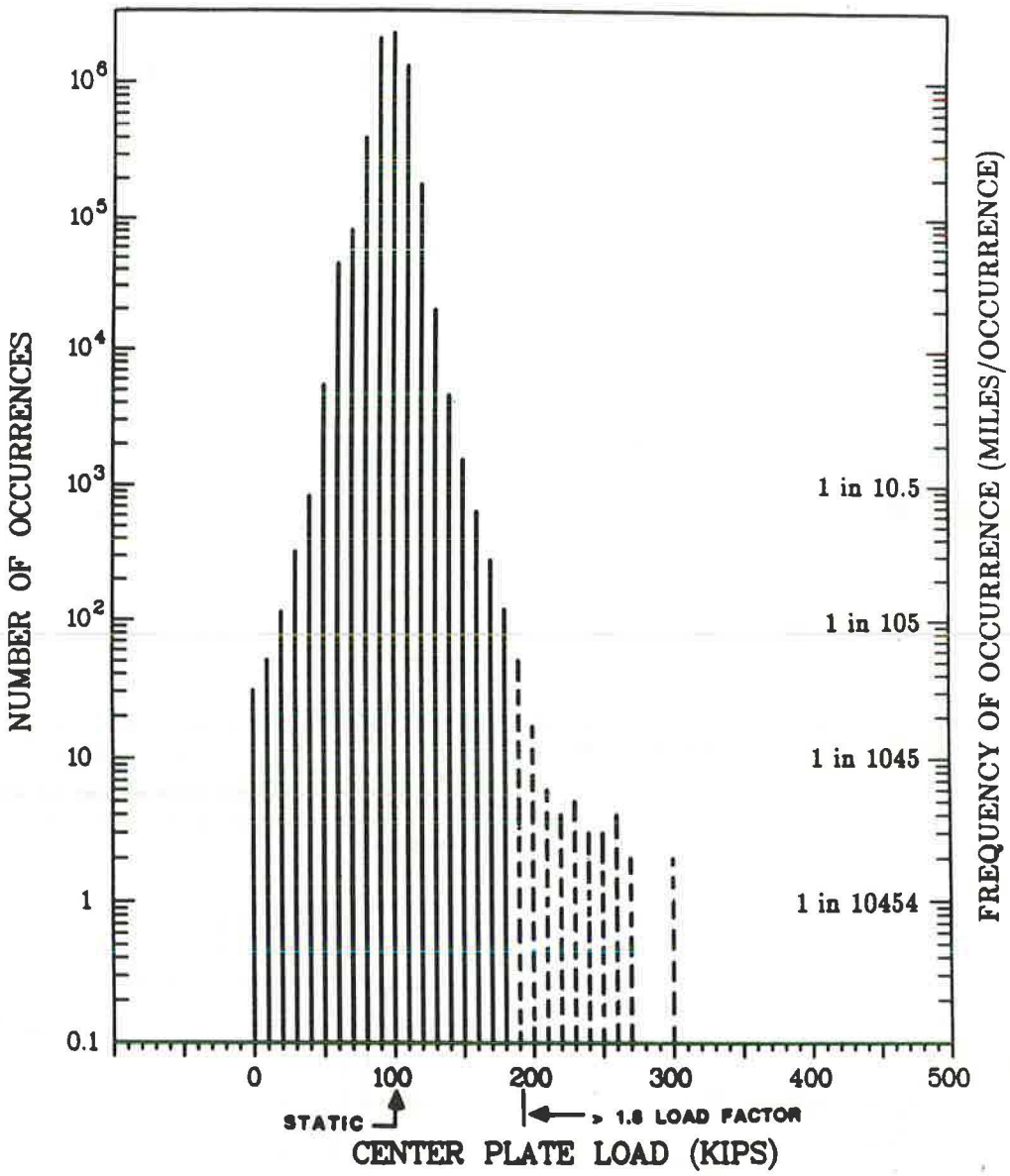

FIGURE 11 Histogram of center plate loads for a 70-ton loaded boxcar, measured with FEESTs using instrumented truck bolster data.

experienced (*8*). An analysis of the effects of the loads that are in excess of the design values on the fatigue life of a freight car was made. It was found that these high-magnitude, low-occurrence loads cause considerable fatigue damage. Figure 11 shows the occurrence histogram of center plate loads, collected over 12,000 mi for a fully loaded 70-ton boxcar. It can be seen from this figure that the design value of 1.8 *g* is exceeded, approximately two times every 100 mi.

In order to locate the track geometry that causes these high loads, the 70-ton boxcar was instrumented with a new unattended data collection system and operated in conjunction with a track geometry car on a major railroad (*15*). A paint-spray system was installed on the test car to identify the location of these high loads.

Sixteen locations were identified and spotted with a deposit of yellow paint on the track at each location. The measured loads varied from 183 to 328 kips on the bolster, which had a static load of 100 kips. The track irregularity sites that caused these high loads fell into two broad categories: those that were characterized by a single irregularity and those that had multiple irregularities.

The single irregularities were usually associated with some type of weak track segment, such as an insulated rail joint, field weld, or engine burn, causing the car to exhibit a pitch response.

Inspection of the multiple irregularity sites indicated that the load-producing irregularities were associated with open track on continuously welded rail having a series of parallel vertical irregularities at intervals equivalent to the rail length of 39 ft. At all sites examined, the dips on the track were coincident with the plant welds on one rail. Figure 12 shows the bolster load time history at a multiple irregularity site where a maximum load of 328 kips was measured.

The paint-spotter tests, in effect, showed that a series of

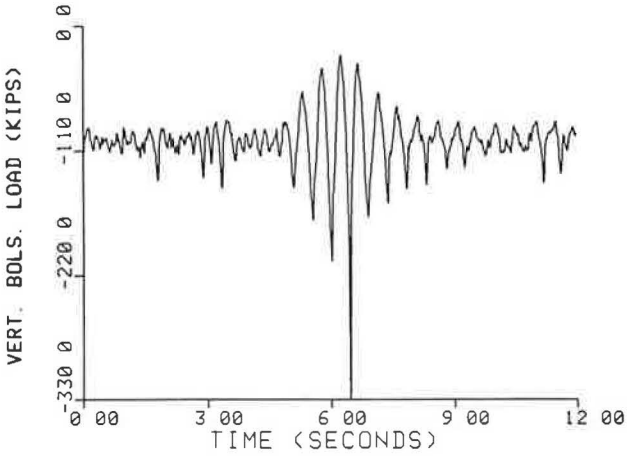

FIGURE 12 Truck bolster load time history for a 70-ton boxcar at 63 mph at a multiple irregularity site.

track profile irregularities can cause car loads in excess of the design level.

The same 70-ton boxcar was further tested under controlled conditions at the TTC's bounce section, which had 10 39-ft nonstaggered vertical irregularities with a maximum amplitude deviation of 0.75 in. (*16*). Both vehicle-borne and wayside instrumentation were used. Truck bolster loads and vertical rail loads were measured at speeds from 30 to 75 mph. The track was instrumented for vertical rail load measurements at the seventh irregularity wave.

The results of the tests showed that truck bolster vertical loads as high as 550,000 lb and car body accelerations as high as 5 *g*, accompanied by consecutive cycles of suspension bottoming and center-plate lift-off, were experienced at a critical bounce speed of 65 mph. Figure 13 shows the maximum and minimum bolster loads plotted versus speed. The vehicle responds to track irregularities with lower vibration amplitudes at speeds from 30 to 50 mph. In this speed range, the bolster loads fluctuate slightly above and below the static load of 100,000 lb, because the suspension system effectively isolates the car body from the external disturbances provided by track irregularities. At speeds near 65 mph, the dynamic activity at both the truck and car body levels sharply increases, indicating a resonance condition. At this speed, the vehicle experiences its maximum bolster load of 550,000 lb and a minimum bolster load of zero.

The results of the track testing using wayside instrumentation are shown in Figure 14, where the maximum wheel/rail loads measured on the seventh irregularity wave are plotted with respect to test speed. A typical bounce resonance characteristic is seen from this figure. The wheel/rail loads sharply increase at speeds above 60 mph, peak at 65 mph as a result of bounce resonance, and decrease as speed increases with the track-forcing-frequency becoming outside of the range of the car body's natural bounce frequency. The truck loads shown in Figures 13 and 14 are not directly comparable because the peak loads shown in Figure 13 occurred on the eighth irregularity wave. However, the maximum load exerted on the test track (the seventh irregularity wave) by the leading truck approaches 420,000 lb—extremely high for any track structure to withstand without experiencing some level of permanent damage.

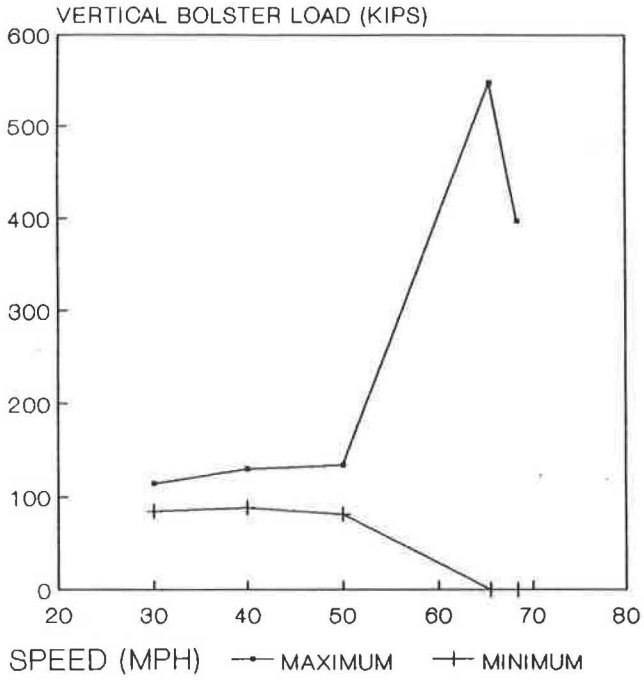

FIGURE 13 Maximum and minimum bolster loads versus speed for a 70-ton boxcar, measured with vehicle bounce tests.

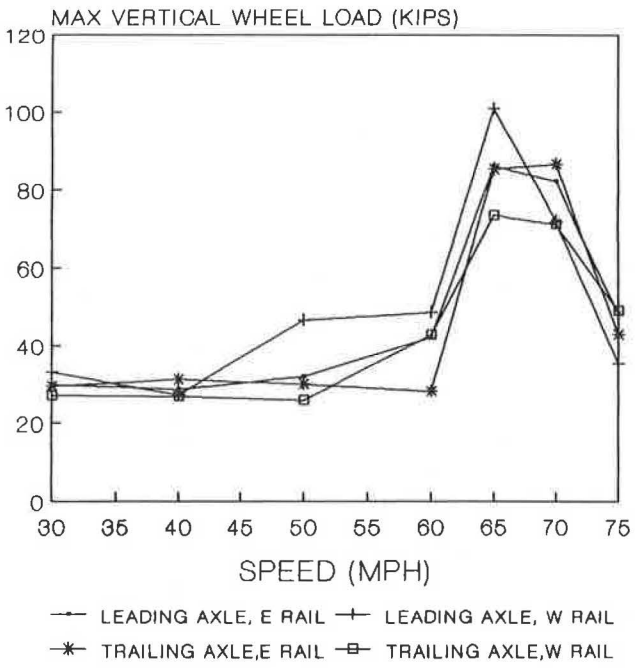

FIGURE 14 Maximum vertical rail loads versus speed for a 70-ton boxcar, measured by bounce tests using wayside data.

100-Ton Car

A 100-ton coal car was tested together with the above 70-ton boxcar for bounce characterization. Figure 15 shows the measured wheel/rail loads at each instrumented crib location at 67 mph, near resonance bounce speed. The leading truck loads peak at the sixth instrumented crib, near the peak of

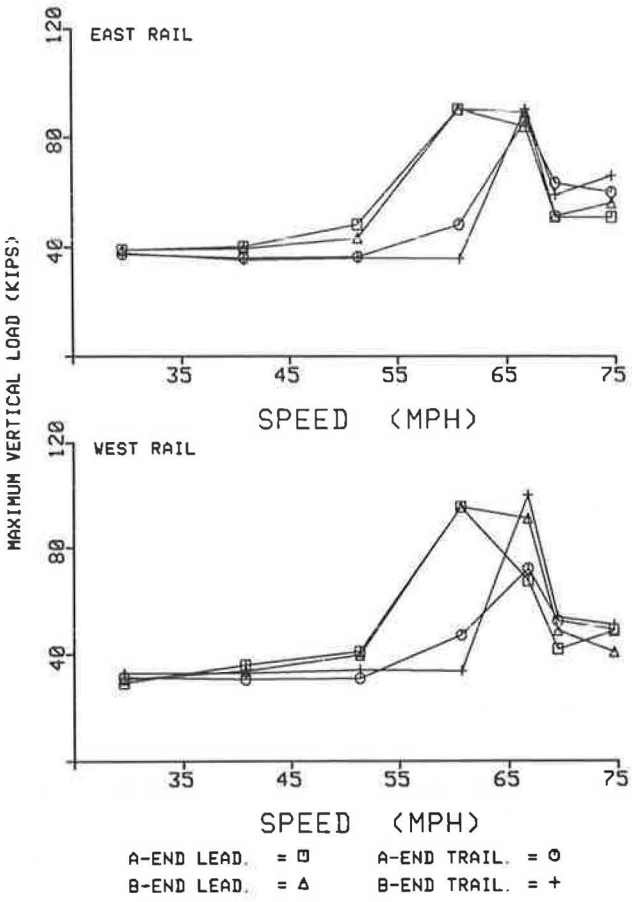

FIGURE 15 Vertical rail loads versus speed for a 100-ton loaded coal car, measured with bounce tests using wayside data.

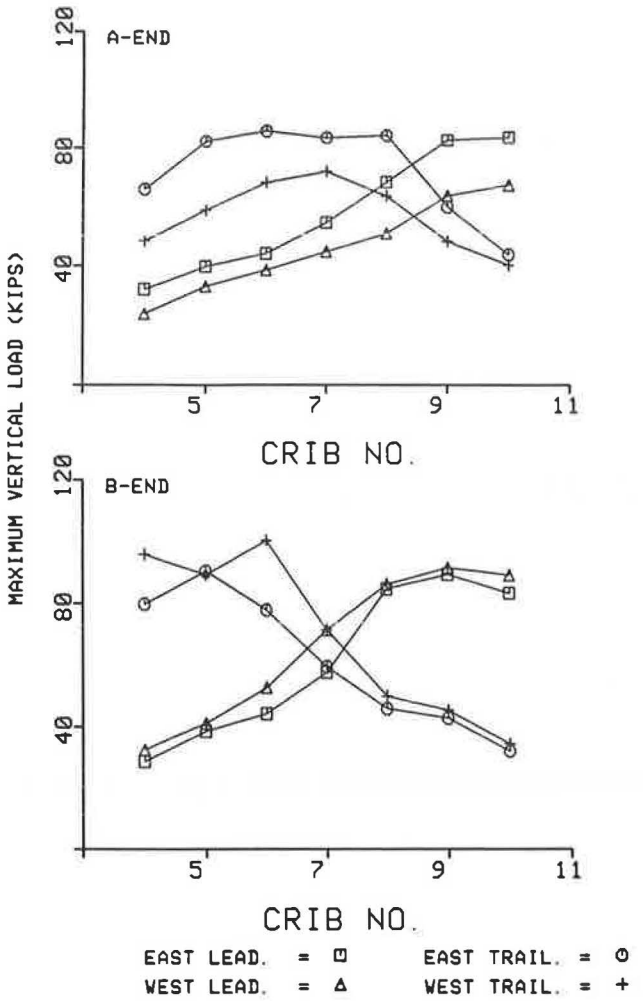

FIGURE 16 Vertical rail load at each instrumented crib for a 100-ton hopper car, measured at 65 mph with bounce tests.

the track irregularity wave. Note that the distance delay between the load peaks of the leading and trailing trucks results from a 70-in. 100-ton truck wheel base (distance extending over four instrumented cribs).

Figure 16 shows a plot of vertical wheel loads as a function of test speed. At speeds between 60 and 65 mph, the vehicle exhibited a severe bounce resonance condition in which the oscillation amplitudes were limited only by the available friction in the suspension system if the springs did not bottom out. The measured wheel/rail loads reached levels above 100,000 lb on a car with 33,000 lb of static wheel load. Above the resonant speed, the vehicle traveled smoothly over the track irregularities with considerably attenuated response amplitudes as the track irregularities were taken up by the suspension springs.

The total vertical bolster load environment encountered by standard 100-ton open hopper and hi-side gondola cars was also measured during FEESTs. Figure 17 shows the frequency of occurrence diagram for the 100-ton loaded open hopper car center plate loads collected over several thousand mi of revenue track at a wide range of operating speeds. Note that the static load on the bolster was about 120 kips. As shown in Figure 11 for the 70-ton car, a considerable number of occurrences is seen at levels above 1.8 times the static load. Also note that the maximum test speed was 60 mph, and the average test speed was 23.3 mph. Similar load levels were reported for the hi-side gondola car in unit train service (AAR-M1001).

125-Ton Cars

A train consist having five 125-ton covered hopper cars—the same consist for which rock-and-roll performance was described earlier—was tested over the same perturbed track for bounce performance. Eleven consecutive cribs were instrumented for vertical rail load measurements.

Figure 18 shows the variation of vertical wheel loads of one of the 125-ton cars over the instrumented track section at 69 mph. The dynamic signal clearly represents the dynamic load response resulting from the track irregularity. The maximum rail load measured on the east rail under the trailing truck was as high as 150,000 lb, which represents a dynamic load factor of 3.9. Evidently, the rail loads under the leading axles on each truck peak first toward the middle of the instrumented track, and the trailing axle loads increase to peak toward the end of the instrumented track because of the time delay introduced by the wheel base. Both the leading and trailing trucks exhibit similar response characteristics partly because of the truck center distance of 36.5 ft, which is fairly close to the irregularity wavelength of 39 ft.

For the five cars tested together, the measured rail loads ranged from 60,000 to 150,000 lb at the maximum test speed of 70 mph, depending on the car types, as shown in the vertical

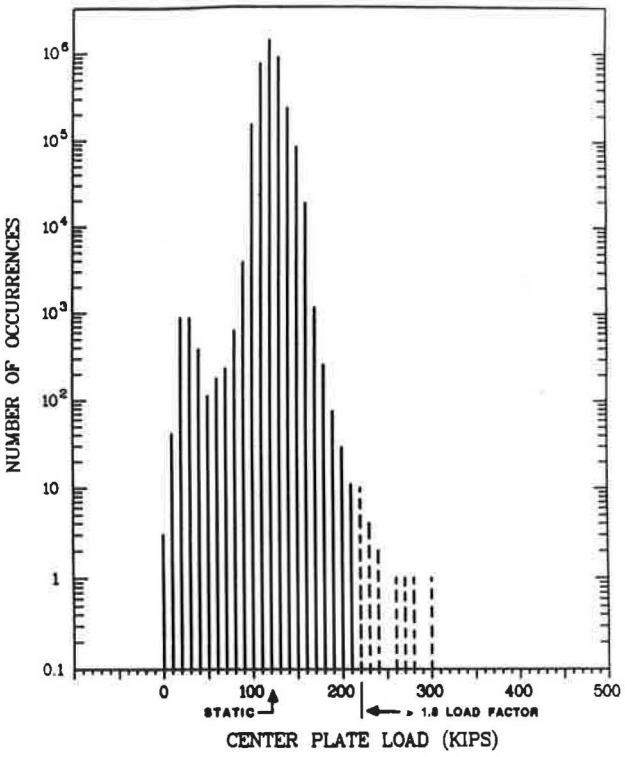

FIGURE 17 Histogram of center plate loads for a 100-ton loaded open-top hopper car FEEST test using instrumental bolster data.

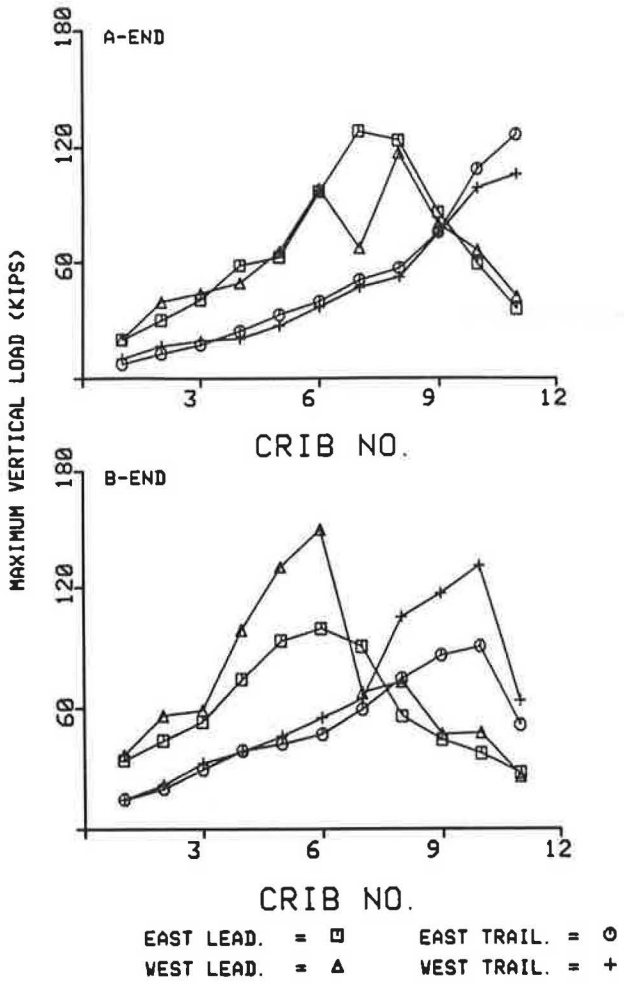

FIGURE 18 Variation of vertical rail loads over instrumented track for a 125-ton loaded car.

load versus speed plot in Figure 19. As seen from this figure, the high-peak loads consistently occurred under two of the 125-ton cars. The maintenance history of these cars is unknown, and it is likely that some suspension characteristic, related either to truck type or physical condition of the trucks, is the primary cause of these high loads. Several follow-up activities are currently under way to help understand the origin of these loads and develop possible corrective actions that might limit the peaks.

The third 125-ton car, the bounce performance of which was given in Figure 19, was tested at a later date by using instrumented wheel sets at the leading axle of the leading truck. Figure 20 shows the variation of the vertical wheel load as a function of speed. The peak load at 70 mph was as high as 130 kips, as shown in Figure 19. Figure 20 shows a comparison of wayside loads to instrumented wheel set loads, with an excellent agreement achieved at almost all test speeds. Truck suspension dependency of a vehicle's bounce response is clearly illustrated in Figure 21, in which the track loads measured under a train consist include, in order, a six-axle locomotive, FRA's T-7 instrumentation car, two 100-ton covered hopper cars, and the aforementioned 70-ton boxcar.

The locomotive and the instrumentation car, which are equipped with premium trucks with both primary and secondary suspension systems, exhibit superb bounce responses. For these cars, no apparent resonant condition is observed, and the dynamic loads virtually remain slightly above the static wheel loads. Obviously, the worst among them all is the 125-ton car tested over the same track at the same speeds.

The data presented here indicated that the vertical loads developed during bounce resonance can be extremely high. The peak dynamic loads measured under the 70-, 100-, and 125-ton cars during bounce resonance varied from 2 to 5 times the static wheel loads. Considering that the track is loaded to a maximum level under a bouncing truck, the transmission of the total load to all track components would lead to serious problems, such as (a) vertical geometry loss resulting from permanent settlement, (b) component fatigue, (c) ballast breakdown, and perhaps (d) subgrade failure.

It should be noted that the data presented here pertain to standard vehicles with average physical condition. The strong dependence of the dynamic bounce response of these vehicles on the suspension system was clearly seen from the data. The 125-ton covered hopper car data are intended to be used for comparison purposes only, because they do not represent the future 125-ton fleet, which may have premium suspension systems.

HUNTING

In some mechanical systems, self-induced oscillations can be maintained by energy sources having no oscillatory properties. The energy sustaining this motion is created by the vibration itself. In railway vehicles, the self-excited lateral oscillations, referred to as hunting, begin spontaneously at a threshold speed. This lateral instability is promoted by the

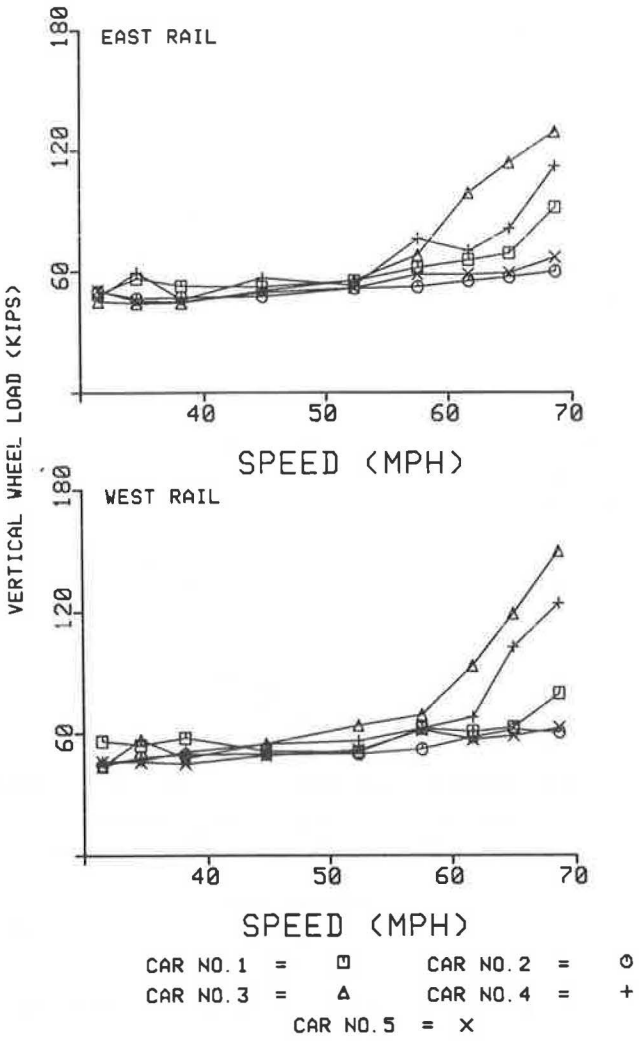

FIGURE 19 Vertical rail loads versus speed for a 125-ton loaded hopper car, measured with bounce tests using wayside data.

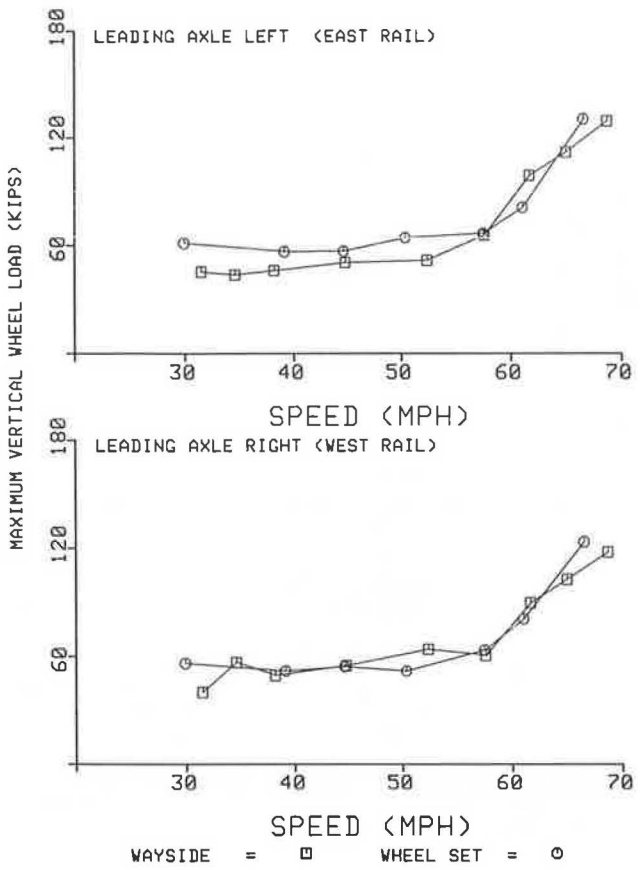

FIGURE 20 Maximum wheel load comparison of wayside and instrumented wheel set measurements from bounce tests of a 125-ton covered hopper car.

self-steering behavior of the coned wheels, and the energy to sustain this motion is provided by the wheel/rail force feedback system.

When the lateral equilibrium state of the vehicle becomes unstable, any initial perturbation (such as that from changes in the rail head profiles, as well as irregularities in the lateral alignment and rail gage) causes the amplitudes of the oscillations to increase. With increasing vehicle speed, one of the truck vibrational modes becomes the least damped mode, and larger oscillations can develop. If the oscillations are large enough, any further increase in the amplitude is precluded by the wheel flanges. In this steady-state-like limit-cycle motion, the amplitude and frequency remain constant.

70-Ton Cars

The Railmaster intermodal concept (its dynamic load environment resulting from rock-and-roll was described previously) was tested for high-speed lateral stability on tangent track at TTC (*12*). The test consist included a locomotive and the three-van Railmaster intermodal car. The trailers were empty, and the trucks were equipped with 70-ton cross-braced trucks with Canadian National Heumann profiled wheels. The test runs started at 30 mph, and a speed increment of 5 mph was chosen. The test runs continued until it was determined that the onset and sustained hunting conditions had been observed or the 80-mph speed limit had been achieved.

The measurements used for the hunting tests included lateral accelerations and displacements at car body and truck levels. The lateral and vertical wheel loads were measured on the leading axle of the lightly loaded rear truck of the rear van using an instrumented wheel set. The analyses of lateral accelerations indicated that the first sign of hunting manifested itself in increased lateral activity at 60 mph. At 70 mph, fully sustained hunting motion was observed at both the truck and body levels of the rear van. At 65 mph, the rms lateral acceleration on the rear truck was about 0.2 *g*. It should be noted that the vehicle was equipped with cross-braced trucks, which provide better lateral stability than the conventional three-piece trucks because of increased interaxle shear stiffness.

The lateral loads at the leading axle of the rear truck were investigated to determine the effects of hunting motions at the wheel/rail interface. The peak lateral loads are shown in Figure 22 as a function of speed. The maximum lateral loads increase with speed to about 5 kips on both wheels at 70 mph, but the 95th percentile of the lateral loads was a maximum of 2.5 kips. It was concluded from the results of the lateral

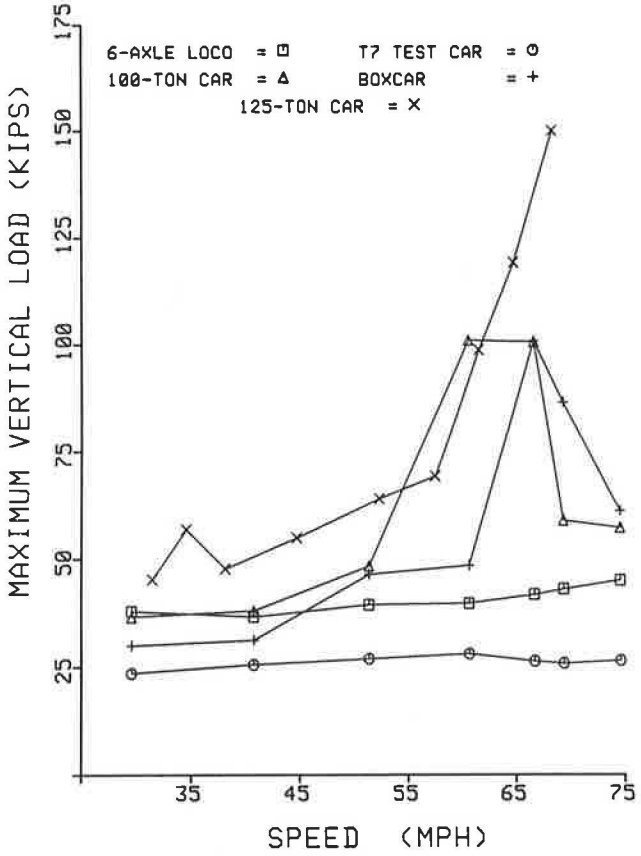

FIGURE 21 Vertical load environment under typical railroad cars, measured with bounce tests.

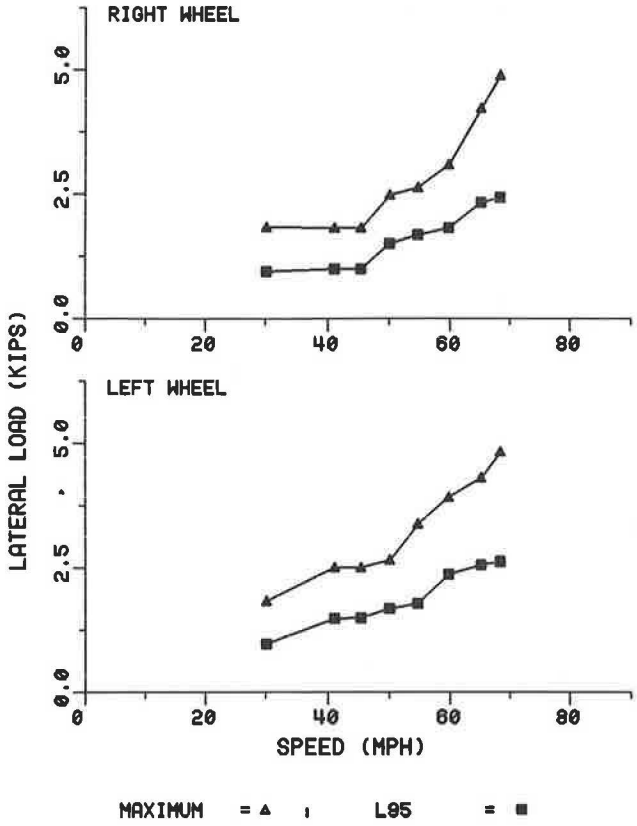

FIGURE 22 Peak lateral wheel load versus speed for a 70-ton truck, measured using instrumented wheel set data.

load response that, during hunting motion of the rear truck, sustained wheel flanging was not evidenced.

100-Ton Cars

As part of the High Performance, High Cube, Covered Hopper Car Project (*4,17*), a 100-ton covered hopper car of current design was tested for dynamic performance at the TTC. The vehicle was instrumented with transducers to measure the accelerations and displacements at both the car body and truck levels. Instrumented wheel sets were used on the leading truck of the test vehicle to measure the vertical and lateral loads of a hunting vehicle. The tests were run on a mile-long tangent track at speeds from 30 to 70 mph, in 5-mph increments. The dynamic load environment developed under the test car is presented in the following paragraphs.

The lateral loads produced at the onset of hunting, as well as those developed during fully sustained hunting, are shown in Figure 23. Absolute peak and L95 lateral load levels on the leading axle show a sharp increase at 51 mph, indicating the onset of hunting. Peak lateral loads of up to 15,300 lb were developed at speeds above 60 mph when the wheel flanges hit against the rails during violent hunting motions of both the car body and its trucks. The frequency of this motion took place at about 3.5 H, as seen in the time history plot of Figure 24.

Truck hunting is not a prevalent loaded car phenomenon because of the stabilizing effect of the increased axle load on hunting. It does, however, occur at relatively higher speeds than on an empty car. The loaded car hunting tests were conducted by using the same test car on the same tangent track on which the empty car was tested. The lateral wheel/rail forces recorded at the wheel/rail interface are shown in Figure 25, in which the sharp increase in the load levels at 60 mph indicate the onset of hunting. Peak maximum and L95 lateral loads experienced on the left wheel of the leading wheel set were about 18,000 and 13,500 lb at 71 mph, respectively. The lateral loads shown in Figure 26 imply that, during sustained hunting, frequent flange contacts occurred.

At and above the critical hunting speed of a vehicle, the wheel flanges contact the rail resulting in excessive wear of the wheels and rails and increased maintenance. During hunting, large lateral loads are exerted on the vehicle and track. These loads tend to develop wide gage (*18*) and lateral alignment problems on track. Truck hunting, when combined with track irregularities, creates a potential for derailment. Moreover, the excessive lateral and yaw motions of the wheel set increase the rolling resistance, resulting in increased energy consumption.

Despite being conducted on well-maintained, good quality track, both the empty and loaded car hunting tests indicated severe high-frequency lateral wheel loads, which changed direction as the wheel sets moved from flange to flange. These loads were certainly capable of creating high alternating stresses. These stresses could cause fatigue damage of the wheels and various vehicle components, as well as the rails, while weakening the track structure.

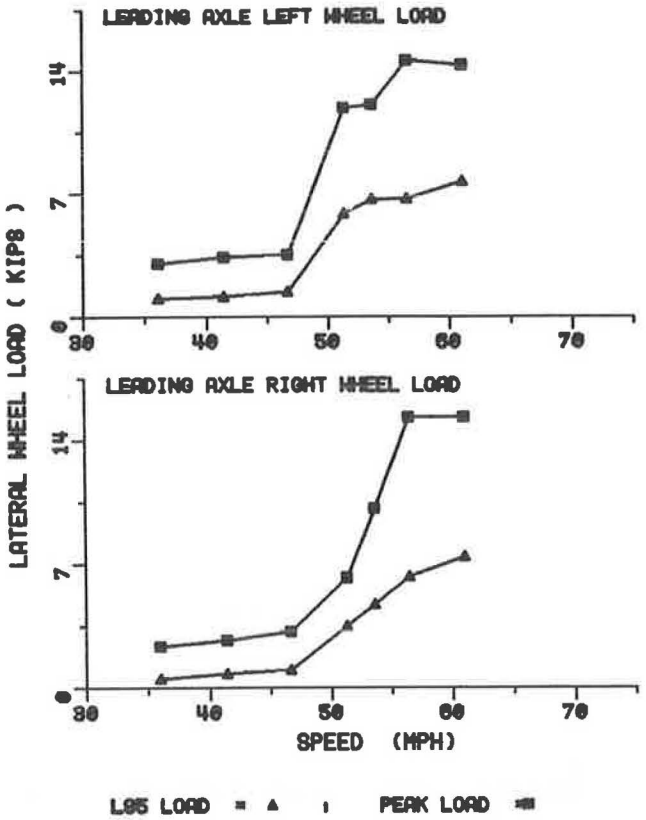

FIGURE 23 Peak lateral wheel load versus speed for a 100-ton empty, covered hopper car, measured during hunting using instrumented wheel set data.

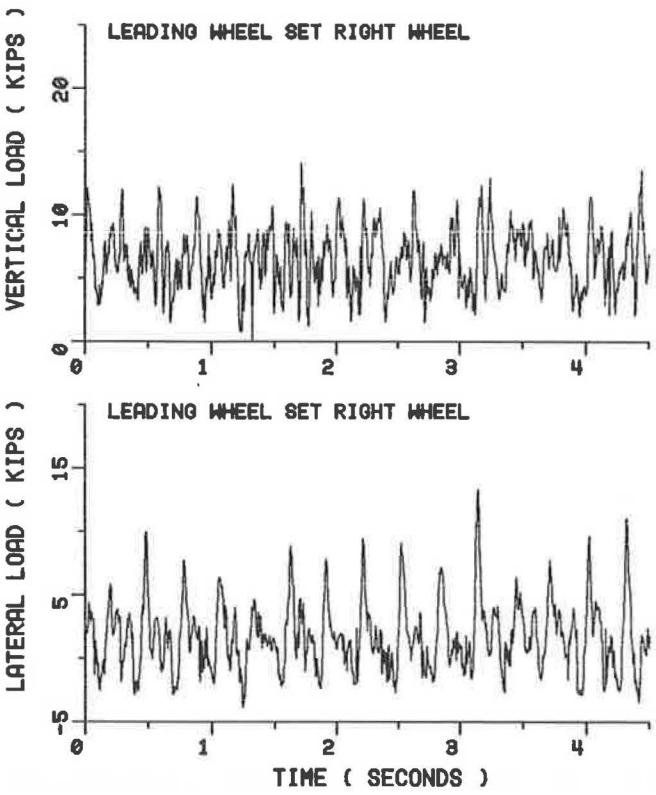

FIGURE 24 Wheel load time histories for a 100-ton empty, covered hopper car, measured at 61 mph during hunting using instrumented wheel set data.

The dynamic load environment produced by 125-ton cars during hunting is not reported in this paper because these data are not currently available.

CURVING

Negotiating curves with low wheel/rail forces is important from both the economic and safety points of view. The economic importance of curving ability can be viewed from the perspective of energy consumption and track maintenance. During curve negotiation, curve resistance, which is the power dissipated at the wheel/rail contact patch, must be overcome by added tractive effort that requires increased energy consumption. Excessive wheel/rail loads cause accelerated wheel/rail wear, truck component deterioration, and track damage. The ramification of all this is increased maintenance of vehicles and track structures, increased potential for derailment, and higher operating costs.

The forces developed between the wheel and rail depend on wheel/rail geometry (e.g., wheel profiles, degree of curvature, superelevation, etc.) and, most importantly, on the truck's primary suspension characteristics.

In sharp curves, depending on the speed of the vehicle, the outer wheel of the lead axle may assume flange contact with the high rail. This situation contributes to the wear of the wheel flanges as well as the gage face of the high rail. High lateral-to-vertical load ratios can cause the wheels to climb the rail or overturn the rail. The peak transient forces resulting

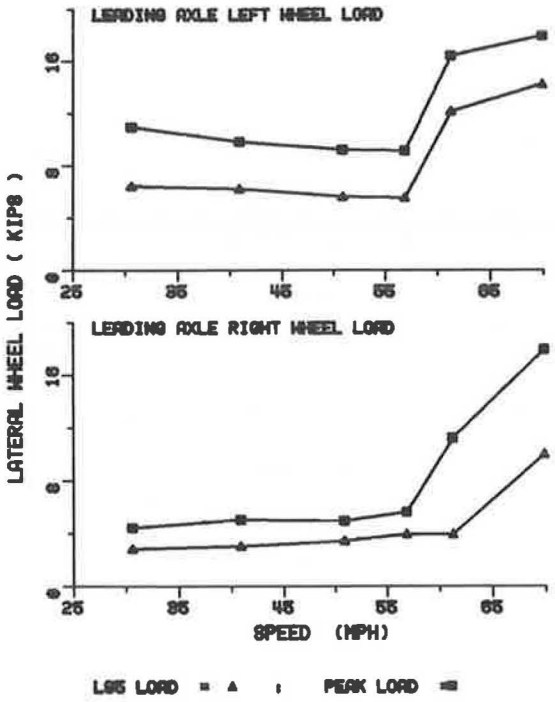

FIGURE 25 Peak lateral wheel load versus speed for a 100-ton loaded, covered hopper car, measured during hunting using instrumental wheel set data.

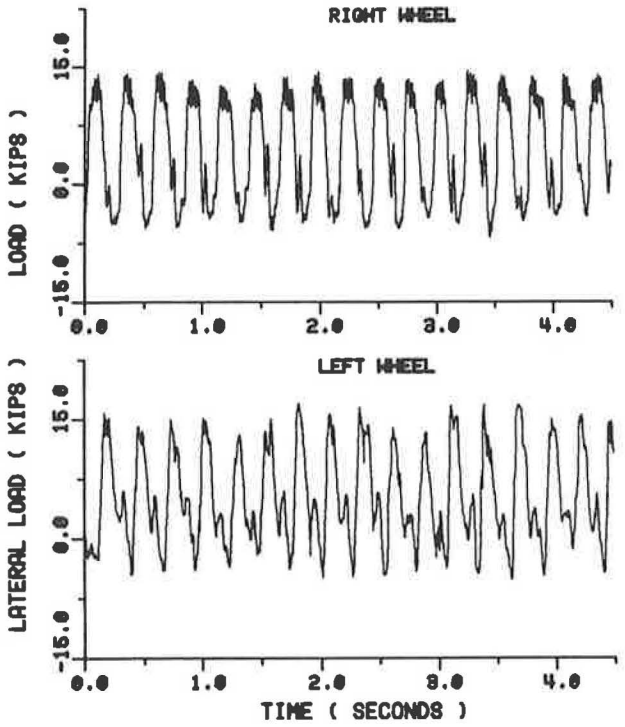

FIGURE 26 Lateral wheel load time histories for a 100-ton loaded, covered hopper car measured at 71 mph during hunting.

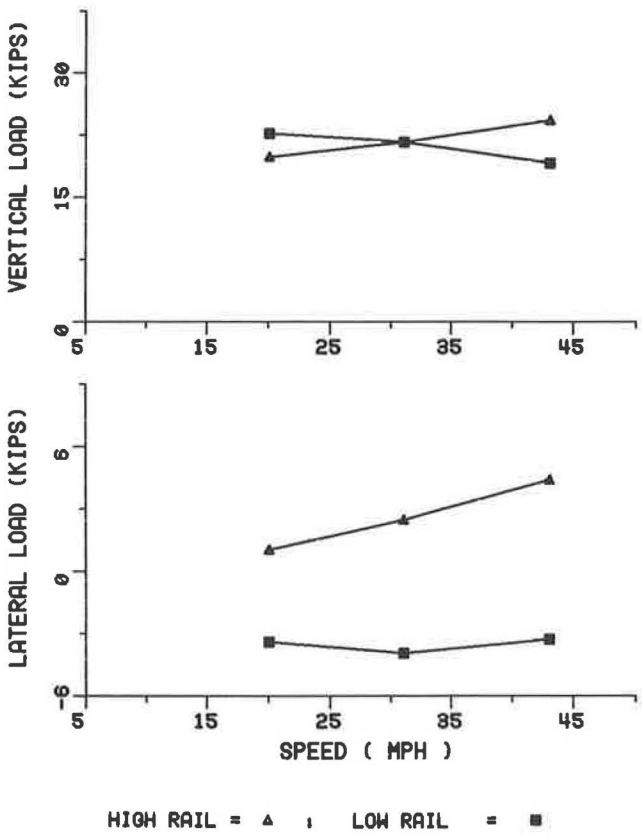

FIGURE 27 Average vertical and lateral load versus speed for a 70-ton loaded frame-braced truck, measured using instrumented wheel set data.

from hard flange impacts during curve entry and exit conditions can be larger than the steady-state forces. Some vehicles experience difficulties in entering and exiting sharper curves of relatively short spiral lengths. A loss of superelevation in such a spiral could create excessive body twist, and, if the torsional stiffness of the vehicle is high, wheel lifts and possible derailments could occur. Therefore, it is of utmost importance to determine the levels of the lateral wheel/rail loads, as well as the vertical load distribution on all four wheels of a truck.

70-Ton Cars

The Railmaster intermodal concept with 70-ton trucks was tested for curving performance at TTC (*12*). The steady-state curving performance characteristics were determined by evaluating the wheel/rail lateral and vertical forces, wheel set angles-of-attack, and L/V ratios at balance and underbalance speeds on curves ranging from 3 to 7.5 degrees.

The lateral and vertical wheel loads on the leading axle of the shared truck located at the leading end of the trailing van were measured using instrumented wheel sets. The curving tests were conducted on the FAST loop and the Balloon loop, providing track curvatures from 3.0 to 7.5 degrees. All curving tests were made with loaded cars in dry rail conditions at balance, overbalance, and below-balance speeds. The 3.0-, 4.0-, 5.0-, and 7.5-degree curved tracks had 2-, 3-, 4-, and 4.5-in. superelevations corresponding to 30.9-, 31.6-, 34.0-, and 29.3-mph balance speeds, respectively.

Figure 27 presents the results of mean lateral and vertical loads on the 5-degree curve. Note that the negative sign in this figure indicates that a low-rail lateral load is directed toward the flange. As seen in the figure, the lateral loads on the high rail increase with increasing speeds, as loads are shifted to the high rail. It should be noted that the individual lateral forces exerted on the rail act to spread the rails apart. Intersection of the vertical loads near 34 mph indicate that the theoretical balance speed was attained. The static wheel load on this lightly loaded truck was about 19 kips.

The mean values of the lateral loads, computed near balance speed as a function of track curvature, are shown in Figure 28. Note that the mean high-rail lateral loads increased from 1.7 kips on the 3-degree curve to 2.9 kips on the 7.5-degree curve. The corresponding low-rail lateral loads were 2.7 kips on the 3-degree curve and 5.2 kips on the 7.5-degree curve. The maximum high- and low-rail L/V ratios were 0.16 and 0.27 on the 7.5-degree curve, respectively.

The load environment seen under conventional 70-ton vehicles is not reported here because of a lack of curving data for this type of cars. The curving performance of this intermodal vehicle equipped with frame-braced trucks, high conicity wheels, and resilient primary suspension pads is believed to be superior to conventional vehicles with standard three-piece trucks.

100-Ton Cars

The High Performance, High Cube, Covered Hopper Car Project included a series of comprehensive tests to charac-

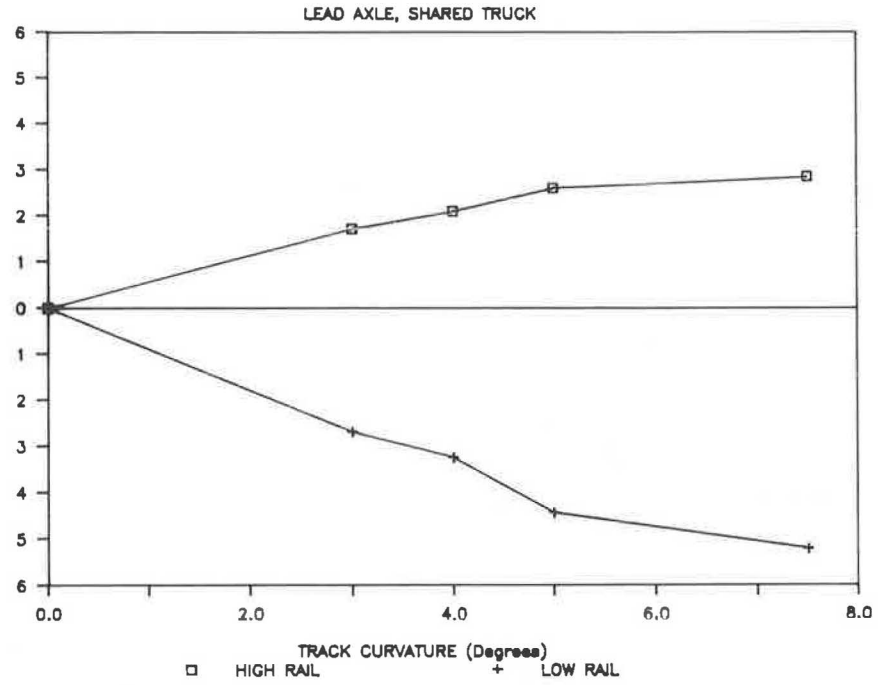

FIGURE 28 Average lateral load versus track curvature for a 70-ton loaded cross-braced truck, measured using instrumented wheel set data.

terize the curving performance of the baseline 100-ton covered hopper car described previously (*19*). The primary objective of the curving tests was to determine the vertical and lateral loads and the angles-of-attack developed during curve negotiation of the vehicle under various operating and track conditions.

The curving tests were conducted on various test tracks at the TTC, providing track curvatures ranging from 50 min. to 5 degrees. Instrumented wheel sets were used on the leading axle of the leading truck. The test runs were made at balance speed for each curve, as well as two speeds above and two speeds below the balance speed.

Figure 29 presents the results of mean lateral and vertical loads on the 5-degree curve versus test speed. The signs of the low-rail lateral wheel loads were changed to avoid overlapping of the curves; the negative sign indicates that a low-rail lateral load is directed toward the wheel flange. On the 5-degree curve, at severe unbalance speed of 10 mph, the mean lateral loads were as high as 14,000 lb on the low rail. At an above-balance speed of 45 mph, the mean values of the high-rail lateral loads increased to 13,000 lb. The individual wheel reaction forces were found to act to spread the rails apart, possibly resulting in gage widening on the track.

The vertical wheel loads showed similar trends in which the low-rail vertical loads decreased and the high-rail loads increased with increasing speeds for most of the curves. For the 5-degree curve, the mean values of the vertical wheel loads ranged from 25,000 to 43,000 lb, depending on the unbalanced superelevation. The intersection of the measured vertical wheel loads near 35 mph indicates that the theoretical balance speed on a 5-degree curve with 4 in. of superelevation was attained.

Figure 30 shows the mean lateral loads computed near balance speed, as a function of track curvature. As expected, the lateral loads increase with increasing curvature.

The lateral wheel loads produced on most curved tracks were in general compliance with fundamental curving behavior: they (a) tended to increase with increasing track curvatures and (b) shifted to the high-rail wheels with increasing speeds. On sharp curves below balance speed, the low-rail wheel of the lead axle experienced lateral loads up to 50 percent higher than the high-rail wheel. The net lateral load resulting from individual wheel loads on the track points toward the inside of the curve at these low speeds. Similarly, at above-balance speed, the high-rail wheel of the lead axle experiences higher lateral wheel loads than the low-rail wheel, partly because of flanging with the gage face of the high rail. The net lateral load exerted on the tracks by the lead wheel set points away from the center of the curve.

To evaluate the maximum levels of the lateral loads, which could cause permanent track deformation, the net axle loads with duration distance of 6 ft were investigated at severe unbalance conditions. It was found that the maximum net lateral lead axle load produced on the 5-degree curve at 45 mph (corresponding to 3 in. of deficiency in superelevation) was as high as 15,700 lb, pointing toward the outside of the curve. At 10 mph, corresponding to 3.6 in. of excess superelevation, the maximum net lead axle lateral load was on the order of 13,200 lb, pointing toward the inside of the curve.

125-Ton Cars

A test program undertaken to gather data to further the understanding of the 125-ton axle load environment and to develop a comparison between the 125- and 100-ton cars was conducted. The curving tests were conducted in the 5-degree curve and on tangent sections of the FAST loop. A total of three cribs was instrumented in the curved section for load

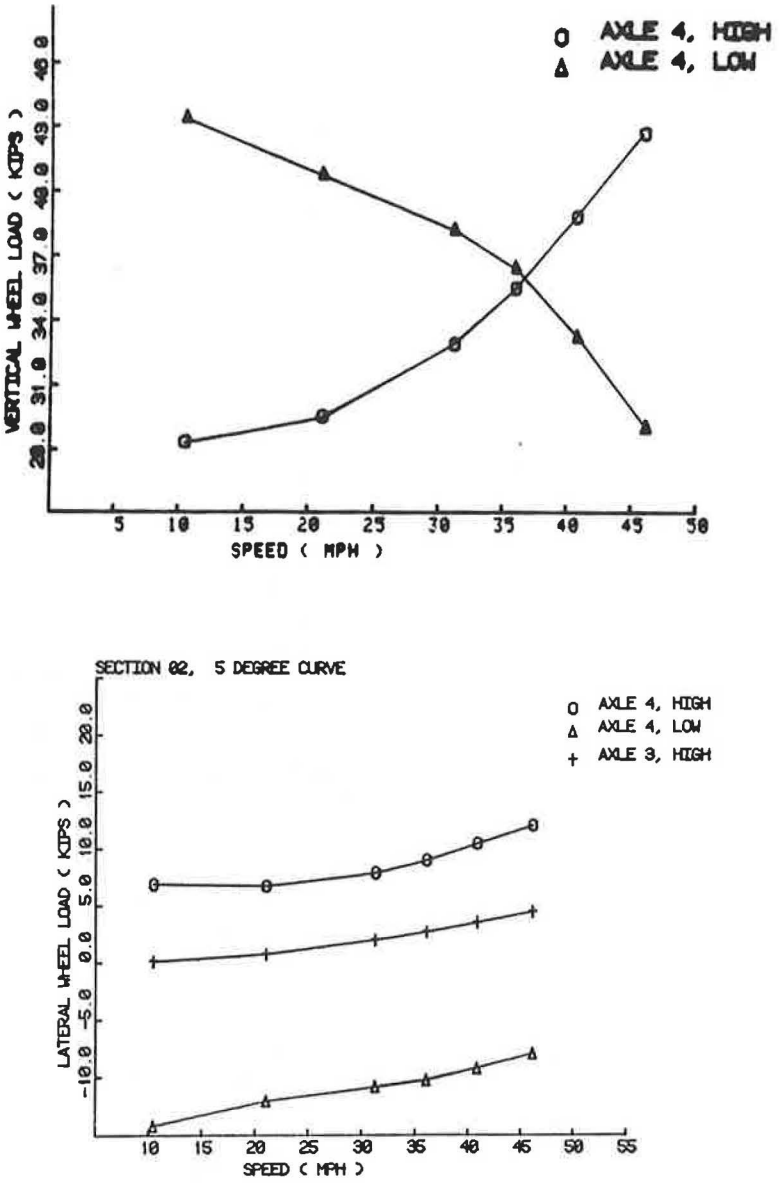

FIGURE 29 Wheel loads versus speed for a 100-ton loaded, covered hopper car, measured on a 5-degree curve using instrumented wheel set data.

and deflection measurements. The tests were run at speeds of 10, 20, 25, 30, 35, and 40 mph on tangent and curved tracks. A total of 25 laps was also run at 40 mph in order to get statistical distribution of the wheel loads.

Figure 31 shows the maximums of vertical and lateral wheel loads (averaged over three instrumented cribs) of leading trucks of all five 125-ton cars on the 5-degree curved and tangent track as a function of test speed. The peak vertical loads on tangent track remain slightly above the static load level of 39 kips at speeds from 10 to 40 mph. The maximum vertical loads show a general trend in which the high-rail loads increase and low-rail loads decrease with speed because of excess superelevation. However, intersection of the vertical load curves does not occur at the theoretical balance speed of 34 mph, because the loads shown in Figure 31 represent maximum vertical loads rather than average vertical loads.

The low-rail lateral loads in Figure 31 appear to be higher than the high-rail loads at all speeds except 40 mph. In general, the low-rail steady-state lateral loads should follow the same trend and decrease with speed like the low-rail vertical loads, but they increase along with the high-rail loads at speeds above 30 mph. The reason is that the lateral loads shown in Figure 31 are the dynamic lateral rail loads that occur over approximately 10 ft of curved track segment. Consequently, the lateral rail loads include steady-state as well as dynamic loads and do not follow the trend displayed by the vertical rail loads.

The statistical analysis results are shown in plots of probability distribution functions in Figure 32, for peak vertical loads. For the 125-ton cars, the median vertical loads on the high rail were about 46,000 lb, and they were 36,000 lb on the low rail at 40 mph.

Comparison of the load distribution curves indicates that the 125-ton car vertical load frequency of exceedance levels

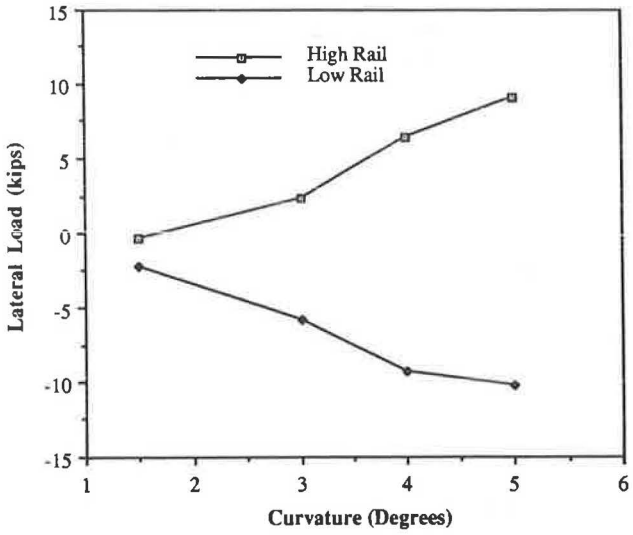

FIGURE 30 Mean lateral wheel load versus track curvature for a 100-ton loaded, covered hopper car, measured using instrumented wheel set data.

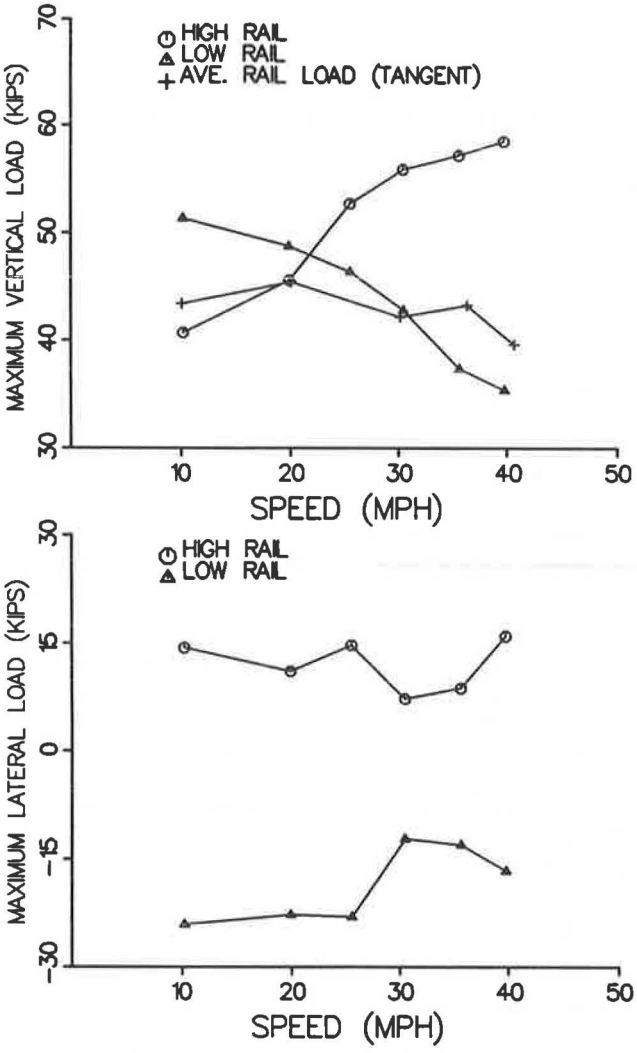

FIGURE 31 Maximum vertical and lateral rail loads versus speed for a 125-ton covered hopper car, measured using wayside data.

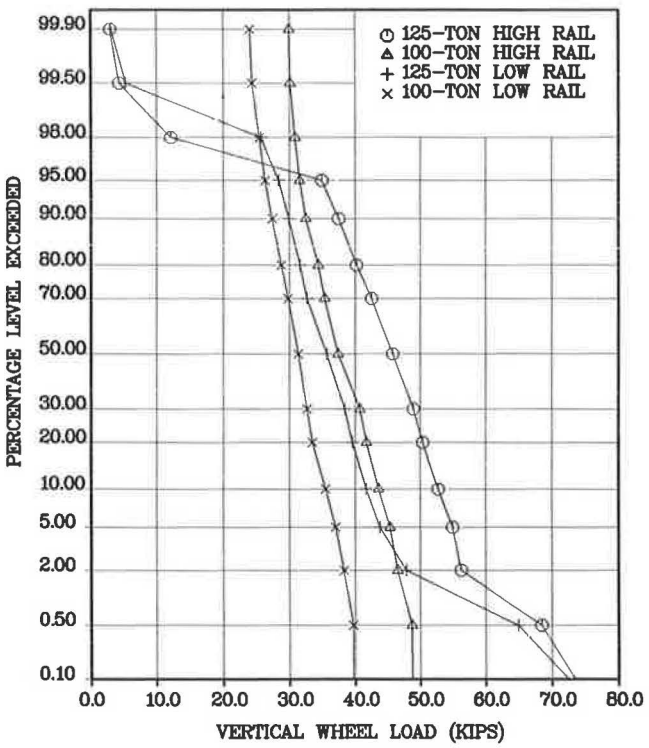

FIGURE 32 Probability distribution of peak vertical rail loads for 100- and 125-ton cars, measured at 40 mph.

from 2 to 98 percent was 20 percent higher than that of the 100-ton cars. The maximum vertical loads with a frequency of less than one per 100 axles were up to 45 percent higher for the 125-ton cars than for the 100-ton cars. The importance of this information is that higher dynamic loads developed under 125-ton cars would be significantly more damaging to the track structure than those under 100-ton cars.

CONCLUSIONS

Based on the results presented herein, the following observations and conclusions were made:

- The high-speed track testing of standard 70-, 100-, and 125-ton freight cars indicated that these cars experience bolster loads in excess of 1.8 times the static load as a result of a variety of track irregularities. The most damaging sites with multiple periodic vertical track irregularities excite the vehicles harmonically. The loads produced by the harmonically excited vehicles appear to be causing further loss of track geometry from the initial irregularity. At these sites the extent of damage appears to be growing with traffic.
- Because of a lack of effective damping during bounce resonance of a standard freight car, successive cycles of suspension spring bottoming produce extremely high vertical loads. The controlled test results indicate that when excited by periodic, parallel, 39-ft low-rail joints with 0.75-in. maximum surface profile deviations, peak dynamic vertical wheel loads for 70-, 100-, and 125-ton cars can be as high as 3 to 5 times the static wheel load. The revenue track test results agree with the controlled test results in that the vertical wheel loads in

excess of three times the static load occur as a result of a series of parallel rail joints occurring on open track with continuously welded rail.

- The maximum dynamic vertical loads resulting from roll resonance ranged from 1.8 to 3 times the static wheel load for loaded 70-, 100-, and 125-ton cars. All car types exhibited extensive wheel unloading.
- As a result of excessive car body roll, suspension bottoming occurs, and the resulting violent undamped body motions cause excessive loading of one side of the track with the other side lifting clear of the track structure. Asymmetric loading of the track structure along the direction of travel results in accelerated deterioration and additional loss of track geometry. With increasing cross-level elevation, the vehicles operating over the same track section would experience higher and higher loads bringing about additional geometry loss resulting in increased derailment propensity.
- At and above the critical hunting speed of a vehicle, very large dynamic lateral loads are exerted on the vehicle and track at frequencies from 2 to 4 H. The peak cyclic lateral loads measured on a 100-ton empty and loaded covered car were as high as 15 to 20 kips, respectively. These loads can cause wide gage and lateral alignment problems on tangent track. Truck hunting, when combined with track irregularities, can create a potential for wheel climb derailment.
- Because the energy necessary to sustain hunting motions is eventually provided by the forward motion of the vehicle, the excessive lateral and yaw motions of the wheel set increase the rolling resistance, resulting in increased energy consumption.
- During curve negotiation of a railway vehicle, the lateral and vertical loads shift to high rail with increasing speeds as a result of overbalance superelevation. The individual lateral loads exerted on the rail act to spread the rails apart.
- A standard North American freight car equipped with conventional three-piece trucks with no primary suspension system achieves its guidance on sharper curves by the wheel flanges. The resulting high wheel/rail forces lead to problems associated with increased wear, truck deterioration, and track damage.
- The increased energy consumption during curving results from the energy dissipated at the contact patch, which must be overcome by added tractive effort.
- Preliminary results obtained from a series of recent track testing of 100- and 125-ton cars indicate that the average 125-ton car vertical wheel loads were 20 percent higher than those of the 100-ton cars on a 5-degree curve. The peak wheel/rail impact loads during curving were 45 percent higher for the 125-ton cars than for the 100-ton cars. Higher dynamic loads developed under 125-ton cars would be more damaging to the track structure. The ongoing 150 million gross tons of operation of heavy axle load cars on the FAST loop will verify and translate this load environment into track deterioration.
- The results of dynamic load testing suggest that vehicle suspension characteristics of heavier cars will have a major effect on the performance and life of the track structure.
- For conventional North American freight cars, the low-frequency dynamic wheel/rail loads associated with suspension dynamics are transmitted to and damaging for the vehicle/track structure. The analysis of the effects of loads in excess of the design values on fatigue life indicates that these high-magnitude, low-frequency loads cause considerable component fatigue damage.
- Inadequate suspension damping adversely influences the dynamic loads imposed on track with imperfect surface characteristics. Even with "questionable" track conditions, railway vehicles equipped with premium suspension systems do not produce excessive dynamic loads. However, standard suspension systems do produce dynamic loads beyond the design limits of vehicle/track components.
- An economic study focusing on the relative cost of maintenance of track and truck components as affected by excessive dynamic loads should be conducted.

REFERENCES

1. E. H. Law and N. K. Cooperrider. A survey of Railway Vehicle Dynamics Research. *Journal of Dynamics Systems, Measurement, and Control*, ASME, Vol. 96, No. 2, June 1974.
2. F. B. Blader. Development and Applications of a General Rail Vehicle Dynamic Computer Model (NUCARS). Presented at the ASME Winter Annual Meeting, Nov. 1988.
3. *Proc., International Conference on Wheel/Rail Load and Displacement Measurement Techniques.* Report DOT-TSC-UMTA-82-3. UMTA, U.S. Department of Transportation, Jan. 19, 1981.
4. S. Kalaycioglu and S. K. Punwani. *High Performance/High Cube Covered Hopper Program, Base Car Dynamic Performance Tests, Volume 4—Summary.* Report R-581. Association of American Railroads, Chicago, Ill., June 1984.
5. P. V. RamaChandran and M. M. ElMadany. *Truck Design Optimization Project Phase-II.* FRA/ORD-81/48; Final Report. FRA, Sept. 1981.
6. N. K. Cooperrider, E. H. Law, and R. H. Fries. *Freight Car Dynamics, Field Test Results and Comparison with Theory.* Report FRA/ORD-81/46. FRA, June 1981.
7. R. H. Prause, H. D. Harrison, J. C. Kennedy, and R. C. Arnlund. *An Analytical and Experimental Evaluation of Concrete Cross Tie and Fastener Loads.* Report FRA/ORD-77/71. FRA, Dec. 1977.
8. V. Sharma, W. H. Sneed, and S. K. Punwani. Freight Equipment Environmental Sampling Test—Description and Results. *Proc., ASME Rail Transportation Spring Conference*, Chicago, Ill., April 1984.
9. R. A. Poclington. The B. R. Load Measuring Wheel. *Proc., International Conference on Wheel/Rail Load and Displacement Measurement Techniques.* Report DOT-TSC-UMTA-82-3. U.S. Department of Transportation, Jan. 1981.
10. H. D. Harrison and D. R. Ahlbeck. Development and Evaluation of Wayside Wheel/Rail Measurement Techniques. *Proc., International Conference on Wheel/Rail Load and Displacement Measurement Techniques.* Report DOT-TSC-UMTA-82-3. U.S. Department of Transportation, Jan. 1981.
11. S. K. Punwani. Measurement of Wheel/Rail Forces on the High Cube, High Performance Covered Hopper Car Project. *Proc., ASME Rail Transportation Spring Conference.* Chicago, Ill., April 1984.
12. G. B. Anderson, S. Kalaycioglu, and S. P. Singh. *High Productivity Integral Train Program, Railmaster System Concept Tests, Volume 1, Summary.* Report R-653. Association of American Railroads, Chicago, Ill., Aug. 1987.
13. S. Kalaycioglu and S. K. Punwani. *High Performance/High Cube Covered Hopper Program, Base Car Dynamic Performance Tests. Volume 1—Rock-and-Roll and Bounce.* Report R-566. Association of American Railroads, Chicago, Ill., April 1984.
14. P. Singh Satya, J. T. Dincher, and S. K. Punwani. *High Performance/High Cube Covered Hopper Program, High Cube 2000 Prototype Dynamic Performance Tests, Summary.* Report R-636. Association of American Railroads, Chicago, Ill., Aug. 1987.
15. S. Kalaycioglu and A. Tajaddini. *Locating Vertical Track Irregularities Which Cause Excessive Vehicle Loads.* Report R-694. Association of American Railroads, Chicago, Ill., March 1988.
16. S. Kalaycioglu and A. Tajaddini. Investigation of Vertical Track Irregularities: Phase 2, Vehicle Track System Testing. Presented at the ASME Winter Annual Meeting, Nov. 1988.

17. S. Kalaycioglu and S. K. Punwani. *Lateral Stability of a 100-Ton Covered Hopper Car Equipped with Conventional Trucks*. Presented at the ASME Winter Annual Meeting, Nov. 1985.
18. D. R. Ahlbeck, H. D. Harrison, and S. L. Noble. *An Investigation of Factors Contributing to Wide Gage on Tangent Track*. Presented at the ASME Winter Annual Meeting, Nov. 1975.
19. S. Kalaycioglu, A. V. Arslan, and S. K. Punwani. *High Performance/High Cube Covered Hopper Program, Base Car Dynamic Performance Tests, Volume 3—Curving*. Report R-572. Association of American Railroads, Chicago, Ill., April 1984.

Publication of this paper sponsored by Committee on Railroad Track Structure System Design.